REVERSIBLE NERVE CONDUCTION BLOCK USING LOW FREQUENCY ALTERNATING CURRENTS

by

Maria I. Muzquiz

A Thesis

Submitted to the Faculty of Purdue University

In Partial Fulfillment of the Requirements for the Degree of

Master of Science in Biomedical Engineering

Department of Biomedical Engineering

Indianapolis, Indiana

August 2020

THE PURDUE UNIVERSITY GRADUATE SCHOOL

STATEMENT OF COMMITTEE APPROVAL

Dr. Ken Yoshida, Chair

Department of Biomedical Engineering

Dr. John Schild

Department of Biomedical Engineering

Dr. Ed Berbari

Department of Biomedical Engineering

Approved by:

Dr. Julie Ji

Head of the Graduate Program

This thesis is dedicated to my parents, Miguel and Ivette Muzquiz, who have taught me the value of hard work and perseverance, to my grandfather, Arturo Garcia, for his words of wisdom, and to my husband, Cole Van Dyke, who may not have understood when I discussed my work but engaged in the conversation and was proud regardless.

ACKNOWLEDGMENTS

I wish to gratefully acknowledge and extend my gratitude towards Dr. Yoshida for taking me into his lab. He challenged my thinking and pushed my limits to help me become the engineer I am today. Without his guidance, support, and supply of coffee this thesis would not have come to full fruition.

I also extend my gratitude towards my former colleague, Landan Mintch, for his collaboration with the rat experiments as well as for his patience with my questions and experiments that carried into the evening at times.

I wish to thank Lindsay Richardson, a colleague and dear friend of the Bioelectronics Lab. Without the fabrication of custom made electrodes this work would have not been possible. I greatly appreciate her guidance, engaging conversation, advice, and moments of laughter.

I would like to thank my colleagues and friends of the Bioelectronics Lab: Awadh Al-Hawwash, Christian Vetter, Macallister Smolik, Nathaniel Lazorchak, Chrisopher Hoffman, Ryne Horn, and Onna Doering. This work would have not been possible without their dedication in collaborating and application of their vast knowledge. I have learned so much from each of you.

To my high school teachers Pam Thurner, Evie Ames, and Andrea Clinkenbeard for seeing my potential and pushing me to strive for more.

To my husband Cole for his patience, advice, and bad jokes. And for helping me stay sane with adventures throughout.

This work was supported by an Exploratory Research Grant from GSK/Galvani Bioelectronics (#100040339). Additional research funding was provided through a NIH Traiblazer R21 award (R21EB028469). The authors also acknowledge support from the Familien Hede-Nielsens Fonden which enabled purchase of the 3D printers and PCB printers used in this project. Additional funding was received from the IUPUI Undergraduate Research Opportunities Program and the BME Department Faculty Development Fund.

TABLE OF CONTENTS

LIST OF TABLES

LIST OF FIGURES

LIST OF ABBREVIATIONS

ANS	autonomic nervous system
AP	action potential
BP	blood pressure
BRrate	breathing rate
CAP	compound action potential
CE	caudal electrode
CNAP	compound neural action potential
CNS	central nervous system
DC	direct current
ECG	electrocardiograph
ENG	electroneurograph
HR	heart rate
H^+	hydrogen ions
K^+	potassium ion
kHFACb	kiloHertz frequency alternating current block
LFAC	low frequency alternating current
Na^+	sodium ion
OH^-	hydroxide ions
RE	rostral electrode
SFAP	single fiber action potential
SNS	somatic nervous system
PNS	peripheral nervous system
VNS	vagal nerve stimulation

ABSTRACT

Muzquiz, Maria I M.S.B.M.E., Purdue University, August 2020. Reversible Nerve Conduction Block Using Low Frequency Alternating Currents. Major Professor: Ken Yoshida.

This thesis describes a novel method to reversibly and safely block nerve conduction using a low frequency alternating current (LFAC) waveform at 1 Hz applied through a bipolar extrafascicular elecrode. This work follows up on observations made on excised mammalian peripheral nerves and earthworm nerve cords. An *in-situ* electrophysiology setup was used to assess the LFAC waveform on propagating action potentials (APs) within the cervical vagus nerve in anaesthetized Sprague-Dawley rats (n = 12). Two sets of bipolar cuff or hook electrodes were applied unilaterally to the cervical vagus nerve, which was crushed rostral to the electrodes to exclude reflex effects on the animal. Pulse stimulation was applied to the rostral electrode, while the LFAC conditioning waveform was applied to the caudal electrode. The efferent volley, if unblocked, elicits acute bradycardia and hypotension. The degree of block of the vagal stimulation induced bradycardia was used as a biomarker. Block was assessed by the ability to reduce the bradycardic drive by monitoring the heart rate (HR) and blood pressure (BP) during LFAC alone, LFAC with vagal stimulation, and vagal stimulation alone. LFAC applied via a hook electrode (n = 7) achieved 86.6 $\pm$ 11 % block at current levels 95 $\pm$ 38 μA_p (current to peak). When applied via a cuff electrode (n = 5) 85.3 $\pm$ 4.60 % block was achieved using current levels of 110 $\pm$ 65 μA_p. Furthermore, LFAC was explored on larger vagal afferent fibers in larger human sized nerve bundles projecting to effects mediated by a reflex. The effectiveness of LFAC was assessed in an *in-situ* electrophysiological setup on the left cervical vagus in anaesthetized domestic swine (n = 5). Two bipolar cuff electrodes were applied unilaterally to the cervical vagus nerve, which was crushed caudal to the electrodes to eliminate cardiac effects. A tripolar extrafascicular cuff electrode was placed most rostral on the nerve for recording of propagating APs induced by electrical stimulation and blocked via the LFAC waveform.

Standard pulse stimulation was applied to the left cervical vagus to induce the Hering-Breuer reflex. If unblocked, the activation of the Hering-Breuer reflex would cause breathing to slow down and potentially cease. Block was quantified by the ability to reduce the effect of the Hering-Breuer reflex by monitoring the breathing rate during LFAC alone, LFAC and vagal stimulation, and vagal stimulation alone. LFAC achieved 87.2 $\pm$ 8.8 % (n = 5) block at current levels of 0.8 $\pm$ 0.3 mA_p. Compound nerve action potentials (CNAP) were monitored directly. They show changes in nerve activity during LFAC, which manifests itself as the slowing and amplitude reduction of components of the CNAPs. Since the waveform is balanced, all forward reactions are reversed, leading to a blocking method that is similar in nature to DC block without the potential issues of toxic byproduct production. These results suggest that LFAC can achieve a high degree of nerve block in both small and large nerve bundles, resulting in the change in behavior of a biomarker, *in-vivo* in the mammalian nervous system at low amplitudes of electrical stimulation that are within the water window of the electrode.

CHAPTER 1. INTRODUCTION

1.1 Discovery

The novel waveform explored in this thesis was discovered in the lab by Horn and Yoshida while investigating high-frequency nerve conduction block. This discovery was quickly followed up by *ex-vivo* work on excised mammalian nerves and *in-vitro* on earthworm nerves [1, 2]. This work provided cursory observations that block occurred intermittently when the high frequency (10's kHz) was switched to a low frequency sinusoidal waveform at 0.1 Hz. The conditioning waveform was deemed low frequency alternating current (LFAC) as it fills the gap between direct current block (0 Hz) and kilohertz frequency alternating current block (kHFACb, > 1 kHz). The *ex-vivo* and *in-vitro* work showed successful block of conducting action potentials (AP), which suggested that the technique could be a viable means to block nerve activity. Computer models for kHFACb were adjusted to the LFAC waveform and block was demonstrated *in-silico* [1]. These observations suggested that LFAC block could be a potential means to block nerve activity as a tool to complement electrical activation of nerve (FES). However, it was unclear if LFAC block could induce relevant functional, organ level, changes in function. The work presented in this thesis aims to fill the knowledge gap regarding the novel LFAC waveform.

1.2 Significance and Overview of System

The nervous system is a highly complex system that is composed of a vast variety of nerves. It is important in coordinating voluntary and involuntary movements. It is also crucial in our interaction with the environment. The most basic function of the nervous system is to send and receive signals from one cell to another or from one body part to another. At a more integrative level, the function of the nervous system is to maintain the body within a homeostatic range. Signaling is often complex and thus not always well defined. However, it is well understood that the nerves that produce the signals are an end target for modulation of neural activity that affect many end organs. The purpose of this chapter is to dive into the general components of the nervous system to understand why it has become a target for electrical therapies.

1.2.1 Anatomy and Physiology

The nervous system is a complex system composed the brain, spinal cord, and a vast network of nerves and specialized cells that innervate organs. There are two main divisions of the nervous system (*Figure 1.1*), the central nervous system (CNS) and the peripheral nervous system (PNS). The CNS is composed of the brain and spinal cord, meanwhile, the PNS is everything else, consisting of both sensory and motor components. The PNS is the method in which the CNS communicates with the rest of the body. The sensory, or afferent, portion links sensory receptors found at the surface (exteroreceptors) and within the body (interoreceptors) with circuits in the CNS. The sensory ganglia and nerves carry sensory information to the CNS to be integrated. Alternatively, the motor, or efferent, portion consists of two divisions that carry impulses away from the CNS to the effector organ. The PNS is composed of the somatic nervous system (SNS) and the autonomic nervous system (ANS). The SNS connects the brain and spinal cord to skeletal muscles. It is responsible for voluntary muscle movements and motor responses. It is also important in transmitting information regarding touch, pain, and temperature below the head and neck region. Meanwhile, the autonomic nervous system (ANS) is responsible for involuntary motor movements and is further divided into two antagonistic divisions deemed the sympathetic and parasympathetic divisions. These two divisions have opposite effects on its visceral targets and are analogous to a gas and brake pedal in a motor vehicle. The sympathetic division is associated with the fight or flight response and has a stimulating effect. It can cause an increase in heart rate and cardiac output, skeletal muscle vasodilation, and the release of catelcholamines. Meanwhile, the parasympathetic division is associated with ‘rest and digest’ and has a relaxing effect. It is responsible for the restoration of homeostasis, conservation of energy, and maintaining a resting heart rate.

The autonomic system innervates and regulates the activity of many vital organs including the heart, pancreas, spleen, liver, kidneys, lungs, and reproductive organs among others. In the case of chronic disease, the regulation of these organs is pushed out of its homeostatic range. The disease can either alter the sensory information or alter the control signals that regulate these vital organs. Surgical or pharmaceuticals interventions are available to treat these diseases. Surgical procedures are invasive and result in irreversible effects. Meanwhile, there are many systemic side effects due to pharmaceutical interventions. Therefore, this division of the PNS, the autonomic nervous system, has been a target for neuromodulation and bioelectronic medicines with the hopes of developing a less invasive and safe alternative to current blocking techniques.

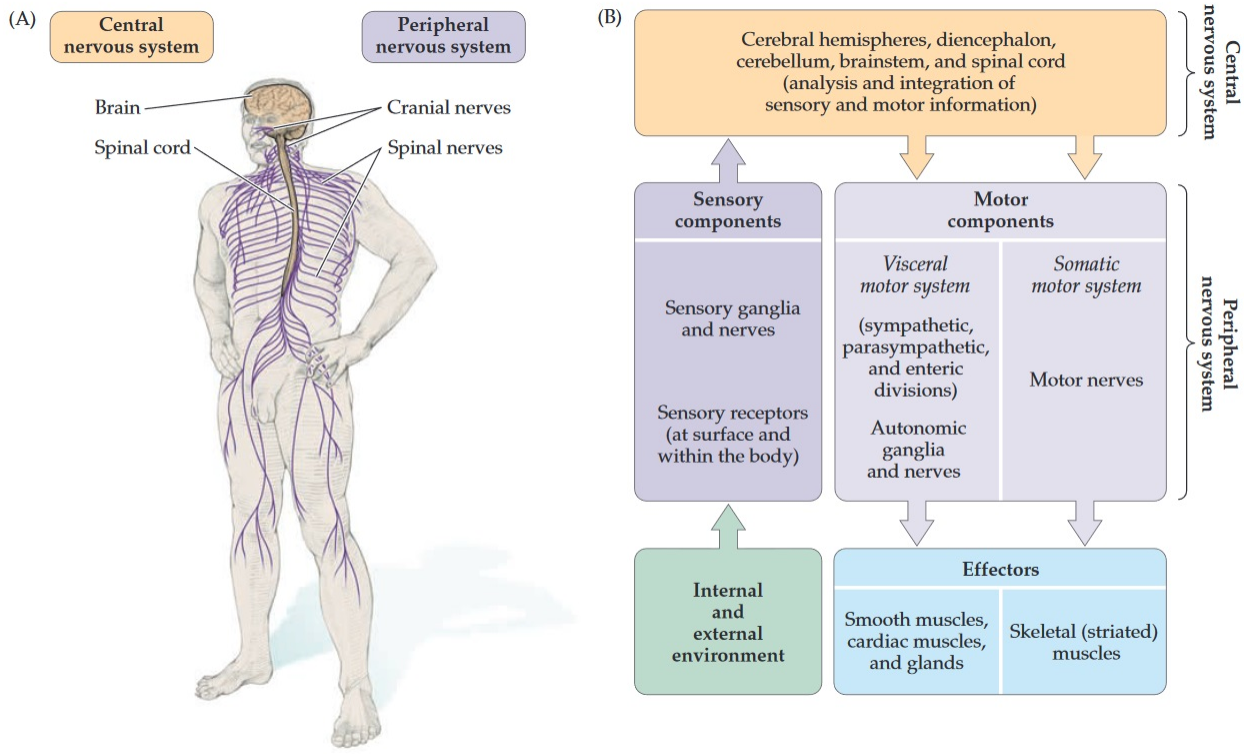

Figure 1.1. Nervous system classification and organization [3]. *Reproduced with permission of the Licensor through PLSclear, PLSclear Ref No: 39114 from Neuroscience, 6th edition, Purves et al, Oxford Publishing Limited, 2018

1.2.2 Hodgkin-Huxley Channel Dynamics

The nervous system communicates through electrical impulses known as APs. Information is transmitted by a combination of both chemical and electrical activity through neurons. Neurons vary in structure and function throughout the nervous system, but a general structure of a neuron is shown in *Figure 1.2*. They have 3 main functional regions: integrative/receptive region, conducting region, and a secretory region. The soma and dendrites are part of the integrative/receptive region. The axon is the conducting region, and the secretory region is at the axon terminal.

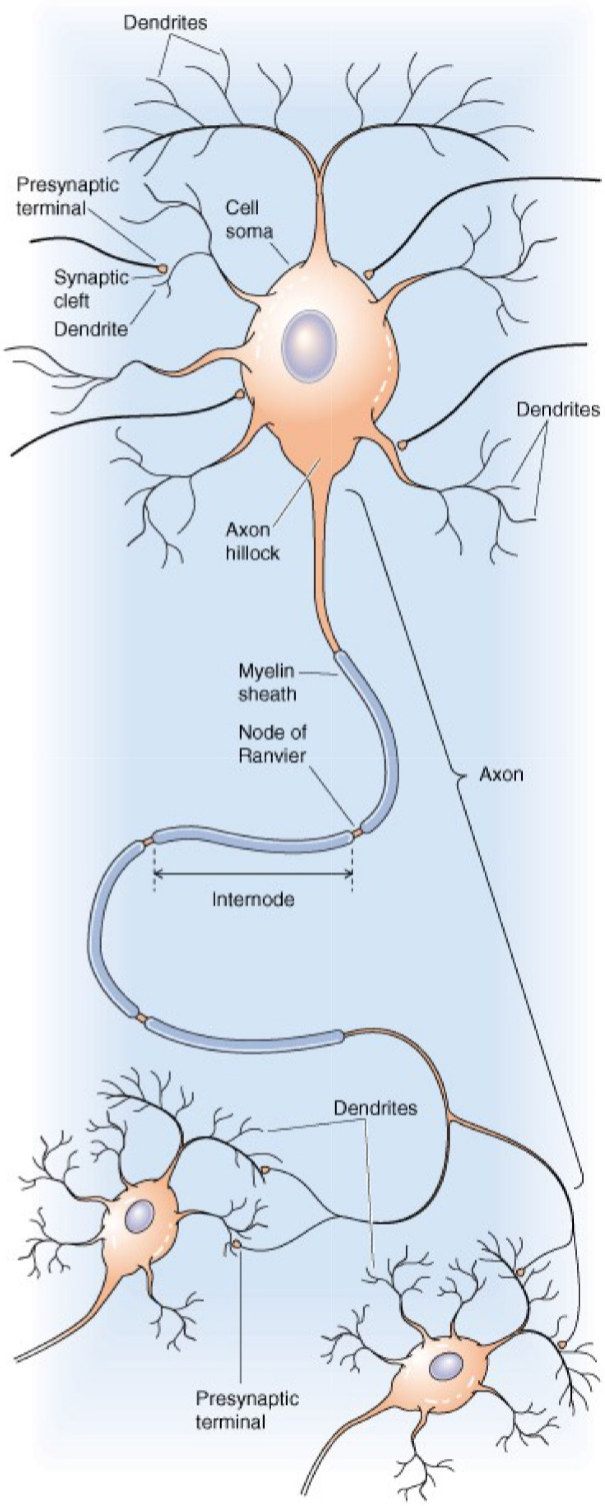

Figure 1.2. General structure of a neuron [4]. *This figure was reproduced with permission from Medical Physiology, 2nd edition, Boron et al, Copyright Elsevier, 2012

Information comes in through the dendrites and cell bodies which produces a change in resting membrane potential or graded potential. An AP is an 'all or none' response to the magnitude of the graded potential which is dependent on the strength or concentration of stimulus. There are two types of graded potentials. A receptor potential is generally associated with sound, light, and touch. In other words, these cells are transducing a type of energy. Alternatively, a synaptic graded potential occurs when neurotransmitter interacts with the receptor. Meanwhile, an AP is the result of a significant change in resting membrane potential. The AP has the ability to cause downstream effects. If the graded potential is large enough, it will trigger APs which travels in an orthodromic and antidromic fashion. The orthodromic AP travels forward into the axon, without loss of amplitude, until it reaches the axon terminal where it will trigger the release of chemical messengers. The antidromic AP travels backwards into the cell body or soma with great attenuation due to absolute refractoriness [4]. The absolute refractory period is the window in time in which an AP can not be triggered again no matter the stimulus strength.

The waveform of an AP can generally be described in 4 phases. Phase 1 is the resting membrane potential. The rapid upstroke, or depolarization, is Phase 2 and is due to sodium (Na^+) channels opening and Na^+ entering the cell. Repolarization, or Phase 3, is due to Na^+ channels closing and potassium (K^+) channels opening thus, K^+ ions leaving the cell. The undershoot, or Phase 4, is due to K^+ channels remaining open while the Na^+ channels are closed. Finally, it goes back to the resting state (Phase 1) in which the Na^+ activation gates are closed and inactivation gates are open.

Voltage clamp experiments on the giant axon of a squid described the voltage-dependent and time dependent parameters that are the underlying basis of an AP [5]. In the work of Hodgkin and Huxley, they define 3 dimensionless gating variables, m, n, and h, that take on a value between 0 and 1. Parameter n, the activating variable, describes the probability that K^+ channels are open. Meanwhile, the sodium Na^+ channel dynamics are ruled by m and h. The probability that the Na^+ is open is described by the activating variable m. The inactivating variable is deemed h. The mathematical model they developed describes the total membrane current which predicts the shape of the AP. In addition, it explains the refractory period and threshold behavior which are observed in *Figure 1.3*. The movement of the various ions across the membrane result in a potential difference. If the difference is great enough, it can trigger an AP.

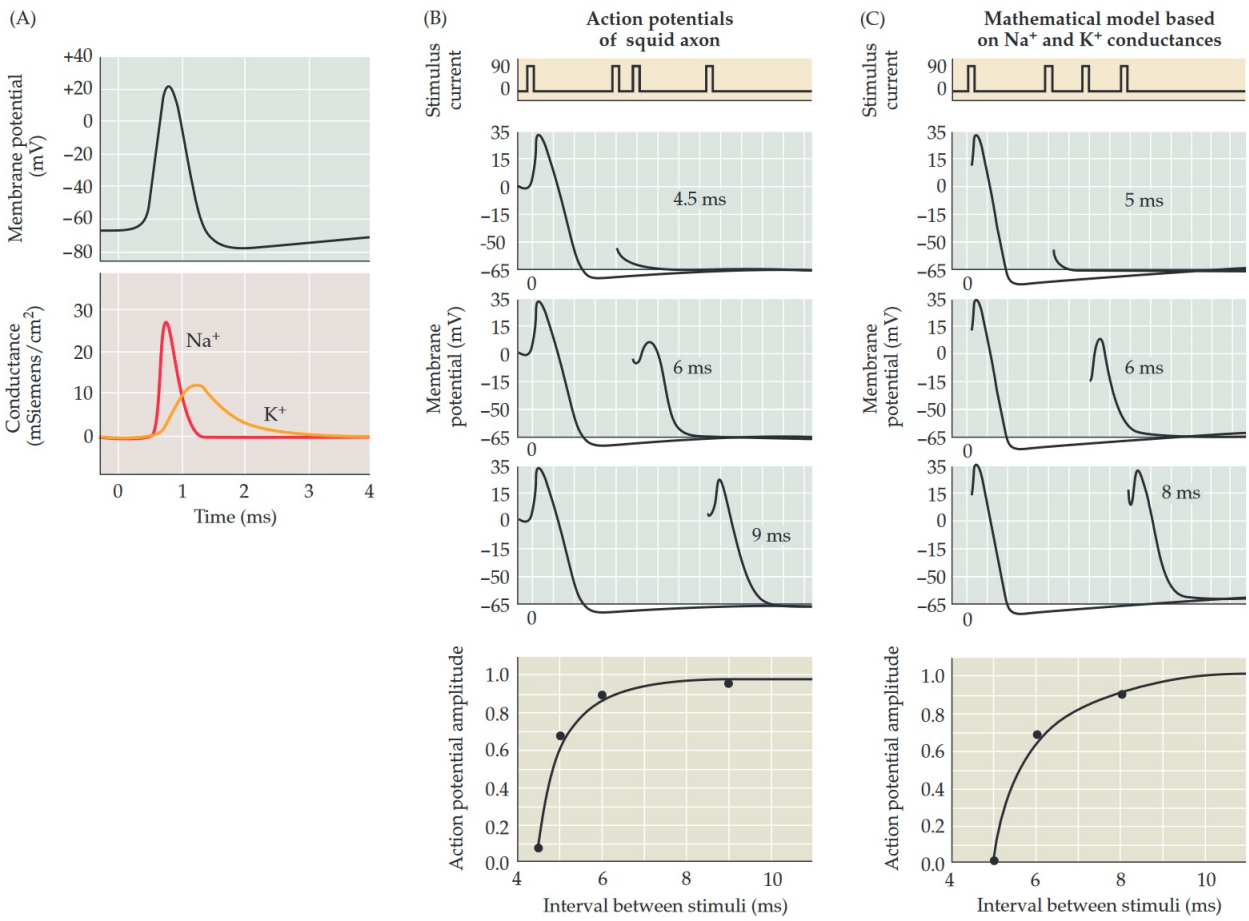

Figure 1.3. Simulation of an action potential. (A) Shows the general shape of an action potential and underlying changes in channel conductance that result in an action potential. (B) Shows the refractory period of actual action potential measurements in a squid axon. (C) Shows the refractoriness prediction of the Hodgkin-Huxley model. [3] *Reproduced with permission of the Licensor through PLSclear, PLSclear Ref No: 39114. Reproduced from Neuroscience, 6th edition, Purves et al, Oxford Publishing Limited, 2018

There are two types of conduction that can occur which depends on the type of axon. Action potentials travel in a continuous manner in unmyelinated nerve fibers. The depolarization and repolarization, or renewal of the AP, occurs step-wise and must move down the entire membrane. Alternatively, APs in myelinated axons travel in a saltatory manner in which the APs are regenerated at the inter-node regions, or Nodes of Ranvier (NoR).

This results in much faster conduction of APs. Action potentials are encoded by population and rate code. The frequency or rate of action potentials increases with increasing stimulus strength or concentration. Additionally, it can result in an increase in the number of neurons that are firing APs, known as population code.

1.2.3 Nerve Fiber Classification

Nerve fibers are classified according to conduction velocity and diameter. The A-C fiber classification along with the subdivisions, only applied to the A class, (α,β,γ) was introduced by Joseph Erlanger and Herbert Gasser [6, 7]. They were awarded the 1944 Nobel Prize in Medicine or Physiology for their work in classifying fiber type according to conduction velocity, function, and diameter [8]. As mentioned above, conduction occurs differently depending on whether the nerve fiber is myelinated or unmyelinated. Myelination offers insulative properties which allow the AP to conduct or propagate faster along the axon. In unmyelinated axons, the currents leak through leakage channels and must be regenerated in a step-wise fashion along the nerve of the axon. Thus, unmyelinated nerves have a slower conduction velocity. *Table 1.1* shows the classification of nerve fibers according to conduction velocity and diameter.

Table 1.1. Nerve fiber classification by conduction velocity and fiber diameter [3]. *Reproduced with permission of the Licensor through PLSclear, PLSclear Ref No: 39114. Reproduced from Neuroscience, 6th edition, Purves et al, Oxford Publishing Limited, 2018

Axon	Conduction velocity (m/s)	Diameter (μm)	Myelination
Squid giant axon	25	500	No
Human			
Motor axons			
Aα type	80–120	13–20	Yes
Aγ type	4–24	5–8	Yes
Sensory axons			
Aα type	80–120	13–20	Yes
Aβ type	35–75	6–12	Yes
Aδ type	3–35	1–5	Thin
C type	0.5–2.0	0.2–1.5	No
Autonomic			
preganglionic B type	3–15	1–5	Yes
postganglionic C type	0.5–2.0	0.2–1.5	No

Different nerve fibers conduct at different velocities. Additionally, different nerve fibers carry different information, therefore, they provide a target for altering a diseased state or modulating neural over-activity with the use of bioelectronic medicines.

1.3 Neuromodulation

Bioelectronic medicine is an emerging interdisciplinary field that combines various engineering disciplines with the fields of neuroscience and medicine. The objective is to modulate neural activity by either stimulating or inhibiting neural signals to alter a diseased state, modulate motor movement, or alter sensations. The modulation of neural activity using electricity is otherwise known as neuromodulation. In the late 1700's, Aloysio Luigi Galvani used electricity to stimulate a dissected leg muscle of a frog to cause it to contract or twitch [9]. This was the first documented evidence of bioelectronic medicine and more specifically, neuromodulation. Neuromodulation can be implemented at the level of the PNS to modulate the activity between the CNS and end organs. One such targets of interest has been the vagus nerve. The vagus nerve, or cranial nerve X, is the longest of the cranial nerves. It is a mixed nerve with both somatic and autonomic branches, 80% of the fibers carry afferent, or sensory, information and the remaining 20% carry efferent or motor information [10]. The autonomic branches of the vagus nerve innervate the heart and organs of the gastrointestinal system such as the stomach and colon. It also provides somatic input to the muscles of the pharynx, larynx, and the palatoglossus muscle of the tongue [11]. It is easily surgically accessible which makes it an important clinical target. Vagal nerve stimulation (VNS) is the term used to describe any technique that stimulates the vagus nerve. This can include physical, chemical, or electrical methods. Electrical vagus nerve stimulation has a variety of clinical applications [10, 12–15]. Clinical applications include the treatment of epilepsy [10], depression [16], obesity [17], anxiety [10], cognitive enhancement for people with Alzheimer's disease [18], migraines [19], rheumatoid arthritis [20], and cardiac diseases [21–24].

There are many associated side effects to current pharamaceutical treatments. Systemic side effects occur due to lack of localization of the treatment. These include drowsiness, mental confusion, insomnia, withdrawal symptoms and many more are among the most common [25, 26]. In comparison, neuromodulation allows for a customizable therapy without the many adverse effects of pharmaceuticals and is therefore, a more attractive option to conventional medical treatments. Neuromodulation has many characteristic features that make this treatment a superior alternative. These include localization, reversibility, rapid onset, and tunability to application and individual.

Modes of neuromodulation include stimulation (or activation) and block (or inhibition) of neural activity. Activation is the mode through which electrical pulses introduce activity to the nerve. Activation of nerve fibers using electrical discharges has been known and understood for centuries [9]. Methods to block propagating APs using electrical stimulation are a more recent discovery and a current topic of investigation.

1.4 Review of Blocking Techniques

Several types of nerve block currently exist to prevent the transmission of nerve signals to the brain or end organ. These include physical, chemical (pharmacological), temperature, and electrical nerve block. Physical nerve block is an irreversible surgical procedure to prevent conduction. The primary method occurs through crushing the nerve or through surgical sectioning. There are two different types of surgical nerve block which include a neurectomy and a rhizotomy. A neurectomy blocks a specific pain signaling pathway via the removal of part or all of the peripheral nerve mediating the pathway. Alternatively, a rhizotomy is a procedure in which the root of the nerve from the spine is destroyed. While the procedures are generally considered safe, they are irreversible. [27]

Chemical treatments can be either reversible or irreversible depending on the pharmacological agent used. Sympathetic blockade is an example of an irreversible or permanent procedure in which the doctor injects a drug, usually phenol or alcohol, to destroy a nerve. With the injection of alcohol, it has been observed that the nerves undergo neuropraxia with Wallerian degeneration of axons. The clinical effect is directly proportional to length of exposure and concentration [28]. There have been studies that point to preferential effects on alpha motorneurons to reduce spasticity with the use of phenol. The method of action is similar to that with the use of alcohol, i.e., through Wallerian degeneration. With the use of chemical agents, reinnervation can occur and have long-term consequences [28, 29]. Reversible nerve block can be achieved through local anesthetics such as botulinum toxin (BTX-A) injections to treat spasticity [28, 30].

Another method of block uses temperature either as heat, cold, or infrared heat. Heat block has been shown to effectively block conduction in simulations of the giant axon of the squid [31]. Alternatively, cooling of the nerve has been shown to slow conduction and reversibly block nerve conduction. This has been shown in earthworms [32], rats [33], and canine [34]. Infrared and a combined infrared energy with electrical nerve block has also shown to be effective in conduction block [35, 36]. Stability and safety are a concern with the use of temperature block.

The conduction block methods outlined above via surgical means, pharmacological agents, and varying temperatures can have unwanted systemic side effects. Furthermore, many are irreversible and can cause unforeseen damage. Therefore, alternative methods to block nerve conduction are necessary. Other methods being investigated use electricity to block nerve conduction. Electrical nerve block offers many properties that are more attractive than pharmaceutical options such as reversibility, localization, and tunability for nerve caliber and type. However, many of these techniques have associated drawbacks which are outlined below.

1.4.1 Collision Block

Collision block is a method of block in which artificial unidirectional antidromic APs can annihilate natural orthodromic APs. This method of block requires that the waveform produce only antidromic APs and not produce orthodromic APs that could be received by the end organ.

1.4.1.1 Quasi-Trapezoidal Stimulation for Collision Block

Quasi-trapezoidal stimulation is a waveform that has been shown to produce only antidromic APs. When the artificial antidromic impulses meet the orthodromic impulses, mutual annihilation occurs. The waveform is similar to a rectangular pulse, however the falling edge decays exponentially. The use of an exponential falling edge yields a slow removal of hyperpolarization to suppress the 'anode break' excitation that occurs from the abrupt removal of hyperpolarization. Monophasic and charge balanced biphasic waveforms have been used in both acute and chronic studies [37, 38], applications have been to block efferent motor activity [37–39].

Cuff electrodes have been used for such applications, however they vary in design. Monopolar [40], tripolar [40, 41, 41], and an asymmetrical two electrode cuff [38, 39, 42] have been used to achieve collision block through the production of antidromic unidirectional action potentials. Waveform parameters vary greatly in frequency, amplitude, and rates of decay. Block has been demonstrated at amplitudes from $1 - 17mA$ [37, 38, 41, 43, 44]. This method of block is not a safe option for clinical studies due to the high currents needed and the production of cytotoxic byproducts that are produced at the tissue/electrode interface due to the charge imbalanced waveform. The cytotoxic byproducts occur due to hydrolysis, the breakdown of water into respective hydrogen (H^+) and hydroxide ions (OH^-). These ions can irreperably damage the nerve and cause the electrode to become polarized. They can also erode the contacts of the electrode.

1.4.2 Direct Current Block

Direct current (DC) block is otherwise termed 'preferential block' or 'differential block' since it was initially used to preferentially block larger axons for the purpose of solely studying small axons [45]. Bhadra et al studied the mechanism of DC block using simulations in Neuron [46]. This study differentiates depolarization block (or cathodal block) from hyperpolarization block (or anodal block), both of which fall under the umbrella of DC block.

The cathode refers to the negative electrode and the anode refers to the positive electrode. Current at the cathode is flowing outward resulting in a depolarizing current. Hyperpolarizing currents occur at the anode due to current flowing inward. Standard rectangular or square wave pulses have associated make or break excitation that occurs at the cathode and anode. Make excitation, or cathode-make excitation, causes an AP to occur at the cathode due to the depolarizing current. Break excitation results from the abrupt removal of the pulse and also causes an AP to occur at the anode, referred to as anode-break excitation. Anode-break excitation occurs due to the hyperpolarization under the anode which results in an increase in membrane excitability. This increase occurs due to a change in the Hodgkin-Huxley gating variables h and n. The sodium inactivating variable, h, approaches a value of 1.

Alternatively, the potassium gating variable n approaches 0. These changes allow the membrane to depolarize and produce an AP [47]. The make or break excitation that occurs must be addressed in the DC blocking mechanism.

Current intensities for DC block have ranged from 50 μA to 10 mA [46]. Meanwhile, pulse duration ranges from 100's of μsec to being constantly on [48, 49]. The mechanisms of anodal and cathodal block differ, however, a property that both anodal and cathodal block share is the onset response [50] and the tissue damage due to hydrolysis that can occur from charge imbalance [45, 51, 52]. A concern of DC block is the 'make or break' excitation that occurs at the cathode when the pulse is turned on and at the anode when the pulse is turned off. Other waveforms have been investigated as a means of preventing the 'make or break' excitation that can occur at the cathode or anode such as: ramped, triangular, and trapezoidal [53–55]. A decaying falling edge has also been used to mitigate the break excitation that occurs at the anode [54], similar to the quasi-trapezoidal waveform mentioned above. However, the formation of cytotoxic byproducts, due to hydrolysis, at the tissue-electrode interface make DC block unsuitable for clinical applications.

1.4.2.1 Anodal Block

Anodal block is one of the mechanisms that falls under the umbrella of DC block and is also referred to hyperpolarization block. Anodal block has been achieved in simulations without the production of anodal-break activation, or the production of APs. Additionally, the use of quasi-trapezoidal stimulation has been used to prevent anodal-break excitation following anodal block [54]. The underlying mechanism has been explored in simulations and is explained as the activation gating variable m approaches zero indicating that the probability of the activating gate m being open is close to zero in the blocked region [46]. When the threshold for an AP is reached there are not enough sodium channels available to open and therefore, can not generate an AP. Thus, block occurs due to failure of sodium channel activation [56].

1.4.2.2 Cathodal Block

Cathodal block, or depolarization block, occurs at generally lower thresholds than anodal block but produces 'make' APs. When a depolarizing current is applied, APs are induced and travel in both directions.

However, with the use of a ramped waveform, make-activation can be prevented. Block occurs after the make-activation, and the h gating variable drops to zero resulting in no sodium current. This indicates that the inactivation gate is being held closed and that most of the gates within the blocking region were inactive [46]. Therefore, block occurs due to inactivation of sodium channels [56].

1.4.3 KiloHertz Frequency Alternating Current Block

Kilohertz frequency alternating current block (kHFACb) has been shown to produce reversible and fast block in peripheral nerves [57]. The charged balanced waveform of kHFACb is a desirable feature of this conduction block technique [58]. The zero net charge delivery significantly reduces the possibility of nerve damage due to the formation of reactive species at the electrode/electrolyte interface. However, a transient of neural activity occurs when kHFACb is turned on, referred to as the onset response. This onset response is a limitation of this technique and can result in painful sensation as well as unwanted muscle contractions [59]. Therefore, efforts have been made to mitigate this onset response which include: adjusting kHFACb parameters such as frequency ramping and amplitude ramping [53, 60, 61], charge imbalance, electrode design [62, 63], and kHFACb used in conjunction with additional blocking techniques [64–66]. Frequencies throughout the literature range from 1kHz-100kHz [67, 68], however, the optimum frequency range is generally between 10-40kHz [59, 69]. Amplitudes of block thresholds vary from 1-10 mA [70]. Additional investigations have identified a linearly increasing relationship between frequency and thresholds of block in the range of 10-30 kHz [57, 71]. KHFACb has been applied and shown to reversibly block electrical nerve conduction across species, class (insecta, amphibia, mammalia), and different nerve diameters. These different models include sea slugs [72], rats [73], frogs [74], cats [75], swine [76], goats [77], and non-human primates [70]. The mechanism of action is still under investigation however, several modeling studies suggest that block occurs due to sodium channel inactivation [67, 69, 73, 78, 79].

Table 1.2 summarizes the blocking techniques reviewed.

Table 1.2. Nerve Block Methods [66]

Blocking Technique	Reversible/Temporary	Permanent
Physical	Compression	Rhizotomy
		Neurectomy
Chemical	Local Anaesthetics	Phenol
	Botulinum Toxin	Alcohol
Temperature	Heat	
	Cold	
	Infrared Energy	
Electrical	Collision	hydrolysis due to direct current (anodal, or cathodal)
	Anodal	
	Cathodal	
	kHFACb	

1.5 Novel Electrical Conduction Block: Low Frequency Alternating Current Block

The data presented in this thesis provides evidence of a novel blocking technique. The *in-vivo* work presented here follows up on *ex-vivo* observations made on mammalian peripheral nerves and earthworm nerve cord. During the course of investigating kHFACb, we discovered that reducing the frequency of the sinusoid to $< 100\ Hz$ achieved phasic blocking of action potentials in *in-vivo* earthworm nerve cords. This discovery prompted us to test the phenomenon in *ex-vivo* canine and porcine vagus nerves and found that the blocking phenomenon was conserved across species. During this discovery, it was known that DC block resulted in hydrolysis and kHFACb caused an onset response. The novel low frequency alternating current (LFAC) waveform fills the gap between DC ($0\ Hz$) and kHFACb ($> 1\ kHz$) while mitigating the negative effects of both.

The LFAC blocking waveform at $1\ Hz$ is a more attractive option to the other electrical blocking methods mentioned above because it has the low threshold characteristics of cathodal block, a charge balanced waveform, and no associated onset response.

1.5.1 Thesis Objectives

The aim of this follow up investigation was to parameterize the voltage and current requirements to obtain block against a relevant functional change in organ function and to ensure safe levels of stimulation are being delivered (i.e. within the water window), identify the 'best' method for delivery, and explore the effect that the LFAC waveform imposes on neural signals *in-vivo*. Findings will verify current models and guide the development of *in-silico* models.

Aim 1: Explore the effect of the LFAC waveform on a bradycardia induced state due to vagal stimulation.

Aim 2: Compare the effect of electrode type on blocking a relevant biomarker.

Aim 3: Scalability of the LFAC waveform to different nerve diameters.

Aim 4: Explore the effect of LFAC on compound action potentials.

CHAPTER 2. A REVERSIBLE LOW FREQUENCY ALTERNATING CURRENT NERVE CONDUCTION BLOCK IN MAMMALIAN AUTONOMIC NERVES

A portion of this chapter will be submitted to Nature. A portion of this work was submitted to the 9th International IEEE EMBS Conference on Neural Engineering in San Francisco, California and to Rehab Week 2019, IFESS in Toronto, Canada.

2.1 Abstract

This paper describes a novel method to reversibly block nerve conduction using a low frequency alternating current (LFAC) blocking waveform at 1 Hz applied through a bipolar extrafascicular (hook or cuff) electrode. The waveform used is a sinusoidal current waveform applied to bipolar electrodes, whose magnitude is parameterized by the current amplitude to peak and sine frequency. This work follows up on observations made on excised mammalian peripheral nerves and earthworm nerve cord. An *in-situ* electrophysiology setup was used to assess the LFAC waveform on propagating action potentials (APs) within the cervical vagus nerve in anesthetized Sprague-Dawley rats (n = 12). Two sets of bipolar cuff or hook electrodes were applied unilaterally to the cervical vagus nerve, which was crushed rostral to the electrodes to exclude reflex effects on the animal. Pulse stimulation was applied to the rostral electrode, while the LFAC conditioning waveform was applied to the caudal electrode. The efferent volley, if unblocked, elicits acute bradycardia and hypotension.The degree of block of the vagal stimulation induced bradycardia was used as a biomarker. Block was assessed by the ability to reduce the bradycardic drive by monitoring the heart rate (HR) and blood pressure (BP) during LFAC alone, LFAC with vagal stimulation, and vagal stimulation alone. LFAC applied via a hook electrode achieved 86.6 $\pm$ 11 % block (n = 7) at current levels 95 $\pm$ 38 μAp. When applied via a cuff electrode 85.3 $\pm$ 4.60 % block (n = 5) was achieved using current levels of 110 $\pm$ 65 μAp. ANOVA and tukey post hoc results showed no statistical significant difference whether LFAC was derived via the hook and cuff electrode. In the test case, block was achieved as soon as the LFAC waveform was applied with no onset activation.

Block was almost immediately reversed, with bradycardia induced, when LFAC was removed. LFAC waveform without vagal pulse stimulation resulted in no change to the HR or BP. Block was not possible when the vagal pulse stimulation was applied to the caudal electrode and LFAC to the rostral electrode, indicating that collision block is not the mechanism of action of the LFAC waveform. These results suggest that LFAC when applied to small nerve bundles can achieve a high degree of nerve block, resulting in the change in behavior of a biomarker, *in-vivo* in the mammalian nervous system at low amplitudes of electrical stimulation that are within the water window of the electrode. Since the waveform is balanced, all forward reactions are reversed, leading to a blocking method that is similar in nature to DC block without the potential issues of toxic byproduct production.

2.2 Introduction

The peripheral nervous system (PNS) is a medium that the body uses to communicate, control, and relay information within itself. Electrical signals are conveyed to and from the brain and spinal cord to muscles, major organs, and sensors embedded throughout the body using the pathways of the PNS. They are used not only to convey sensations and control muscles, but also used to control and regulate how major organs such as the kidneys, pancreas, liver, and heart function. In the case of chronic disease, the pathology alters the set point of the control system, resulting in illness and abnormal function of these organs. Electrical stimulation of the PNS has long held hope as a means to modulate the information within the nervous system to help restore function to dysfunctional or poorly functioning organs.

Electrical stimulation influences neural signals through two modes. Activation is the mode through which electrical pulses introduce activity to the nerve. Activation of nerve fibers using electrical discharges has been known since antiquity and understood for at least a century [9]. Methods to block propagating action potentials using electrical stimulation are a more recent discovery and a current topic of investigation. Many of the current methods being used or investigated for blocking can be effective, however, they have associated drawbacks that limit their application clinically.

Methods such as direct current (DC) block [45, 46, 80], kilohertz frequency alternating current block (kHFACb) [57, 59, 81, 82], anodal block [83, 84], collision block [41, 43], and quasi-trapezoidal stimulation [54]. In the case of DC block, Faradaic reactions occur at the tissue-electrode interface due to charge imbalance. This results in the production of toxic electrochemical byproducts, due to hydrolysis, which damage the nerve. This yields DC block unsafe for long term use. Alternatively, kHFACb is a charged balanced waveform that results in the delivery of zero net charge. This is desirable as it greatly reduces the possibility of nerve damage from the formation of reactive species. However, it is often associated with an onset response. The onset response is characterized by transient nerve firing that can last for several seconds. This can result in a painful sensation along with involuntary muscle contractions. Efforts have been made to mitigate the effects from DC block and kHFACb by generating a blocking waveform that is the combination of the two [53, 64–66].

While investigating kHFACb in *in-vivo* earthworm nerves, we discovered that phasic blocking of action potentials could be achieved by reducing the frequency of the sinusoid to less than 100 Hz. LFAC is a simple sinusoidal waveform applied to a bipolar electrode and is defined by the magnitude of the sinusoid and its frequency. The waveform was tested on *ex-vivo* canine and porcine vagus nerves and was found that the blocking phenomenon was conserved across species (canus - sus) and class (insecta – mammalia) [1, 85]. With further investigation, block was achieved at half of the current levels that was required for kHFACb and was achieved within the water window of the electrodes. Unlike kHFACb, LFAC showed no indication of onset activation [85]. The low thresholds of LFAC are comparable to those of DC block, but unlike DC block since it is a sinusoidal charge balanced waveform, there is no accumulation of unbalanced charge.

The present work aims to build upon the prior work in the earthworm or excised mammalian nerves to determine whether LFAC can achieve a physiologically relevant level of nerve block *in-vivo* on a mammalian peripheral nerve.

2.3 Methods

2.3.1 Animal and Surgical Prep

All animal use protocols were approved by the Purdue School of Science Institutional Animal Care and Use Committee (SoS IACUC) at Indiana University Purdue – University Indianapolis (IUPUI). The electrophysiological preparation mirrored that of Cruz et al [86]. A total of 12 adult ($> 200\ g$) Sprague-Dawley rats of mixed gender were included in this study. The rats were anesthetized to the surgical plane following induction using Isoflurane (Vedco Inc. St. Joseph, MO) followed by an intraperitoneal (IP) injection ($0.8\ mL/100\ g$) of a combination of urethane ($800\ mg/kg$; Sigma-Aldrich Co., MO) and alpha-chloralose ($80\ mg/kg$; Acros Organics, NJ). Once anesthetized, body temperature was maintained using a heating pad (HTP-1500 and ST-017 Soft-Temp Pad, Adroit Medical Systems, TN). Supplemental IP injections of urethane / alpha-chloralose were administered as needed to maintain sufficient depth of anaesthesia at the surgical plane. The left femoral artery was exposed and catheterized using a short length (10 mm) of PE-100 tubing filled with heparinized saline ($30\ U/mL$). A midline incision on the ventral side of the neck was used to obtain access to and visualization of the left carotid artery and left cervical vagus. Finally, a tracheotomy tube was inserted through an incision in the trachea to facilitate mechanical ventilation in event that the animal stopped breathing. The bio-marker of interest, ECG, was monitored continuously in each experiment with the placement of needle electrodes on the chest. The ECG signal was band-pass filtered (4th order Bandpass Bessel Filter; 2nd order Highpass: $0.1\ Hz$; 2nd order Lowpass: $300\ Hz$) and amplified (1000 x gain) via a differential amplifier (DP-311, Warner Instruments, Hamden, CT). Additionally, blood pressure was encoded into a voltage equivalent by a calibrated pressure transducer (#159905, Radnoti LLC, Covina, CA).

2.3.2 Electrode Configuration

Two bipolar extrafascicular electrodes were placed on the exposed left cervical vagus shown in *Figure 2.1*. A platinum-iridium (Pt-Ir) bipolar hook electrode with 800 μm anode/cathode spacing (PBAA0875, FHC, Bowdoin, ME) was used for vagal stimulation. The LFAC waveform was delivered via a platinized Pt-Ir hook electrode for 7 of the experiments. In the remaining 5 experiments, the LFAC waveform was presented through a 0.5 mm i.d. bipolar cuff (1041.5008.01, CorTec GmbH, Neuer Messplatz 3, 79108 Freiburg Germany). As shown in the figure below, the rostral hook electrode (RE) was used for vagal stimulation. Meanwhile the caudal electrode (CE), hook or cuff, was used to deliver the conditioning waveform. The left cervical vagus was crushed and ligated rostral to the stimulating hook electrode to eliminate the visceral afferents as the origin of bradycardia. The right vagus nerve was remained intact to maintain autonomic reflexes for stability.

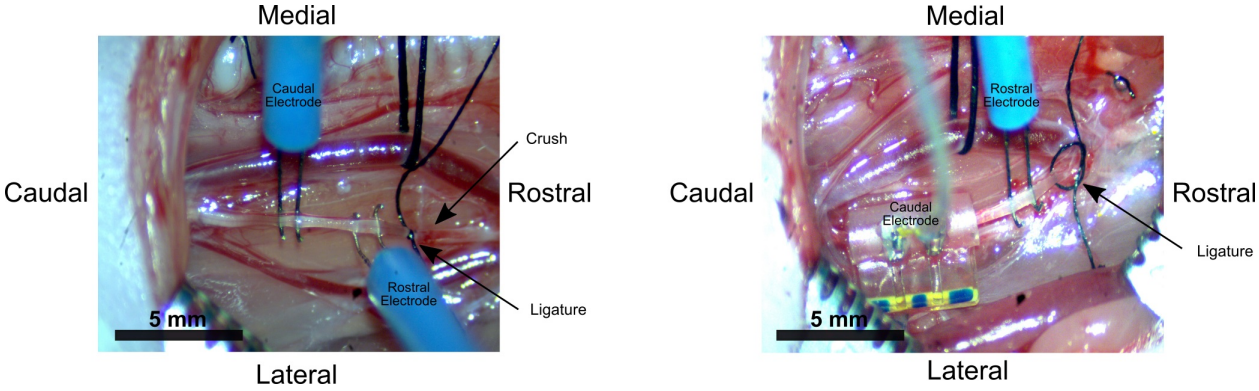

Figure 2.1. Electrode placement for hook (left panel) and cuff (right panel) on the left cervical vagus. The ligature was placed rostral to both electrodes to eliminate cranial reflexes. Additionally, the vagus nerve was crushed with forceps, as shown in the left panel, to further ensure that reflexes were excluded. The right vagus nerve was left intact and not crushed for stability

2.3.3 Nerve Stimulation and Experimental Paradigm

A standard rectangular pulse train of 10 pulses (0.1, 1.0, 2.0 ms pulse width) at 25 Hz repeated at 1 Hz were applied to the vagus nerve using a opto-isolated stimulator (DS3, Digitimer Ltd, Hertfordshire UK) triggered by a pulse generator (33120A, Hewlett Packard, Engelwood, CO) at an adequate level to evoke bradycardia. The stimuli was titrated to cause a visible change in ECG and BP, however would not result in the animal to crash. Without block, the stimulus results in a heart rate drop from ~ 5 Hz to ~ 1 Hz. The drop in heart rate results in an acute drop in mean blood pressure from $\sim 90-110$ $mmHg$ to less than $\sim 50 mmHg$. When the blood pressure dropped below ~ 50 $mmHg$, vagal stimulation was discontinued to enable the blood pressure to return to its normal set point. The LFAC waveform was generated using a dual channel waveform generator (DG5072, Rigol Tech, Beaverton, OR) coupled to an isolated voltage controlled current source (CS580, Stanford Research Systems, Sunnyvale, CA). Adequate block amplitude was determined using a 1 Hz sinusoidal waveform. The amplitude was increased until distortion of the waveform was observed. This indicated that the water window had been reached. The amplitude was then decreased slightly to remain within the water window of the electrode which resulted in block of the effect of the vagal stimulation. Nominally, the block current was ~ 100 μA_p (current to peak) corresponding to a voltage drop across the electrode of between $1-2$ V_p (voltage to peak), which was well within the water window.

To test the effect of LFAC, the vagal stimulus train and the LFAC waveform were presented in a regular continuous sequence as follows: 1 – Pre Phase) 20s baseline period of no stimulation, 2 – LFAC Only Phase) 20s LFAC delivered to the CE, 3 – LFAC+VStim Phase) 20s LFAC delivered to the CE and vagal stimulation at the RE, 4 – Vstim Only) Vagal stimulation at RE until BP falls below $\sim$ 50 $mmHg$. 5 – Post Phase) No stimulation return to baseline.

This test sequence was repeated followed by a control case where the vagal stimulus was applied to the CE and LFAC to the RE. The ECG and BP along with the LFAC waveform and voltage drop across the LFAC electrode were continuously recorded and sampled at 10 kHz (USB-6212, National Instruments, Austin, TX) using Mr. Kick III (Aalborg University, Denmark).

A potential explanation for the apparent block is if there is an interaction between the LFAC waveform or electrode and the vagal stimulation pulse train or electrode. As a control, the vagal stimulation and LFAC sites were reversed such that VStim was presented on the caudal electrode and LFAC was presented on the rostral electrode.

2.3.4 Data Analysis

The analysis of the acquired data sets was performed using custom software written for Matlab (2016a, The Mathworks, Natick, MA). The continuously acquired ECG and BP were segmented into 5 epochs corresponding to the conditioning sequence and identified as follows: Pre, LFAC Only, LFAC+VStim, VStim Only, Post. Based on the R to R interval of the QRS complex, an R-R rate and median R-R rate was calculated for each epoch. The normalized heart rate (HR) during each experimental epoch was calculated using the following equation as a percentage:

$$Normalized\ HR(\%) = 1 - \frac{[cond] - median(RRrate_{pre})}{median(RRrate_{pre}) - median(RRrate_{vstimonly)}} * 100 \qquad (2.1)$$

Where the difference between the median in R-R rate_{pre} and R-R $\text{rate}_{\text{VStimOnly}}$ represents the maximum depression in HR, while the change in R-R rate, and [cond] represents the change for each of the five conditions. This equation normalized the HR in the 'Pre' and 'Stim Only' epochs. 'Pre' was normalized to 100. Meanwhile, 'Stim Only' was normalized to 0. The normalized HR directly correlates 1:1 to the percent block in the 'LFAC+VStim' and 'VStim Only' epochs in both the test and control cases.

The test case repetitions were combined for each electrode and two separate one-way ANOVAs were performed in R Studio (1.2.5042, R Foundation for Statistical Computing, Vienna, Austria) for each electrode type (cuff or hook) to determine if there was a significant difference between each of the 5 epochs of the test sequence. A 2-way ANOVA was performed to determine the effect of electrode type and treatment (Pre, LFAC Only, LFAC + Vstim, Vstim Only, Post) on normalized HR.

Lastly, the test and control case repetitions were each combined into a respective data set and a second 2-way ANOVA was performed to determine the effect of experimental case (test or control) and treatment on normalized HR. Tukey post hoc tests were used to determine where, if any, the significant differences were located.

2.4 Results

The trains of vagal stimulation induced an episodic reduction in heart rate which presented as an increase in the RR interval with dropped heart beats, *Figure 2.2*. As a result of the dropped heart beats, the BP also dropped. However, the response time of the BP due to vagal stimulation was relatively slower than the response time of heart rate. Additionally, BP can drift due to occlusion of femoral catheter, vasoconstriction, or vasodilation. Therefore, the HR provided a more reliable biomarker and measure of block. The change in RR rate is most clearly seen by examining the minima during vagal stimulation alone. Therefore, the RR rates were calculated and the local minima in rate associated with dropped heart beats were used to quantify the effect of the vagal stimulation without block.

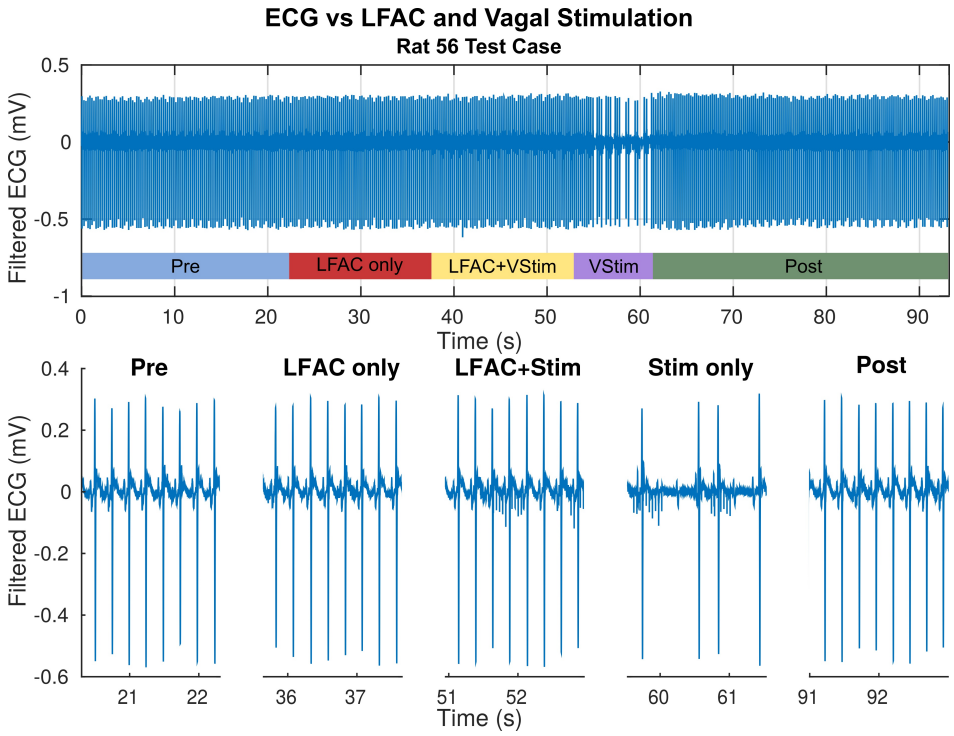

Figure 2.2. The effect on heart rate during a test sequence consisting of 1) Pre (no stim), 2) LFAC only, 3) LFAC and Vagal Stimulation delivered together, 4) Vagal Stimulation only, and 5) Post (Recovery, no stim or LFAC). The top panel shows a continuous recording of the bandpass filtered ECG during the 5 epochs. The bottom panels show 2 second samples of the ECG for each epoch

Figure 2.3 is a representative example of the change in ECG and epoch as a function of epoch of the stimulation paradigm. It shows that LFAC alone does not alter the ECG rhythm or waveform indicating that the LFAC waveform did not activate the vagus nerve. Thus, it does not have an associated onset response. When LFAC is used in conjunction with vagal stimulation, the ECG rhythm shows little to no change suggesting that LFAC is blocking the effect of vagal stimulation. Once LFAC is removed, there is a rapid disruption in the heart rhythm. When vagal stimulation is removed, the heart rhythm returns to its initial state after a slight overshoot due to sympathetic rebound. The BP follows the same trend as the RR rate with little or no change except during the case where vagal stimulation is presented alone. Repetitions were spaced out so that the animal had a similar 'Pre' epoch. Vagal stimulation alone or without block results in the complete stoppage of the heart if not discontinued.

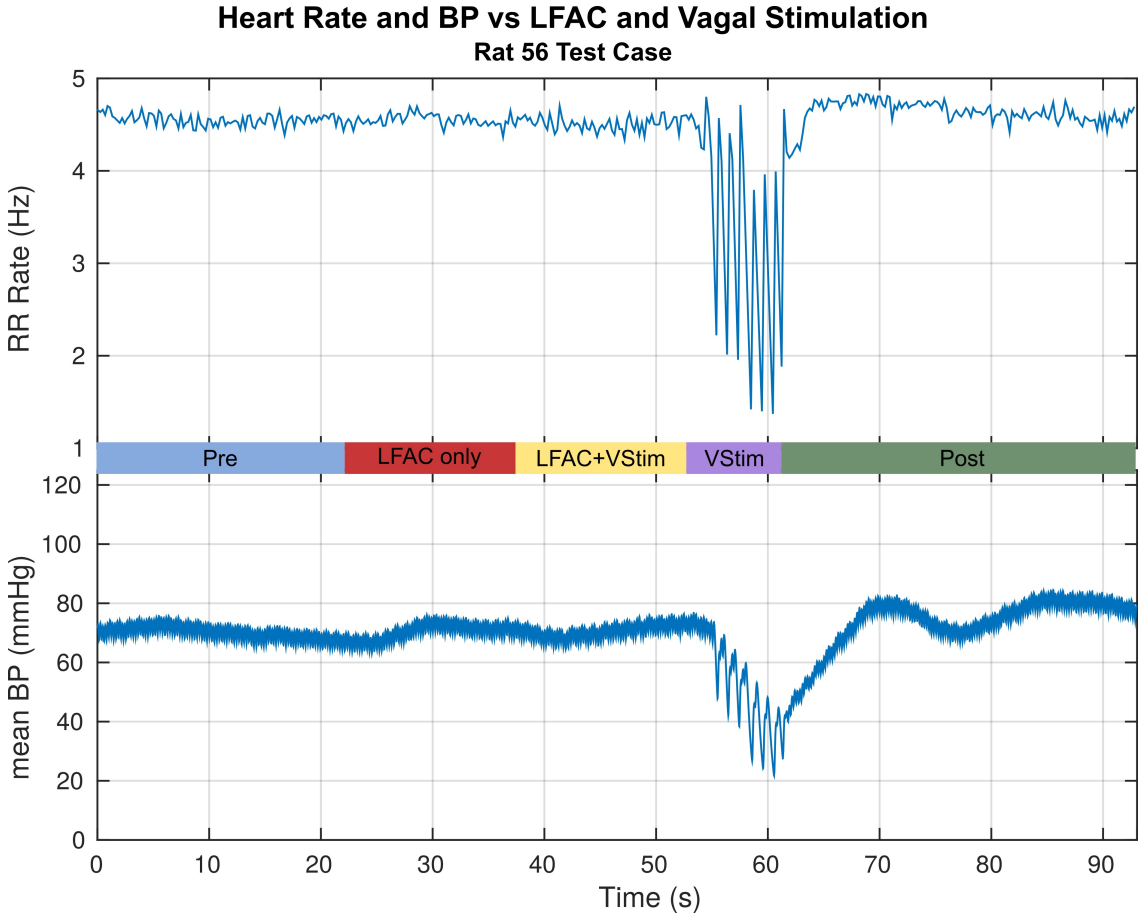

Figure 2.3. Effects of the typical test sequence on the RR rate of the QRS complex and mean arterial BP. The RR rate for this example is for the data presented in *Figure 2.2*. The HR and the BP show no change during LFAC and LFAC+Vagal Stimulation. This suggests that LFAC by itself does not activate fibers, and blocks the descending volley that elicits bradycardia and its accompaniment, hypotension

Taking the local minima of the RR rate and using the prevention of disruption to the heart rhythm as a biomarker, the percent block was estimated (*Figure 2.4*).

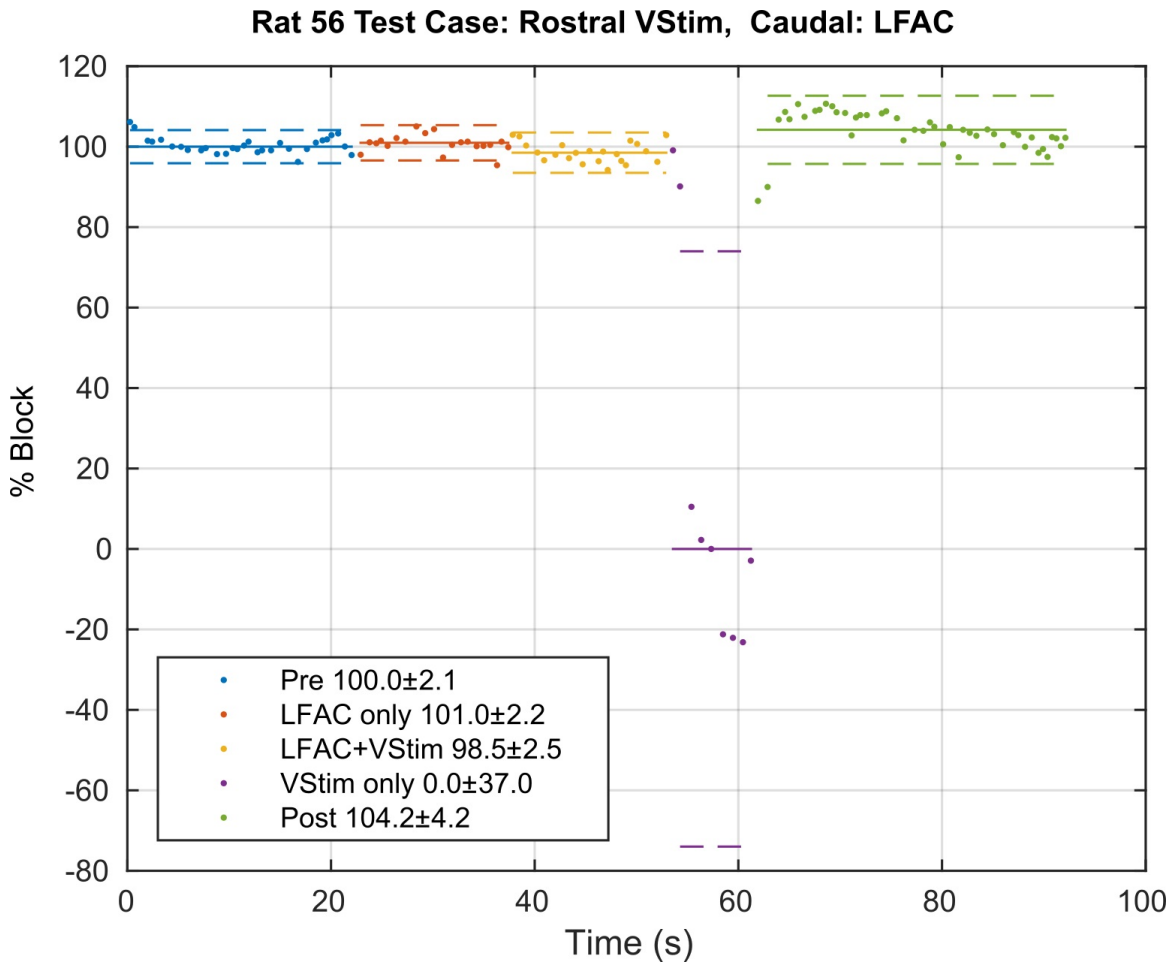

Figure 2.4. Example of RR rate derived percent block as a function of epoch for the test case where vagal stimulation is presented rostral to the LFAC waveform along the nerve. In this example, 98.5 $\pm$ 2.5 % block was achieved. A negative percent block indicates that the data point was below the normalized percent block in the 'VStim Only' epoch. The solid straight lines indicate medians and the dashed straight lines indicate one standard deviation

The absence of RR rate depression during LFAC+VStim suggests that LFAC blocked the effects of vagal stimulation projecting to the heart. In this particular example (*Figure 2.4*), LFAC achieved a 98.5 $\pm$ 2.5 % block of the effects of vagal stimulation. In the example shown in *Figure 2.5*, the 'LFAC+VStim' epoch achieved 100.8 $\pm$ 3.3 % block.

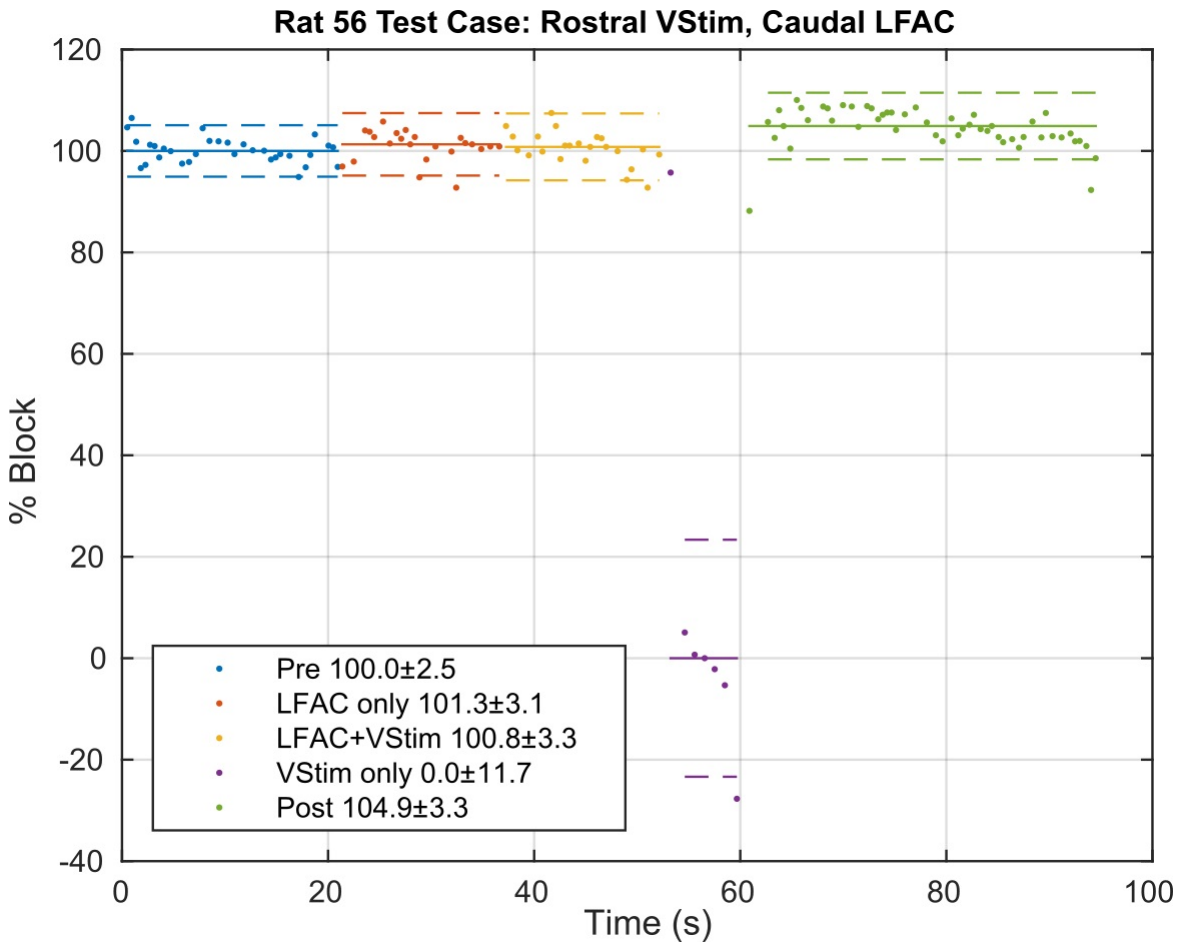

Figure 2.5. Example of RR rate derived percent block as a function of epoch for the test case where vagal stimulation is presented rostral to the LFAC waveform along the nerve. In this example, 100% block was achieved in the 'LFAC+VStim' epoch. A negative percent block, as in the 'VStim only' epoch, indicates that the data point was below the normalized median percent block in the 'VStim Only' epoch. The solid straight lines indicate medians and the dashed straight lines indicate one standard deviation

If an interaction between electrodes or waveforms is the reason for the observed block, reversing the electrodes should also result in a block in the 'LFAC+VStim' epoch. If this is not the mechanism, then the 'LFAC+VStim' epoch should result in a depression of the heart rate. A typical result of the control case is shown in *Figure 2.6*. Swapping the electrodes in the control case results in 2.9% block, indicating that the effects of vagal stimulation are not blocked and discounting the possibility that LFAC block is due to an electrode or waveform interaction between LFAC and vagal stimulation.

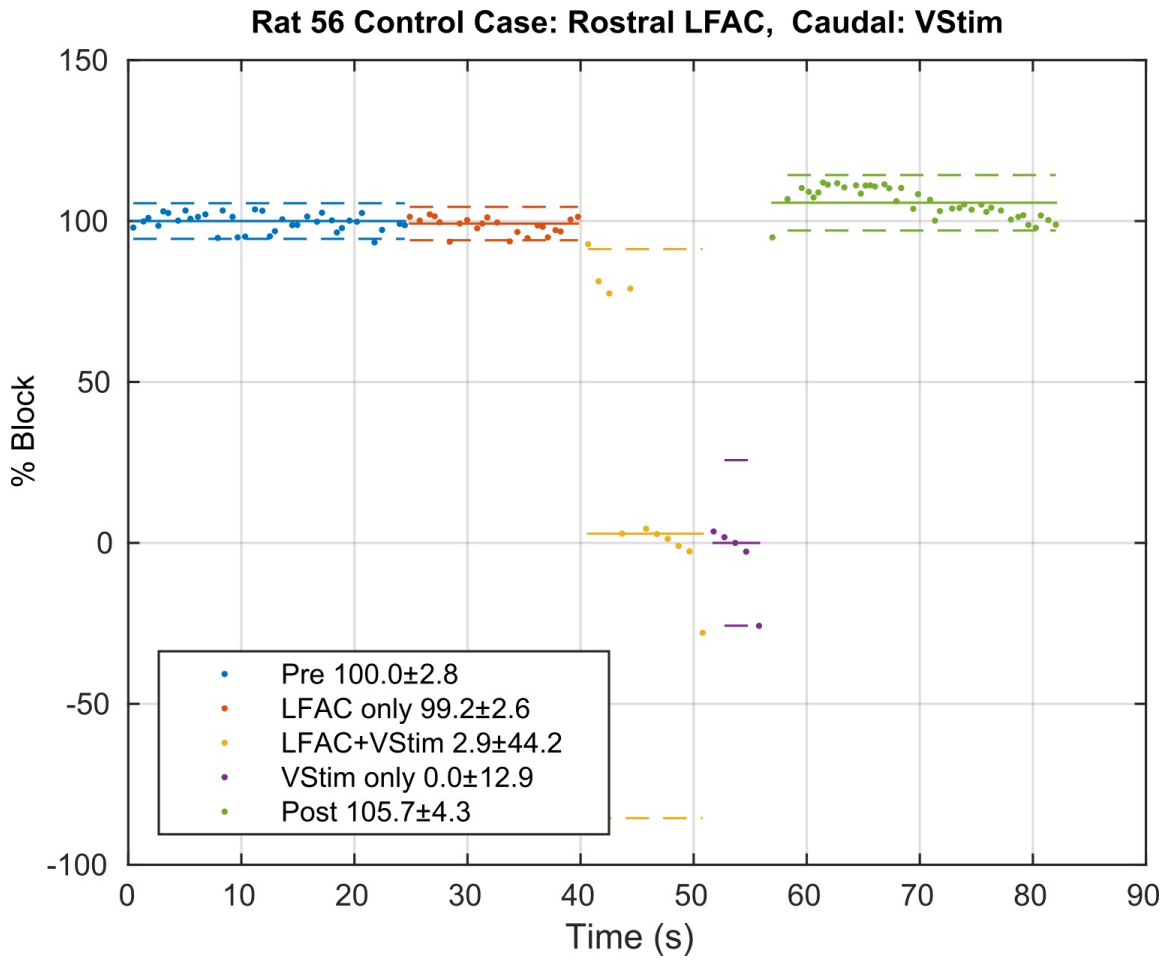

Figure 2.6. Example of the RR rate derived percent block as a function of epoch for the control case where LFAC is presented on the rostral electrode and vagal stimulation on the caudal electrode. Note that the 'LFAC+VStim' epoch does not show block, suggesting that the mechanism of action is not due to electrode or waveform interactions. The solid lines indicate medians and the dashed straight lines indicate one standard deviations

2.4.1 Hook Electrode

Table 2.1 summarizes the experimental parameters used and the percent block that was achieved when using a Pt-Ir bipolar hook electrode to deliver the LFAC waveform. As mentioned, the experimental paradigm was repeated for each animal. The average percent block among all experimental cases was found to be 86.6 ± 11.3 %. In one case, the instrumentation had connection issues which prevented currents $> 2.5\ \mu A$ from being presented to the electrode. Despite the limitation, ~ 60 % block was achieved. In the control case an average percent block of 7.3 ± 26.3 % was achieved during the 'LFAC+VStim' epoch. The negative percentage indicates that the R-R rate during 'LFAC+VStim' was below the normalized 'VStim only' epoch.

Table 2.1. Vagal stimulation and LFAC waveform parameters used in the set of 7 rats in this study. The conditioning waveform was applied via a hook electrode in this set. The average percent block amongst n = 7 experiments was found to be 86.2 ± 11.1 %. *Instrumentation connection issues did not allow currents $> 2.5\ \mu A$. Nonetheless, ~ 60 % block was achieved

Hook LFAC Block Experiments- Test Cases							
Rat ID	LFAC Electrode	Vagal Stimulation			LFAC waveform		% Block
		PW (μs)	PA (μA)	Charge (Q)	Current (μAp)	Freq (Hz)	
Rat 46	Hook	100	270	0.03	160	1	83.0
Rat 50	Hook	1000	63	0.06	2.5*	1	60.3*
Rat 55	Hook	1000	29	0.03	100	1	83.1
Rat 56	Hook	1000	20.75	0.02	75	1	100.0
Rat 57	Hook	1000	19.5	0.02	75	1	68.1
Rat 58	Hook	1000	290	0.29	82.5	1	95.1
Rat 59	Hook	2000	180	0.36	50	1	87.7
N	**Mean**		**124.6**	**0.1**	**90.4**		**86.2**
7	**SD**		**120.0**	**0.1**	**37.7**		**11.1**

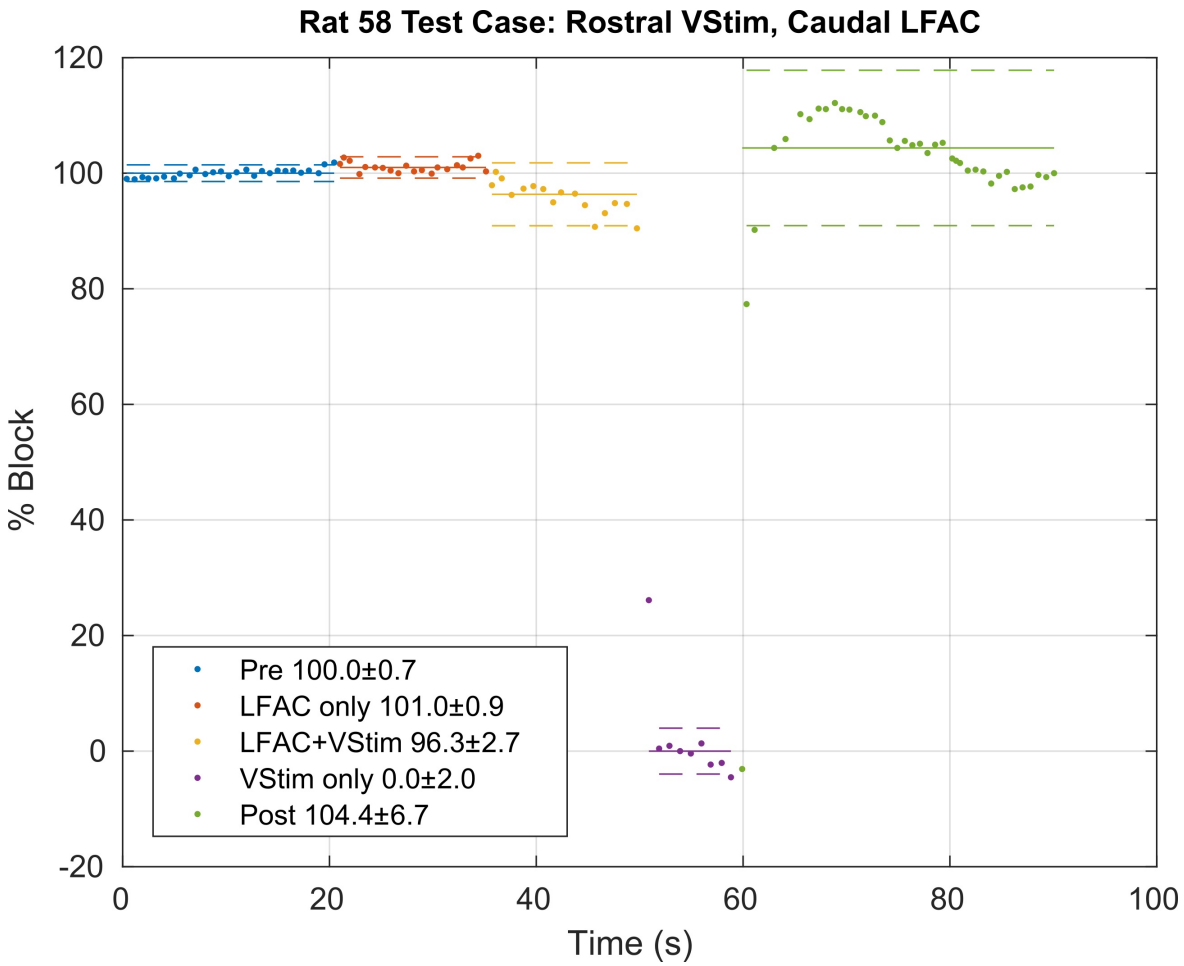

Figure 2.7. Example of a test case with LFAC delivered via a hook

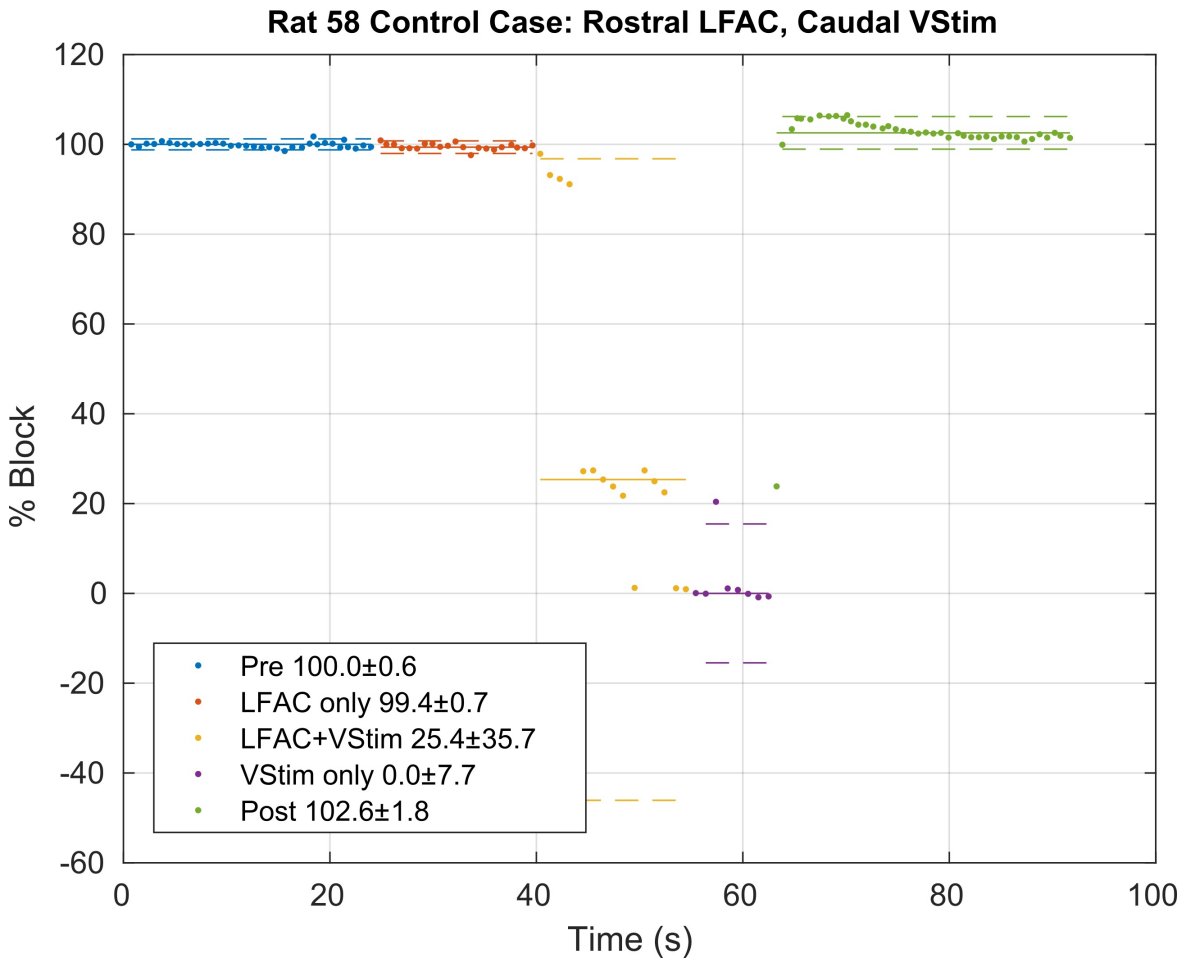

Figure 2.8. Example of a control case with LFAC delivered via a hook

2.4.2 CorTec Cuff Electrode

Table 2.2 summarizes the experimental parameters used and the percent block that was achieved when using a bipolar cuff electrode to deliver the LFAC waveform. The experimental paradigm was repeated for each animal, therefore the average percent block was calculated to be 85.3 $\pm$ 4.6 %. Alternatively, the control case yielded an average percent block of 3.6 $\pm$ 12.6 % during the 'LFAC+VStim' epoch of the test sequence.

Table 2.2. Vagal stimulation and LFAC waveform parameters when LFAC was delivered via a bipolar cuff electrode. An average of 85.3 ± 4.6 % block was achieved in the 'LFAC+VStim' epoch of the test sequence

Cuff LFAC Block Experiments-Test Cases							
Rat ID	LFAC Electrode	Vagal Stimulation			LFAC waveform		% Block
		PW (μs)	PA (μA)	Charge (Q)	Current (μAp)	Freq (Hz)	
Rat 66	Cuff	2000	3500	7	55	1	83.0
Rat 79	Cuff	100	78	0.01	65	1	78.8
Rat 84	Cuff	1000	13.7	0.01	120	1	85.6
Rat 86	Cuff	1000	22.4	0.02	195	1	89.8
Rat 91	Cuff	1000	18	0.02	200	1	89.4
N	**Mean**		**903.5**	**1.4**	**108.8**		**84.3**
5	**SD**		**1731.2**	**3.1**	**64.2**		**4.6**

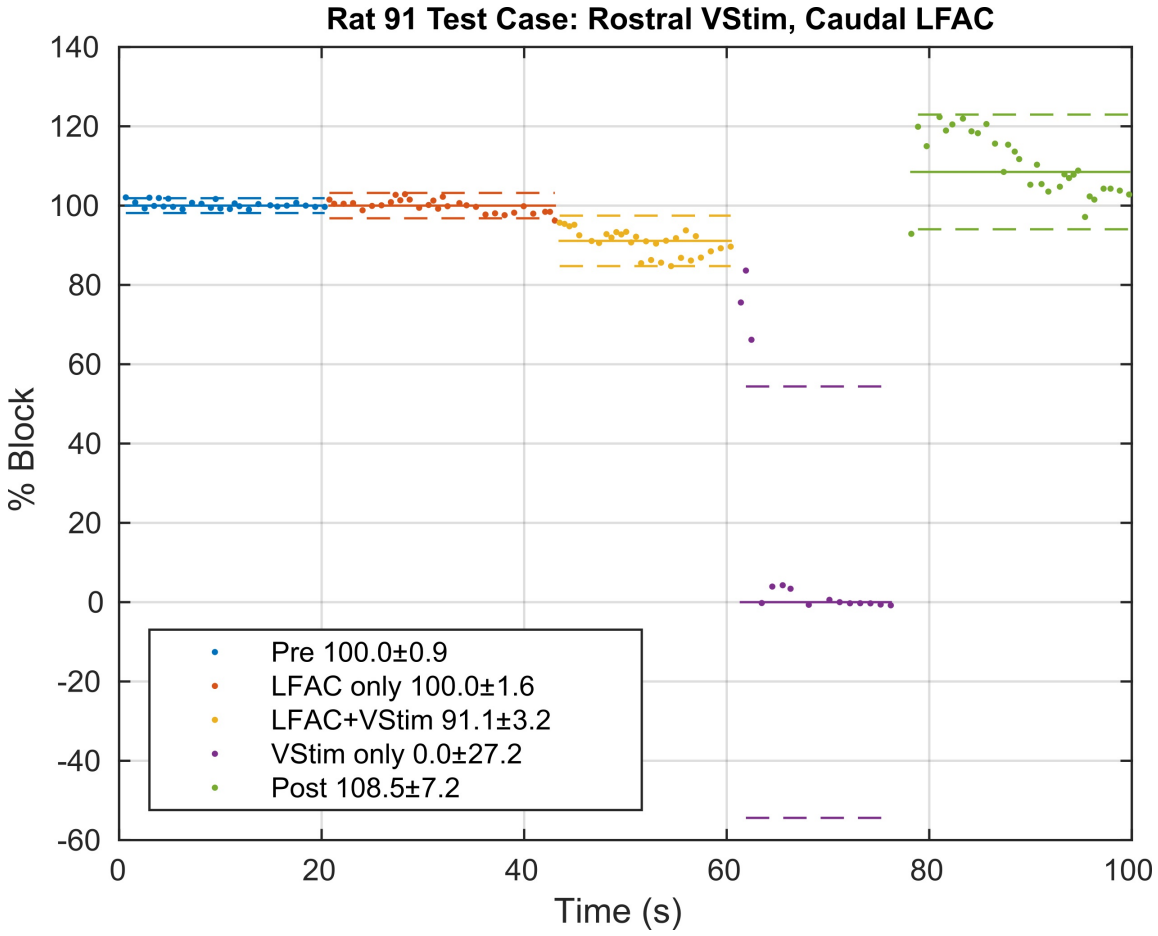

Figure 2.9. Example of a test case with LFAC delivered via a cuff electrode

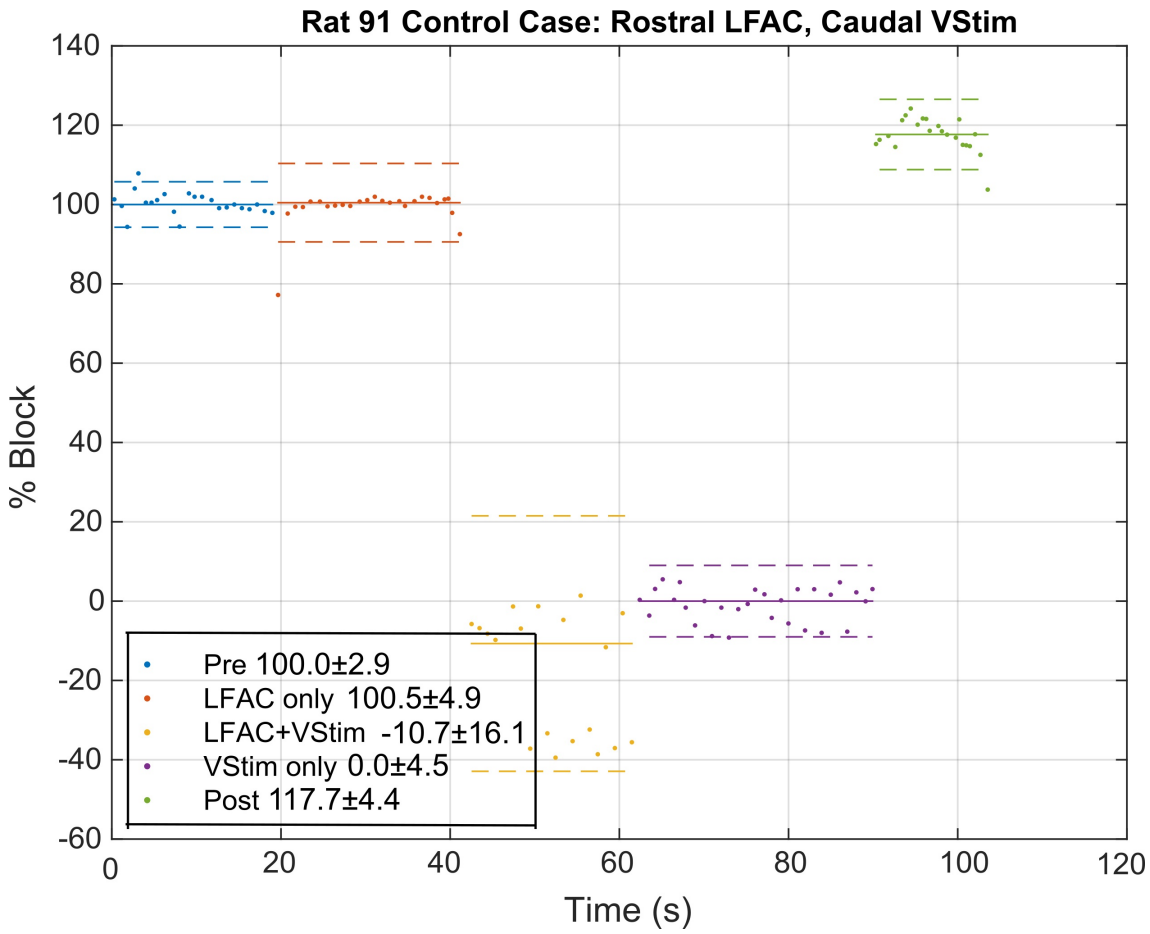

Figure 2.10. Example of a control case with LFAC delivered via a cuff electrode

2.4.3 Statistical Results

One-way ANOVA for the electrodes was performed and showed that there was a statistical difference within the 5 epochs of the test sequence for the hook ($F(4,125) = 755.6$ and $Pr(>F) = 2e^{-}16$) and for the cuff ($F(4,70) = 2271$ and $Pr(>F) = 2e^{-}16$). Tukey post hoc results showed that there was no significant difference between the 'Pre' and 'LFAC only' epochs in both the hook and the cuff ($p-adjusted = 0.99$ and $p-adjusted = 0.77$, respectively). Two-way ANOVA statistical analysis results (*Figure 2.11*) supported the hypothesis that there was no significant difference between cuff and hook. Additionally, Tukey post hoc results indicated that there was no statistical significant difference between 'Pre' and 'LFAC Only' ($p-adjusted = 0.98$). This further demonstrates that there is no onset response associated with LFAC.

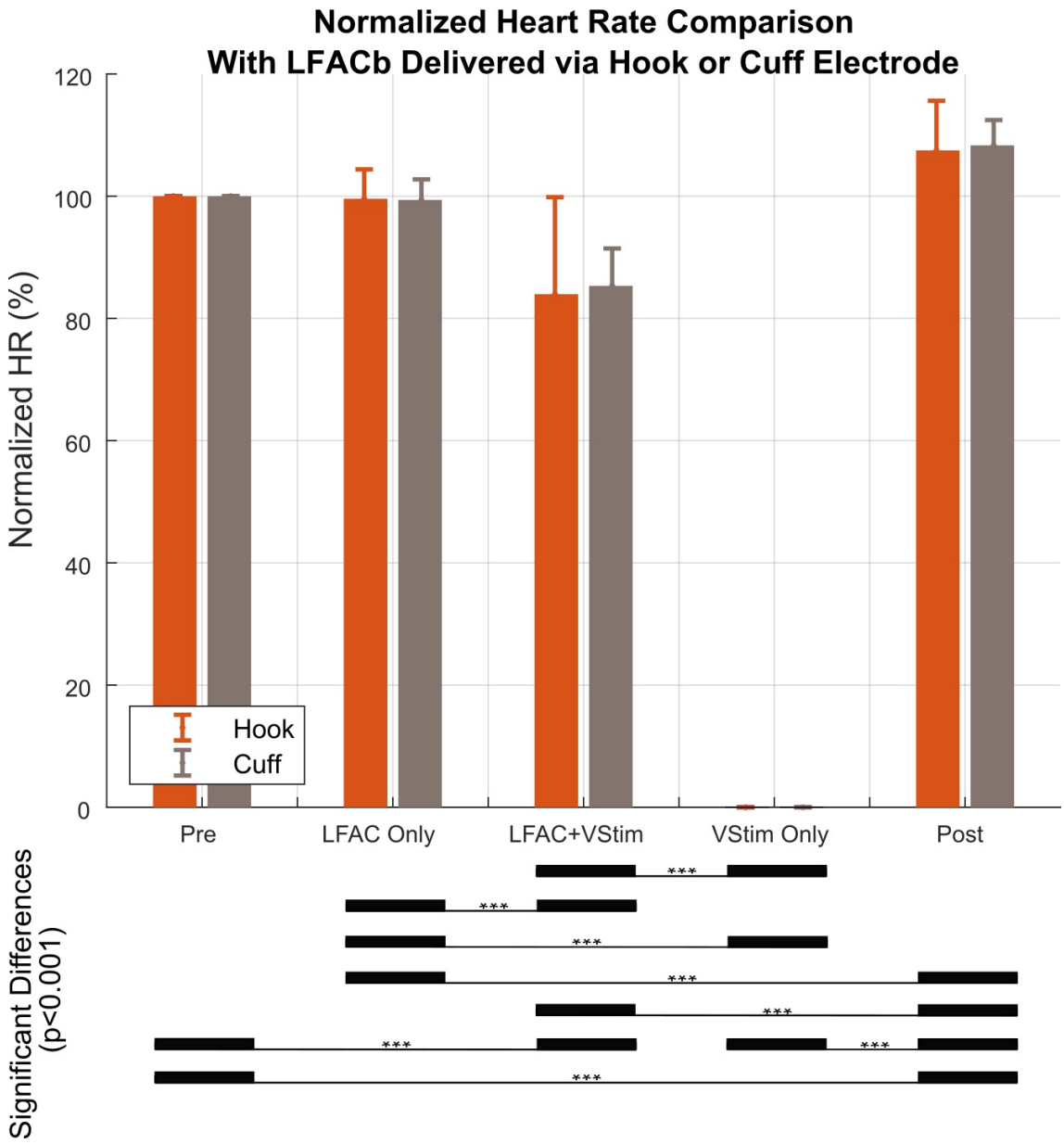

Figure 2.11. Graphical representation displaying the effect of electrode type on normalized HR during each of the 5 epochs of the waveform sequence. For the hook, N = 26 for each segment and N = 15 for the cuff during each segment. ANOVA results revealed that there was no significant difference between the hook and cuff ($F(1,195) = 0.046,\ Pr(>F) = 0.830$). The error bars indicate standard deviations. ***The significant differences ($p = 2e^{-}16$) were only due to treatment type i.e., the 5 five epochs of the waveform sequence

Two-way ANOVA statistical analysis results examining the effect of experimental case (test or control) and treatment, the 5 epochs of the experimental sequence, on normalized HR are shown in *Figure 2.12*. The ANOVA results revealed a significant difference due to experimental case ($F(1,310) = 229.6$ and $Pr(> F) = 2e - 16$), a significant difference due to treatment ($F(4,310) = 1607.5$ and $Pr(> F) = 2e^{-}16$), and a significant difference between experimental case and treatment ($F(4,310) = 229.8$ and $Pr(> F) = 2e^{-}16$). Furthermore, Tukey post hoc results revealed that there were no significant differences between the 'Pre' and 'LFAC Only' epochs between and within the control and test cases. However, there was a significant difference in the 'LFAC+VStim' epoch between the control and test ($p - adjusted = 0$), as expected.

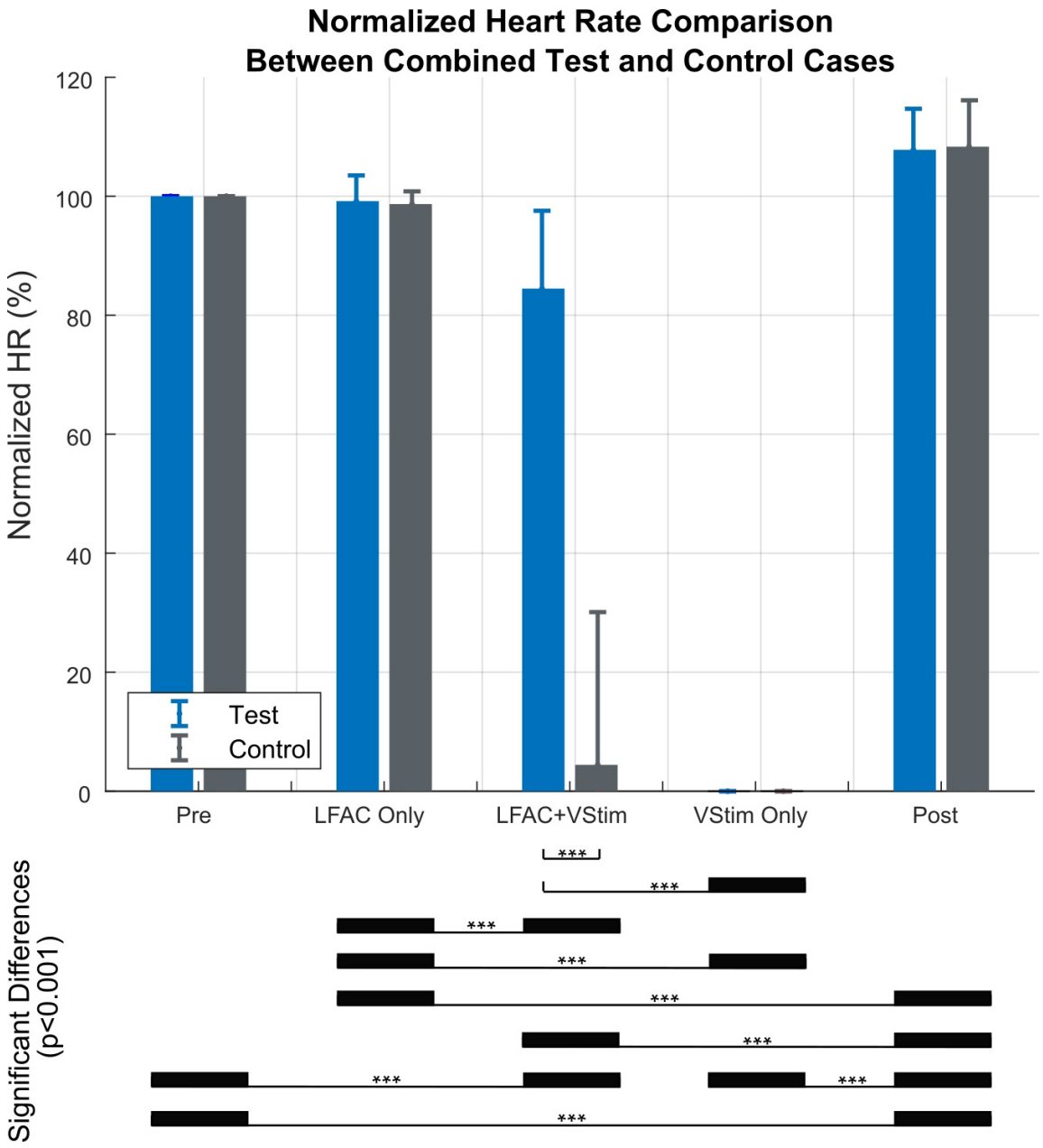

Figure 2.12. Graphical representation displaying the effect of experimental case (test of control) and treatment (Pre, LFAC Only, LFAC+ Vstim, Vstim only, Post) on normalized heart rate. For the test case, N = 41 for each treatment and N = 23 for the control during each treatment. The error bars indicate standard deviations.***The significant differences ($p = 2e^{-}16$) were due to case and treatment type i.e., the 5 five epochs of the waveform sequence

2.5 Preliminary Neural Recordings

The preliminary experiments outlined below explored electroneurograph (ENG) recordings during vagal stimulation to determine which fiber type was eliciting the efferent volley of action potentials responsible for the bradycardic state that was observed. The electrode set up for recording neural activity is shown below in *Figure 2.13*. A set of micro-LIFE needle electrodes were used for ENG recordings. The reference needle electrode was placed on the trachea to minimize noise from muscle activity. Vagal stimulation was delivered via a platinized Pt-Ir bipolar hook electrode. The left cervical vagus was crushed and ligated rostral to the stimulating hook electrode to ensure left cranial reflexes were eliminated. The right vagus nerve was not crushed and was left intact for animal stability.

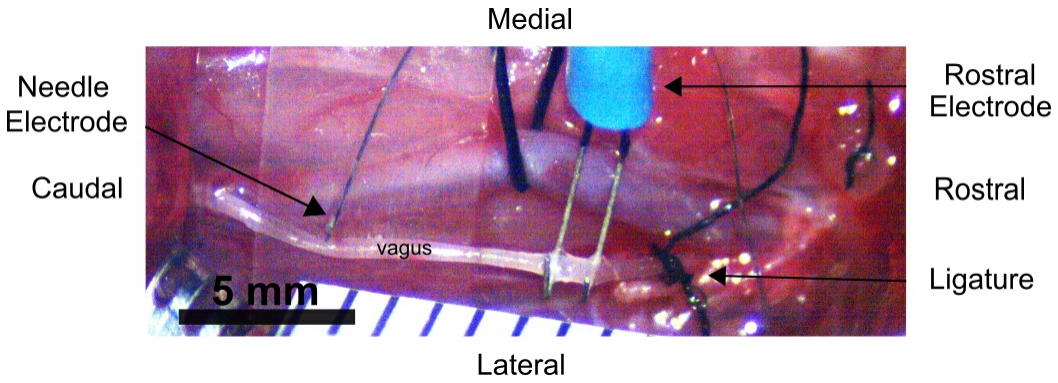

Figure 2.13. Electrode set up for ENG recordings. Left cervical vagus was isolated. A bipolar hook electrode was used for vagal stimulation. A set of micro-LIFE needle electrodes were used for ENG recordings. The working electrode was implanted into the vagus nerve, and the reference electrode was placed on the trachea to enhance the signal to noise ratio

A recruitment curve for the various peaks observed was generated by slowly increasing the amplitude of the stimulus. Post processing analysis and template extraction of the compound neural action potentials (CNAP) responsible for generating the bradycardic state was performed in MATLAB (2016a, The Mathworks, Natick, MA). The stimulus artifact was removed by estimating the step response of the filter characteristics of the amplifier used. This estimate was used to subtract out the stimulus artifact from the ENG recording. The windows of interest were superimposed. The average of the superimposed traces yielded the isolated CNAP template. These analysis steps are outlined in *Figure 2.14*. The CNAPs at the various stimulus thresholds is shown in *Figure 2.15*.

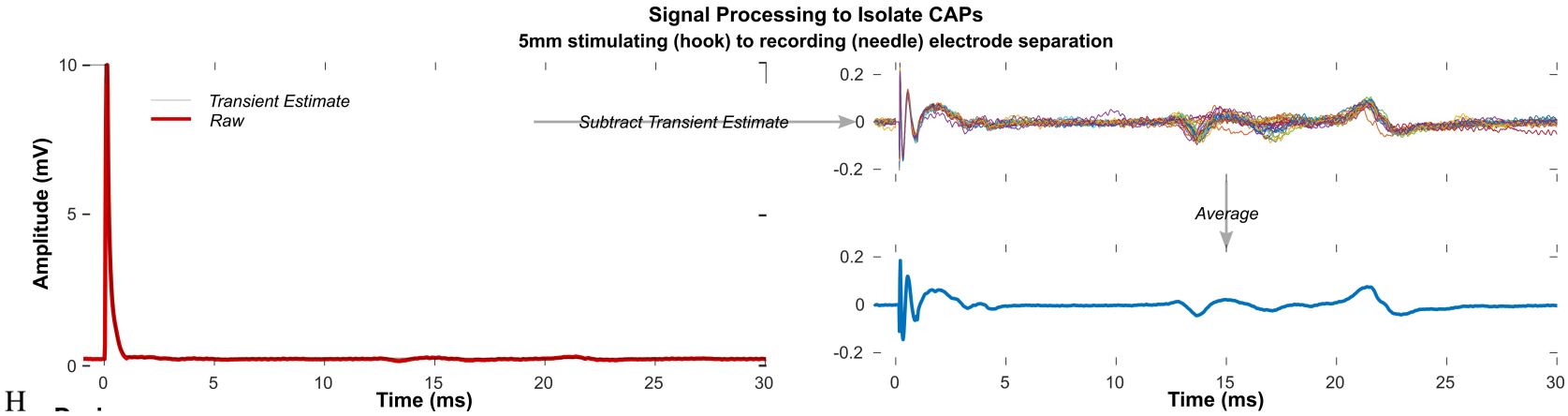

Figure 2.14. Signal processing steps used to reduce the stimulus artifact transient to allow for the visualization of CNAPs. Left panel shows the estimated transient superimposed on the raw signal. Subtraction of the transient and superimposed traces are shown in the top right panel. The bottom right panel displays the CNAP template by averaging the superimposed traces

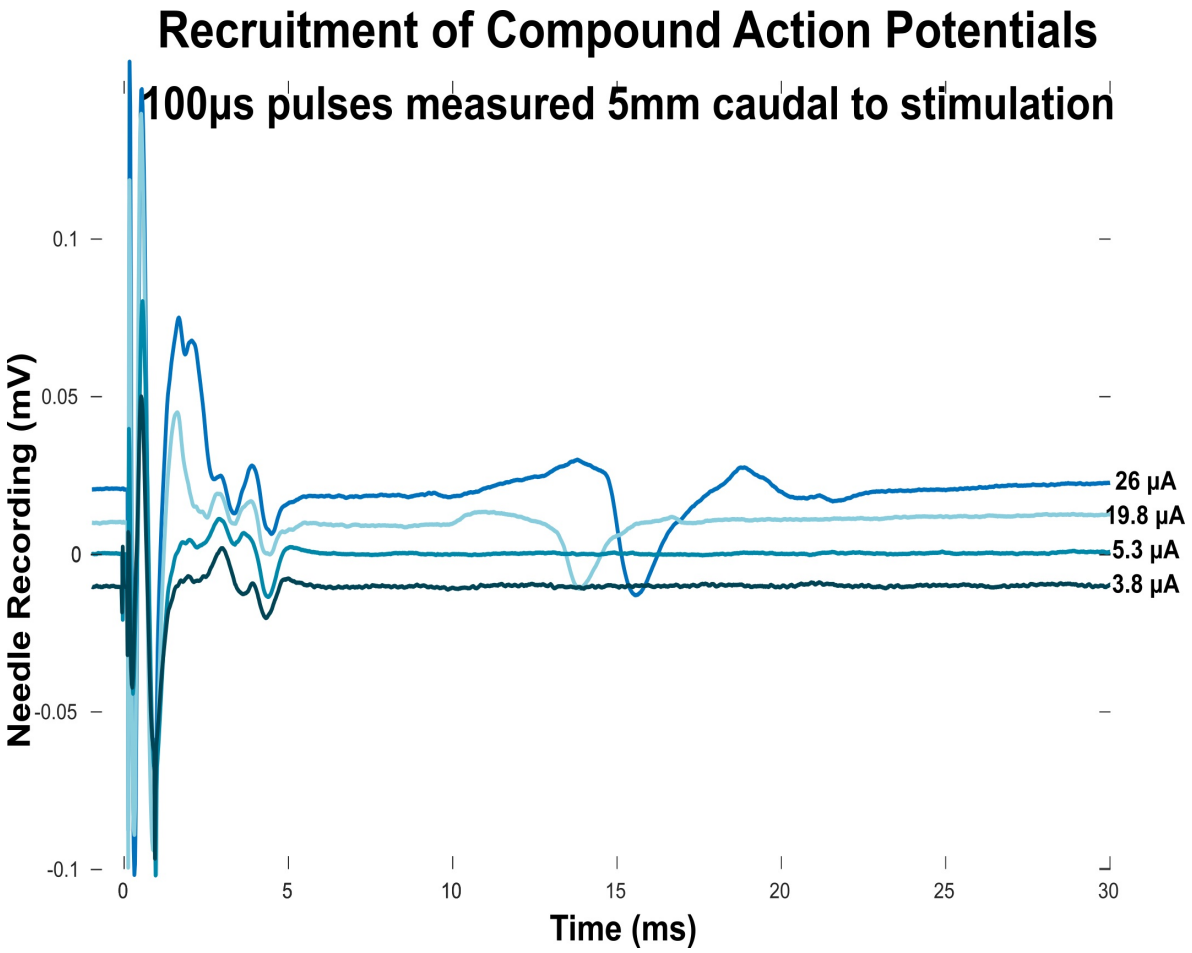

Figure 2.15. Averaged needle electrode recordings showing the recruitment of slower nerve fibers with increasing stimulus amplitude. The development of the CNAPs and the conduction delays were used to identify stimulus strength thresholds for each peak and assign a conduction velocity. The conduction velocity was then used to assign a putative fiber type to the CNAP peaks

Figure 2.16 shows the CNAP recordings at a sufficient stimulation threshold to induce bradycardia using both hook and needle electrodes for recording. This preliminary experiment shows the effect of electrode type on recording capabilities of putative C-fibers based on conduction delay. Both electrodes were able to record the large, fast fibers. However, the hook was unable to record the neural activity of the short wavelength CNAPs.

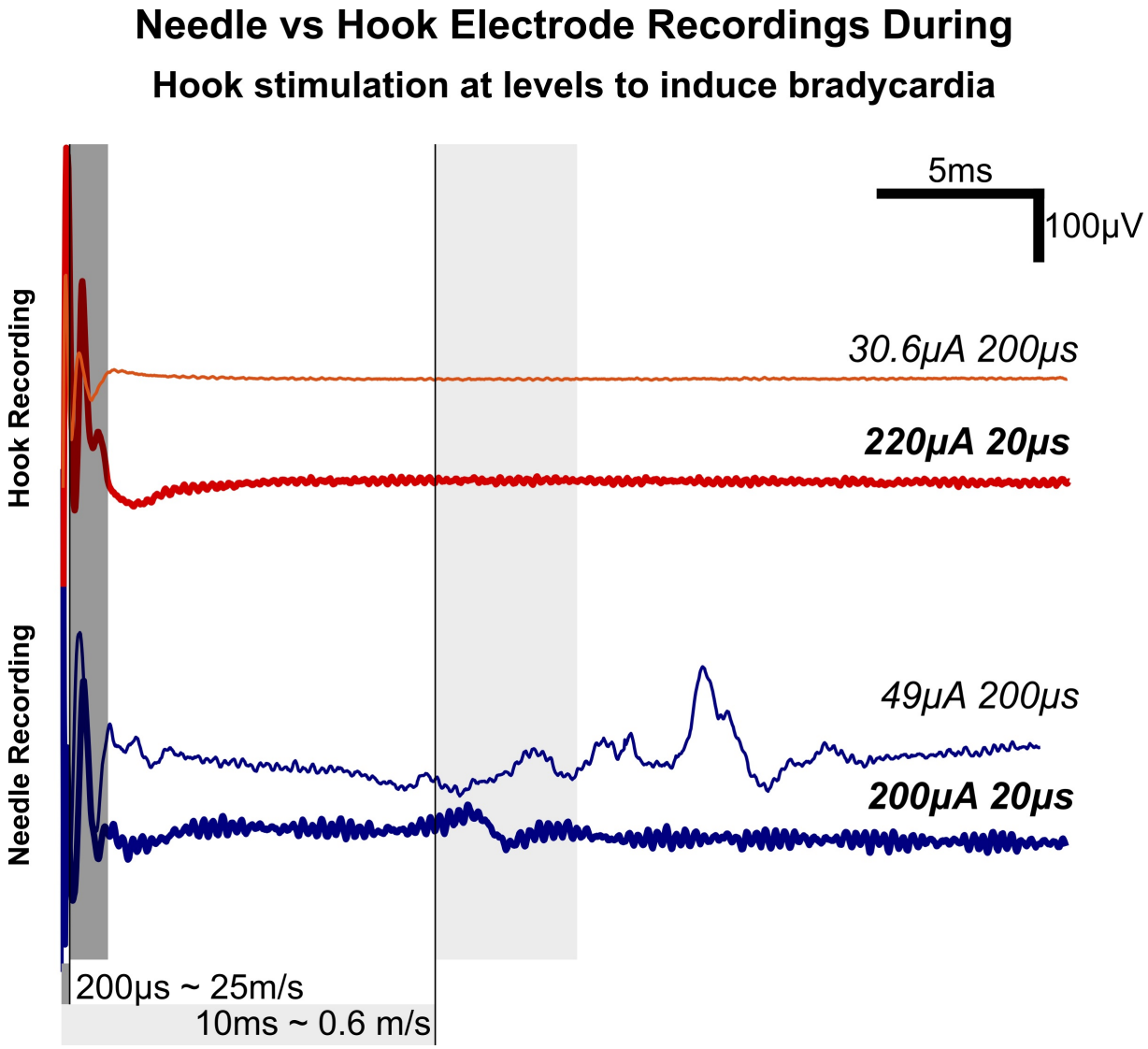

Figure 2.16. Experimental *in-vivo* measurements of CNAPs at stimulus levels sufficient to induce bradycardia. Conduction delays were used to assign putative fiber type to the CNAP peaks observed in this figure. The hook and needle electrodes show comparable A-fiber CNAPs, but only the needle electrodes show C-fiber CNAPs. The 800micron diameter hook electrode contacts' sensitivity function were too long to resolve the short wavelength C-fiber CNAPs. The gray window highlights the location of the C-fibers, which only the needle electrode, with a sharp sensitivity function, was able to record

This observation is due to the difference in electrode sensitivity functions shown in *Figure 2.17*. The electrode sensitivity function gets broader as the distance from the nerve fiber increases. Thus, the electrode sensitivity function of an extrafascicular hook electrode would exceed the wavelength of the action potential of a C-fiber and would not be able to record it. However, an intrafascicular needle electrode would have a sharper sensitivity function and would be able to sample and record the short wavelength CNAPs, such as C-fibers, appropriately, as was shown above.

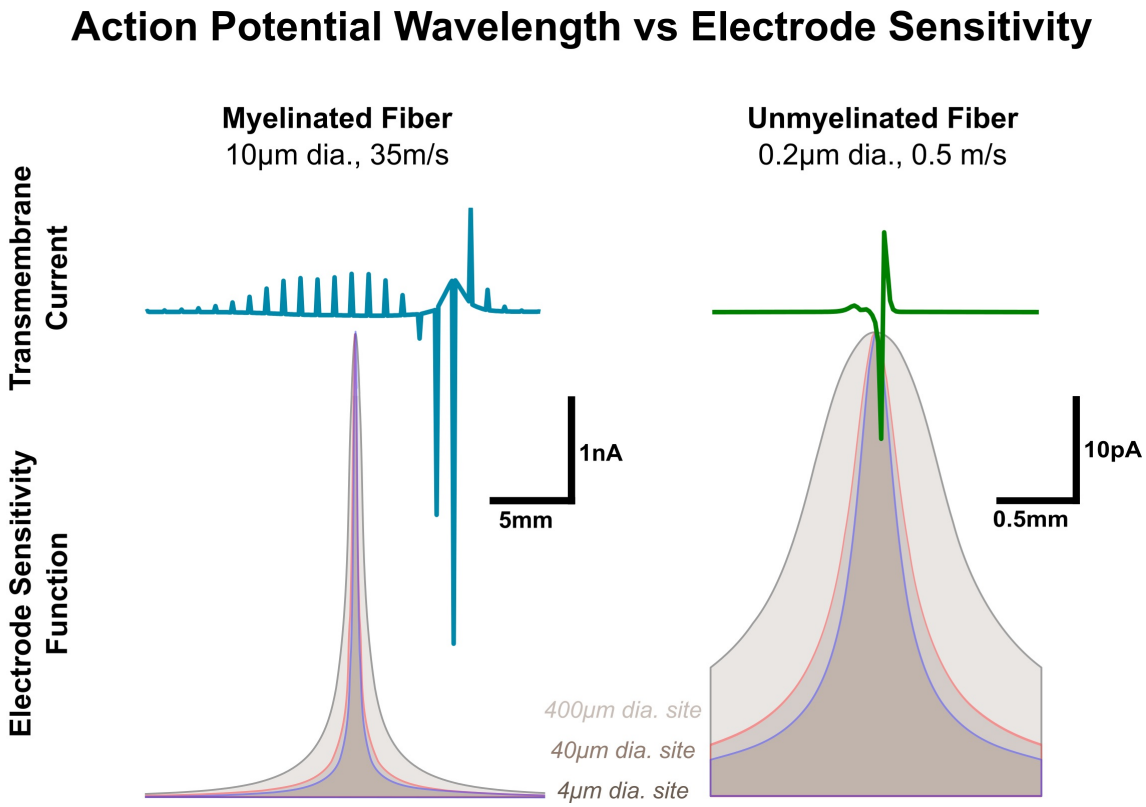

Figure 2.17. The nerve fibers of the ANS differ considerably from the composition of somatic peripheral nerves. ANS nerves can be up to 90% unmyelinated. Moreover, the myelinated fibers tend to be much smaller caliber than those in the somatic PNS. As a result, the wavelengths of the action potential and the length constants of the nerve fibers are considerably shorter. The spatial distribution of action currents in comparison to the electrode sensitivity function of an intrafascicular contact 25μm from the nerve fiber. Note that in the case of the C fiber, the sensitivity function width exceeds the wavelength of the action potential

2.6 Discussion

In this presented work, a LFAC waveform at 1Hz with current levels less than 200 μA_p was sufficient to achieve $> 80\%$ block of the effects of descending activity generated by vagal stimulation. In comparison, kHFACb is generally in the range of $1 - 10$ *mA* [59] [64] [69]. This results in higher power dissipation compared to LFAC block. Larger power dissipation can result in a larger embodiment of a clinical stimulating device. Thus, LFAC block has the potential to yield power savings compared to kHFACb. Alternatively, DC block has been shown to work in the order of 50 μA to 7 *mA* [45] [46]. Thus, LFAC is a viable method for achieving block at much lower current levels deeming it a safer alternative with clinical potential. Similar to bipolar electrode stimulation, the LFAC waveform sends currents from contact to contact. In the bipolar electrode, one contact is the anode and the other is the cathode. Therefore, in one peak or phase of the sinusoid the peak current is what is being delivered. The maximum peak current that can be delivered without the hydrolysis of water is deemed as the water window which is approximately 2.2 V_p. The LFAC waveform generated was well within the water window of the blocking electrodes used and did not cause any apparent injury to the nerve as the nerve was able to conduct and 'VStim only' elicited bradycardia following the removal of the blocking waveform. The blocking effects were approximately immediate without onset activation as is associated with kHFACb. When the LFAC waveform was discontinued, the effects were almost instantaneously reversed. Additionally, unlike DC block, the use of the LFAC alternating waveform allows for the reversal of reactions occurring at the tissue/electrode interface. This recaptures potentially damaging byproducts formed from charge injection. Similar to DC block, an *in-silico* model of LFAC suggests a closed state block of NAV1.7 [1]. Unlike DC block, LFAC blocks by inactivating the activation state variable m, and activating the inactivation state variable h. Whereas DC block there is direct activation of h without activating m. This observation is further supported by the control groups in this study in which LFAC was delivered via the rostral electrode. The control groups showed no block and provided evidence that the block effect observed was not due to an interaction between electrodes or waveforms. Additionally, *in-silico* models suggest a smaller caliber block order, which is congruent with what is seen in DC block, suggesting that the fibers blocked were A-delta or unmyelinated C-fibers [1].

As shown by McAllen et al, the conduction velocities of cardiac vagal fibers that generate bradycardia upon electrical stimulation are between 3 and 15 m/s [87]. Needle recordings of neural activity during bradycardia revealed that the conduction velocity of the fiber generating bradycardia was approximately 0.6 m/s. While this evidence is preliminary, the conduction velocity calculated points to unmyelinated C or A- delta fibers [87]. These fibers are descending due to the vagal crush, preganglionic in origin, and lie rostral to the cardiac ganglion [88]. Therefore, they are likely A-delta or C fibers. Additionally, at low frequencies enough current penetrates the nerve resulting in a functional change in HR, i.e. block bradycardia, while staying well within the water window. However, for larger nerve fibers, this may not hold and the current may not be able to penetrate large nerve bundles at a sufficient level to result in block. An important observation is that the effects of vagal stimulation were not blocked completely, indicating that some fibers were not blocked. Additionally, the stimulation pulses were phased so that the LFAC peak coincided with the train of pulses. This indicates that block does not need to be continuous and disruption of the rate code is sufficient to achieve block. Complete block can be achieved with multiple electrodes in which the peaks of the LFAC waveform are phased in a way that the duty cycle of LFAC approaches 100%, as shown in Horn et al [1]. These observations suggest that LFAC block is a bio-compatible means to achieve reversible block of conducting nerve fibers for long term use.

CHAPTER 3. *IN-VIVO* APPLICATION OF LOW FREQUENCY ALTERNATING CURRENTS ON PORCINE CERVICAL VAGUS NERVE EVOKES REVERSIBLE NERVE CONDUCTION BLOCK

A portion of this chapter will be submitted to the Journal of Neural Engineering.

3.1 Abstract

This paper describes a method to reversibly block nerve conduction. The method was demonstrated *in-vivo* on the cervical vagus nerve of an adult anaesthetised pig using direct application of a low frequency alternating current (LFAC) waveform at 1 Hz applied through a bipolar nerve cuff electrode. Using vagal stimulation evoked bradycardia as a biomarker, this waveform was previously shown to reversibly block the effects of vagal stimulation in the anaesthetised rat model. The present work explores LFAC on larger vagal afferent fibers in larger human sized nerve bundles projecting to effects mediated by a reflex. The effectiveness of LFAC was assessed on the left cervical vagus nerve in anaesthetized domestic swine (n=5) against vagal stimulation to evoke the Hering-Breuer reflex which can only be activated under anesthesia. Two bipolar cuff electrodes were applied unilaterally to the cervical vagus nerve, which was crushed caudal to the electrodes to eliminate cardiac effects. A tripolar extrafascicular cuff electrode was placed most rostral on the nerve for recording of propagating action potentials induced by electrical stimulation and blocked via the LFAC waveform. Standard pulse stimulation was applied to the left cervical vagus to induce the Hering-Breuer reflex. If unblocked, activation of the Hering-Breuer reflex would cause breathing to slow down and potentially halt completely. Block was quantified by the ability of LFAC to reduce the effect of the Hering-Breuer reflex by monitoring the respiration rate during LFAC alone, LFAC and vagal stimulation, and vagal stimulation alone. LFAC achieved $87.2 \pm 8.8\%$ block (n=5) at current levels of 0.8 ± 0.3 mA_p (current to peak), which was well within the water window of the working electrode.

Compound nerve action potential (CNAP) was monitored to directly correlate changes in nerve activity during LFAC, which manifests itself as the slowing and amplitude reduction of components of the CNAP, to changes in organ function.

3.2 Introduction

Electrical nerve conduction block provides a means to interrupt unwanted neural activity in motor or autonomic nerves. It has been shown to reduce spasticity via motor nerve block and modulate the activity of autonomic nerves [59, 75, 89]. Current techniques being investigated that have provided evidence of nerve conduction block include: kilohertz frequency alternating current block (kHFACb) [57, 59, 81, 82], direct current (DC) block [45, 46, 80], anodal block [83, 84], and quasi-trapezoidal stimulation [54]. However, for these methods to be considered safe for clinical applications, the shortcomings associated with each should be addressed. DC block, for example, results in toxic byproduct formation due to charge imbalance which results in hydrolysis. This has shown to not only irreparably injure tissues [45], but the ions can also erode electrodes over time which pushes the electrode outside of its linear operating region i.e., its water window. However, the use of an alternating current has the ability to reverse the Faradaic reactions in order to reduce the possibility of damaging byproduct formation. KHFACb is a method that uses a sinusoidal waveform with frequencies ranging from 1 kHz – 40 kHz [59, 69]. However, it is associated with an onset response which causes the activation of nerve fibers before block can occur [90]. A combined waveform of DC block and kHFACb block is a strategy used in which the DC waveform blocks the onset activation of kHFACb block [53, 64–66]. Although these methods have reportedly been efficacious to varying degrees, a method to safely and reversibly slow or eliminate nerve activity is a shortcoming of the neuromodulation field.

During our investigation of kHFACb, we discovered that a reduction of frequency ($<$ 100 Hz) achieved phasic blocking of action potentials in *in-vivo* testing on earthworm nerves. Furthermore, the waveform was tested on *ex-vivo* canine and porcine vagus nerves and resulted in successful nerve conduction block indicating that the phenomenon was conserved across species (canus – sus) and class (insecta – mammalia) [1].

Block was achieved at current levels that are approximately half of those required for kHFACb block within the linear region of the working electrode. The LFAC waveform applied was a simple sinusoid characterized by amplitude and frequency and presented via a bipolar electrode. LFAC has low threshold characteristics associated with DC block and charge balanced reversibility of kHFACb.

Evidence of LFAC has been shown to block an efferent volley of action potentials producing bradycardia in *in-vivo* rat vagus nerves [85]. The present work aims to build on prior *in-vivo* work to determine whether LFAC can achieve block of larger caliber peripheral nerve fibers whose action is reflected via a reflex in the *in-vivo* swine cervical vagus animal model.

3.3 Methods

3.3.1 Animal and Surgical Prep

All experiments involving animals were approved by an Institutional Animal Care and Use Committee (IACUC) and performed in accordance with the Guide for the Care and Use of Laboratory Animals (National Institutes of Health Publication. No. 85-23, Revised 2011). Adult ($\sim 50\ kg$) male domestic swine were sedated with an intramuscular injection of with Telazol, xylazine, and ketamine (5.0, 2.5, and 2.5 mg/kg respectively). Swine were then intubated, placed in supine position, and anesthesia maintained via inhaled isoflurane anesthesia ($0.5 - 3\%$). A unilateral femoral cutdown was performed and a femorally inserted catheter advanced into the thoracic aorta for continuous maintenance of blood pressure (BP). BP, electrocardiograph (ECG), O^2 saturation, respiration, and body temperature were continuously monitored through the course of the procedure. Respiration was encoded into a voltage equivalent by a calibrated pressure transducer which received input from a blood pressure cuff strapped circumferentially around the chest of the animal. A custom software for MATLAB (2016a, Mathworks, Natick, MA) allowed for the visualization of the voltage equivalent respiration throughout the experiment. Subsequent to placement of all monitoring instrumentation, a midline anterior incision was made in the neck and the vagus nerve was bilaterally isolated.

3.3.2 Electrode Configuration

Two bipolar extrafascicular cuff electrodes were positioned on the exposed left cervical vagus shown in *Figure 3.1*. The LFAC waveform was delivered through the rostral electrode (RE), a bipolar cuff (2mm CorTec GmbH, Neuer Messplatz 3, 79108 Freiburg Germany). A 2 mm bipolar CorTec cuff was placed caudal to the RE and was used for vagal stimulation, as the caudal electrode (CE). Additionally, a custom built 3D printed 3 mm diameter tripolar cuff [91] was placed most rostral on the nerve for recording compound action potentials (CNAPs) and secured with a suture. The left cervical vagus was crushed caudally to all electrodes using a pair of forceps and suture to eliminate caudally directed responses due to electrical stimulation. The right vagus nerve was remained intact and not crushed for stability and to maintain autonomic reflexes. Electroneurograph (ENG), LFAC waveform, respiration, and ECG signals were acquired simultaneously at 48 kHz using a Zoom FN8 sampling front end to Tracktion T7 DAW. Channels whose signals had bandwidths < 20 Hz, respiration and LFAC waveform, were FM modulated using a Vetter FM Recording Adapter (model 2D) prior to acquisition via the Zoom sampling front end to Tracktion. ENG was highpass filtered at 10 Hz (2500x-5000x gain) using a multi-channel gain-filter main amp (CyberAmp 320, Axon Instruments).

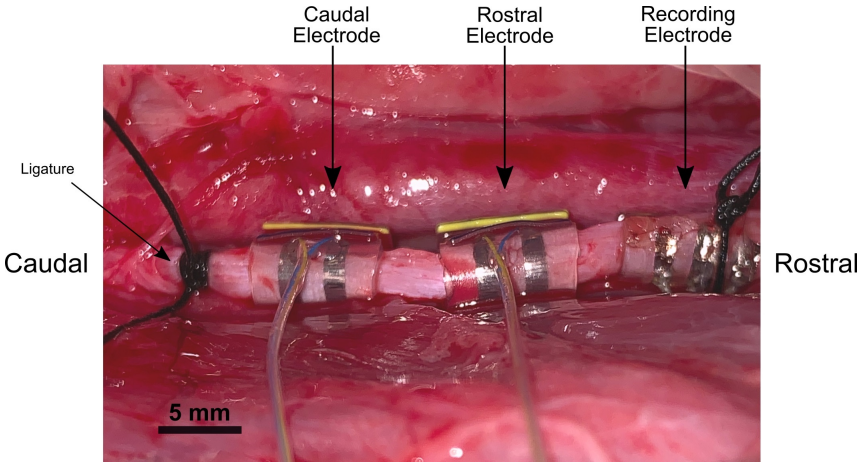

Figure 3.1. Electrode placement on the isolated, left cervical vagus of a swine for the LFAC experiments. The CE, a bipolar cuff, was used for vagal stimulation. The LFAC conditioning waveform was presented at the RE. A tripolar recording electrode for ENG recordings was placed most rostral on the vagus nerve and secured with suture. A ligature was placed caudal to all three electrodes to eliminate cardiac effects due to stimulation of the left vagus nerve

3.3.3 Nerve Stimulation and Experimental Paradigm

The LFAC waveform and stimulation sync pulses were generated using an arbitrary function generator (Analog Discovery 2, Digilent Inc, Pullman WA) controlled via a custom written waveform generation routine written in LabVIEW. The stimulation sync pulses consisted of a train of 10 pulses (100 μsec-1000 μsec pulse width) at 25 Hz repeated at 1 Hz applied to the vagus nerve using an opto-isolated stimulator (DS3, Digitimer LTD, Hertfordshire UK). *Figure 3.2* shows an example of the sync pulses and LFAC waveform generated. The sync pulses were phased to be delivered at the peaks of the sinusoid due to the phasic blocking phenomena observed *ex-vivo* and *in-silico*.

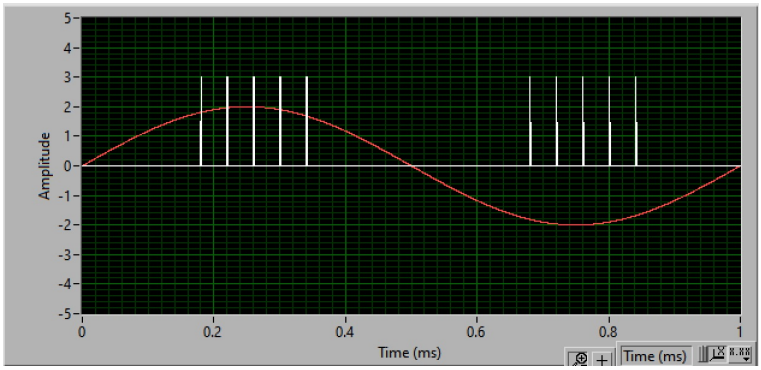

Figure 3.2. LFAC waveform at 1 Hz and sync pulses generated. The sync pulses were phased to trigger at the peaks of the sinusoidal waveform

Adequate stimuli was determined by visually examining the voltage equivalent respiration output on MATLAB. This was a purely qualitative measure. Stimulation was increased until an increase in inter breath interval was identified, indicative of the activation of the Hering-Breuer reflex. However, too large of a stimulus amplitude would result in the complete cessation in breathing. Therefore, the stimulus was titrated to result in a visible effect without complete cessation of breathing.

The LFAC waveforms were presented to the blocking electrode through a custom built analog optical isolator followed by a voltage controlled current source (CS580, SRS, Sunnyvale CA or custom built current source).

The amplitude of the LFAC waveform was increased until distortion of the waveform was visible. This indicated that the voltage had reached or exceeded the water window. At that point, the amplitude was decreased in order to remain within the water window of the electrode. This amplitude resulted in block of the Hering-Breuer reflex.

To test the effect of the LFAC waveform, the vagal stimulus train and the LFAC waveform were presented in a regular continuous sequence as follows: 1 – Pre Phase) 20s baseline period of no stimulation, 2 – LFAC Only Phase) 20s LFAC delivered to the RE, 3 – LFAC+Stim Phase) 20s LFAC delivered to the RE and vagal stimulation at the CE, 4 – Stim Only) Vagal stimulation at CE, 5 – Post Phase) No stimulation return to baseline.

The test sequence outlined above was repeated followed by a control case in which vagal stimulation was presented at the RE and LFAC was delivered at the CE. However, due to different electrode impedance of the RE and CE, the amplitude of the block waveform had to be reduced.

3.3.4 Data Analysis

The analysis of the acquired data sets was performed using custom software written for MATLAB (2016a, Mathworks, Natick, MA). Modulated channels were demodulated using a standard FM demodulation algorithm in MATLAB. The peaks of each breath were located and used to calculate the breathing rate (BRrate) and median BRrate during each of the 5 epochs outlined above. The normalized BRrate during each epoch of the experimental sequence was calculated using the following equation:

$$Normalized\ BRrate(\%) = 1 - \frac{[cond] - median(RRrate_{pre})}{median(RRrate_{pre}) - median(RRrate_{vstimonly)}} * 100 \qquad (3.1)$$

Where [cond] represents the median breathing rate during each of the 5 epochs. Additionally, the denominator, (median(BRrate$_{pre}$)– median(BRrate$_{stimonly}$)), represents the maximum depression in the breathing rate. The breathing rate was normalized to 100% in the 'Pre' epoch, and normalized to 0% in the 'Stim Only' epoch. The normalized breathing rate correlates 1:1 to the percent block in the 'LFAC+Stim' and 'Stim Only' epochs in the test and control experimental cases.

To isolate the CNAPs, the stimulus artifacts were superimposed and averaged within the window of interest. The CNAPs are clearly visible, however, there is an underlying artifact that could not be removed.

3.4 Results

As shown in *Figure 3.3*, the peak of each breath was identified. Upon examination, there is an evident increase in the inter breath interval at approximately 140*s*. This indicates that the breathing has slowed down and that the Hering-Breuer reflex was adequately induced. A further increase in the vagal stimulus would further increase the inter breath interval and eventually lead to cessation of breathing during the vagal stimulation only epoch.

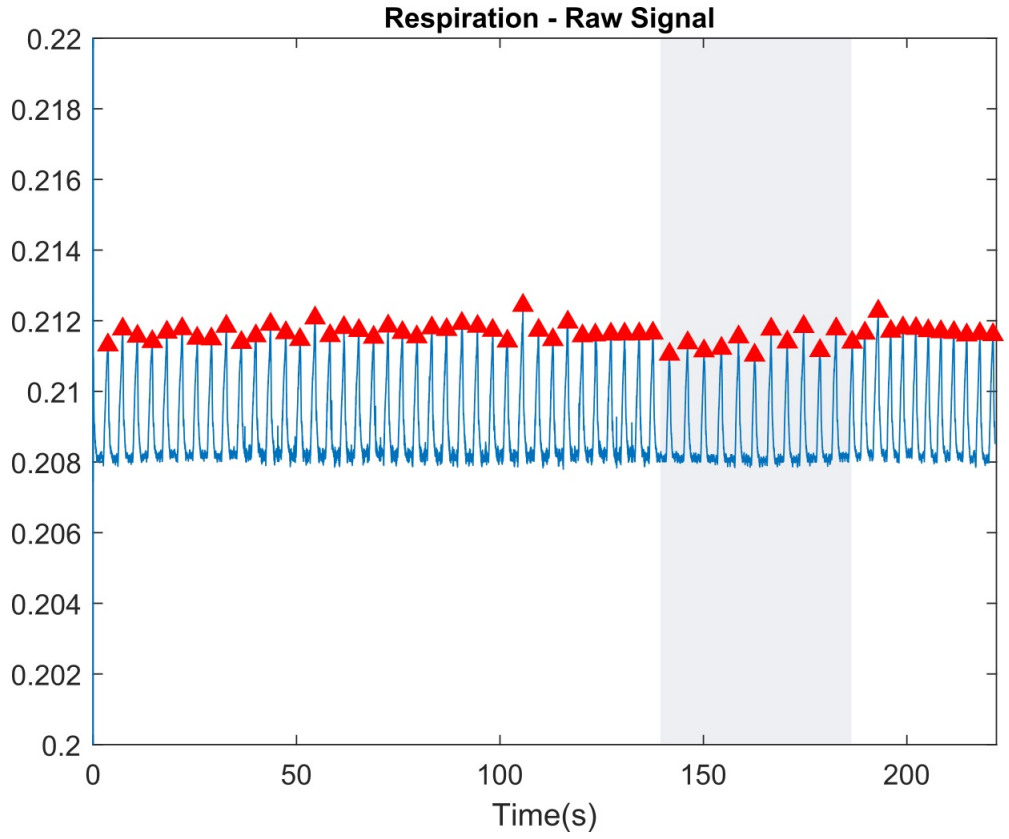

Figure 3.3. Example of a raw respiration data set during experiment. Vagal stimulation alone occurred at approximately 140 seconds, shown as the shaded region. In this period, there is an evident increase in inter-breath interval and a slight decrease in amplitude. This indicates that the Hering-Breuer reflex was adequately activated

The locations of the peaks were used to calculate the breathing rate during each epoch as shown in the *Figure 3.4*. It is clear that application of the LFAC waveform does not cause an onset response as is often associated with kHFACb. It is also evident that during the 'LFAC+Stim' epoch, the breathing rate continues at a comparable rate to that of the 'Pre' epoch. Removal of the LFAC waveform causes an almost instantaneous drop in breathing rate due to vagal stimulation. Turning the stimulus off caused an overshoot likely due to sympathetic rebound before returning to baseline.

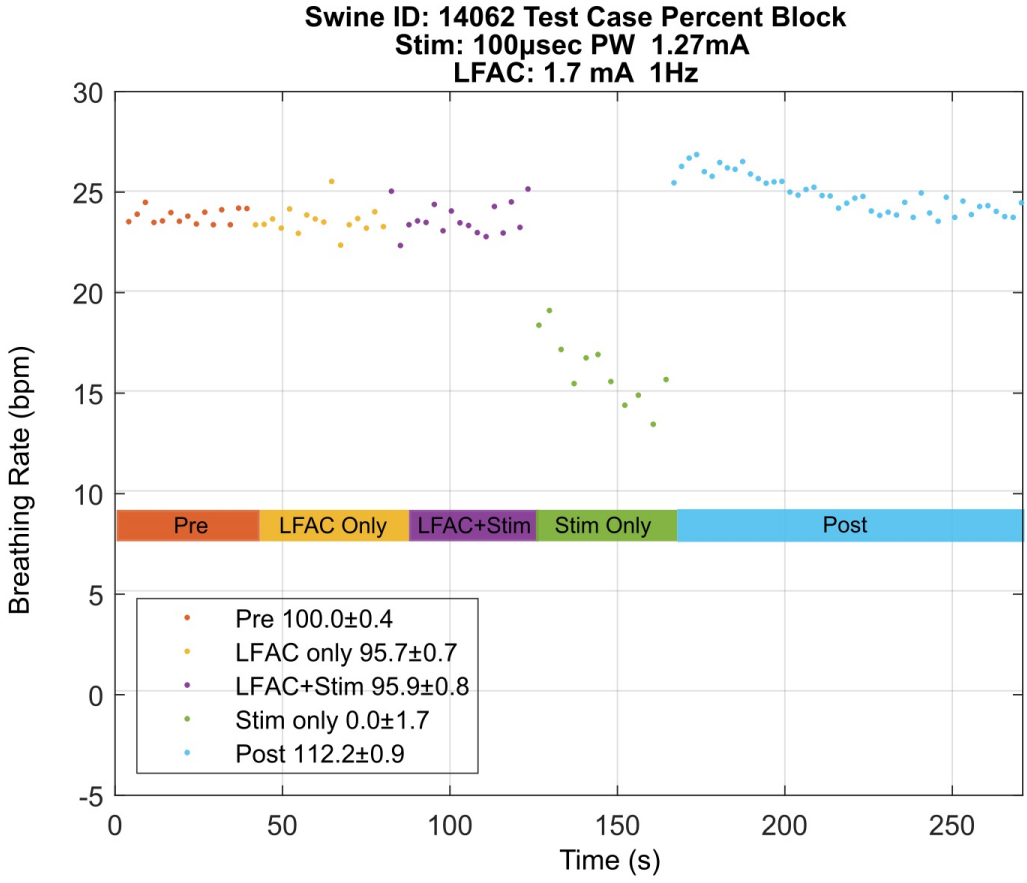

Figure 3.4. Breathing rate during each epoch of the experimental paradigm. The percent block is shown in the legend on the bottom left. The 'Pre' epoch was normalized to 100% block and the 'Stim only' epoch was normalized to 0% block. The overshoot seen in the first few seconds of the 'Post' epoch is likely due to sympathetic rebound before returning to baseline

A possible explanation for the effect of block observed could be that block is occurring due to an interaction between electrodes or stimulation train and LFAC waveform. Therefore, a control case, *Figure 4.1*, was initiated in which vagal stimulation was delivered through the RE and the LFAC waveform was presented through the CE. As in the test case, there is no onset response associated with the application of the LFAC waveform. Conversely, there is a decrease in BRrate during 'LFAC+Stim' indicating that the Hering-Breuer reflex was not blocked. Additionally, the BRrate during 'LFAC+Stim' and 'Stim only' are approximately equal. This provides evidence that the reflex was not blocked, as was expected in the control case, indicating that the block effect is not due to an interaction between electrodes or waveforms.

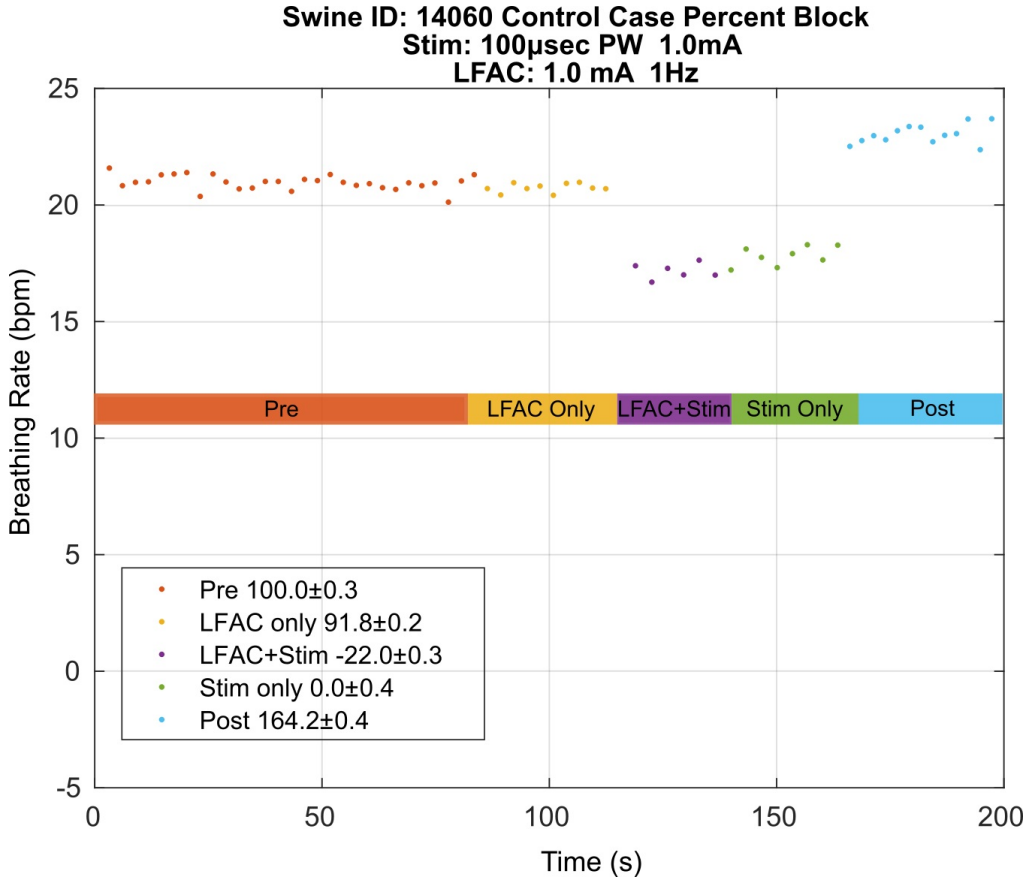

Figure 3.5. BRrate during a control case in which the electrode connections were swapped. Vagal stimulation was delivered via the CE and the LFAC waveform was presented at the RE. In this control case, the percent block during the 'LFAC+Stim' epoch was calculated to be -22%. A negative percent block indicates that the breathing rate during 'LFAC+Stim' was lower than the breathing rate of the 'Stim only' epoch

Out of the 8 experiments, there were 5 successful. The 3 unsuccessful experiments were excluded in the analysis. These experiments were unsuccessful due to synchronization issues between the LFAC and pulse stimulation, no evident Hering-Breuer reflex during vagal stimulation, and insufficient time between runs leading to the accumulation of chemoreceptors. *Table 3.1* summarizes the stimulation and blocking waveform parameters for the successful experiments. All values shown were within the water widow of the blocking cuff. The average percent block achieved during 'LFAC+Stim' was 87.2 $\pm$ 8.8 %. In contrast, the control cases averaged 9.3 $\pm$ 24 % block during 'LFAC+Stim'. A negative percent block indicates that the BRrate during 'LFAC+Stim' was lower than that of the BRrate in the 'Stim Only' epoch.

Table 3.1. Vagal stimulation and LFAC parameters used in the set of n=5 successful experiments. The LFAC waveform was strictly applied at 1 Hz. The average percent block amongst n = 5 experiment was calculated to be 84.3 $\pm$ 4.6 %. Two pulse widths, 1000μsec and 100μsec, were used for Swine ID 13525. The voltages delivered were within the water window of the electrode. *In one case, instrumentation issues did not allow for the retrieval of the LFAC voltage

Swine ID	Vagal Stimulation			LFAC waveform		% Block
	PW (µsec)	PA (mA)	Charge (mC)	Current (mAp)	Voltage (Vp)	Mean
21435	1000	0.22	0.22	1.00	0.20	88.23
13523	1000	1.19	1.19	1.00	0.45	94.48
13525	1000/100	0.35	0.04	0.88	0.47	86.32
14060	100	0.00	0.10	1.18	*N/A	94.20
14062	100	1.21	0.12	1.63	0.62	72.89
Mean		**0.6**	**0.3**	**1.1**	**0.4**	**87.2**
SD		**0.6**	**0.5**	**0.3**	**0.2**	**8.8**

In the test case of Swine ID 21435 (*Figure 3.6*), the test sequence was applied out of order. Following the 'Pre' epoch, the stimulus was applied to elicit the Hering-Breuer reflex. After successful activation of the Hering-Breuer reflex, the LFAC waveform was slowly ramped up until block was achieved. Block was achieved when the waveform reached an amplitude of approximately 1mA$_p$. Upon removal of the LFAC waveform, the Hering-Breuer reflex was activated again. Removal of the vagal stimulation resulted in the return to baseline respiration. In this case, the LFAC waveform was able to block an already activated reflex, which is more difficult to achieve than blocking the Hering-Breuer from being activated. In other words, LFAC was able to block already recruited CNAPs.

Furthermore, neural recordings from the test case, shown in *Figure 3.7*, display the effect of the LFAC waveform on the two CNAPs shown in the 'Stim Only' epoch.

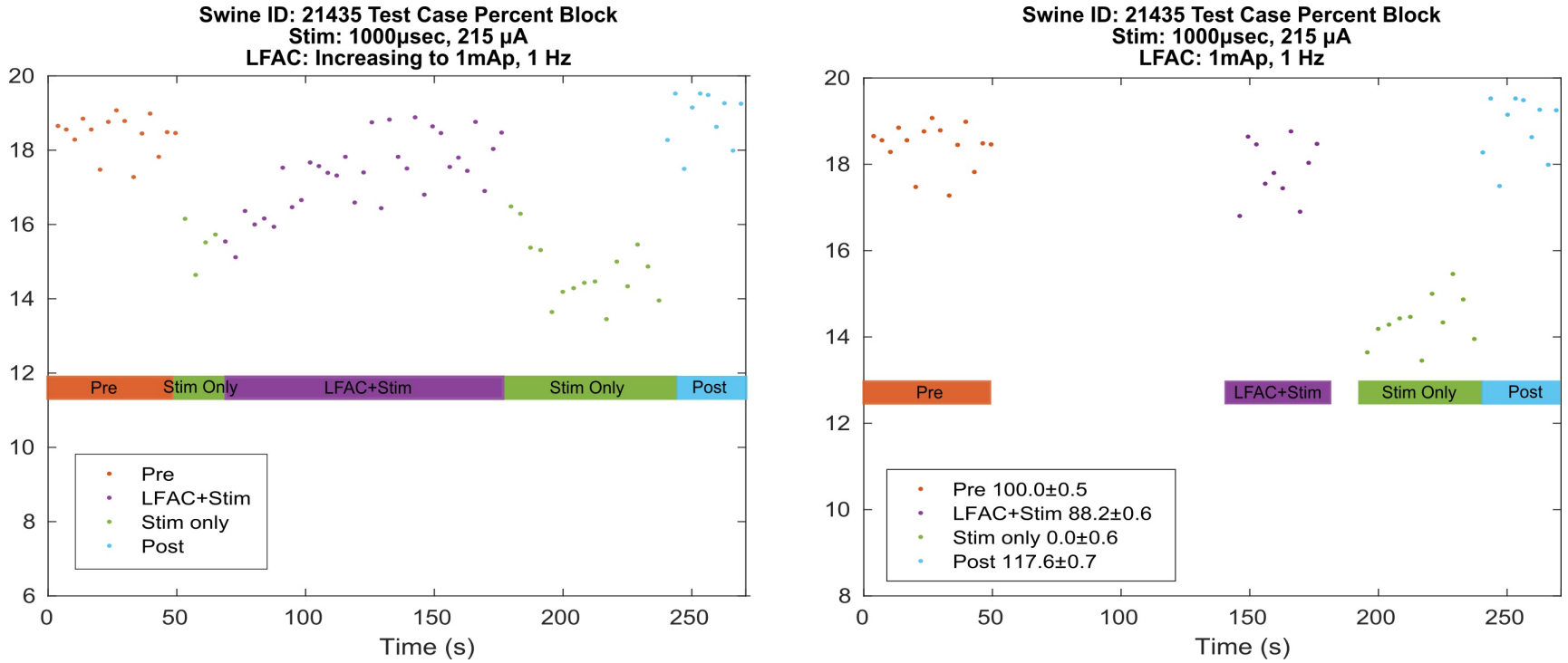

Figure 3.6. Test case of Swine ID 21435. In this unconventional case, the test sequence was applied out of order. Following a baseline reading, the Hering-Breuer reflex was established. The amplitude of the LFAC waveform was then slowly ramped up until block was achieved. The LFAC waveform was then discontinued which resulted in the activation of the Hering-Breuer reflex almost instantly. The left panel shows the unconventional test sequence order. To quantify the percent block, 4 epochs were isolated, shown on the right panel: Pre, LFAC+Stim, Stim Only, and Post. The 'LFAC+Stim' epoch had a max amplitude of $1mA_p$ applied at 1 Hz, thus the window of 'LFAC+Stim' was determined based on the location of the max amplitude

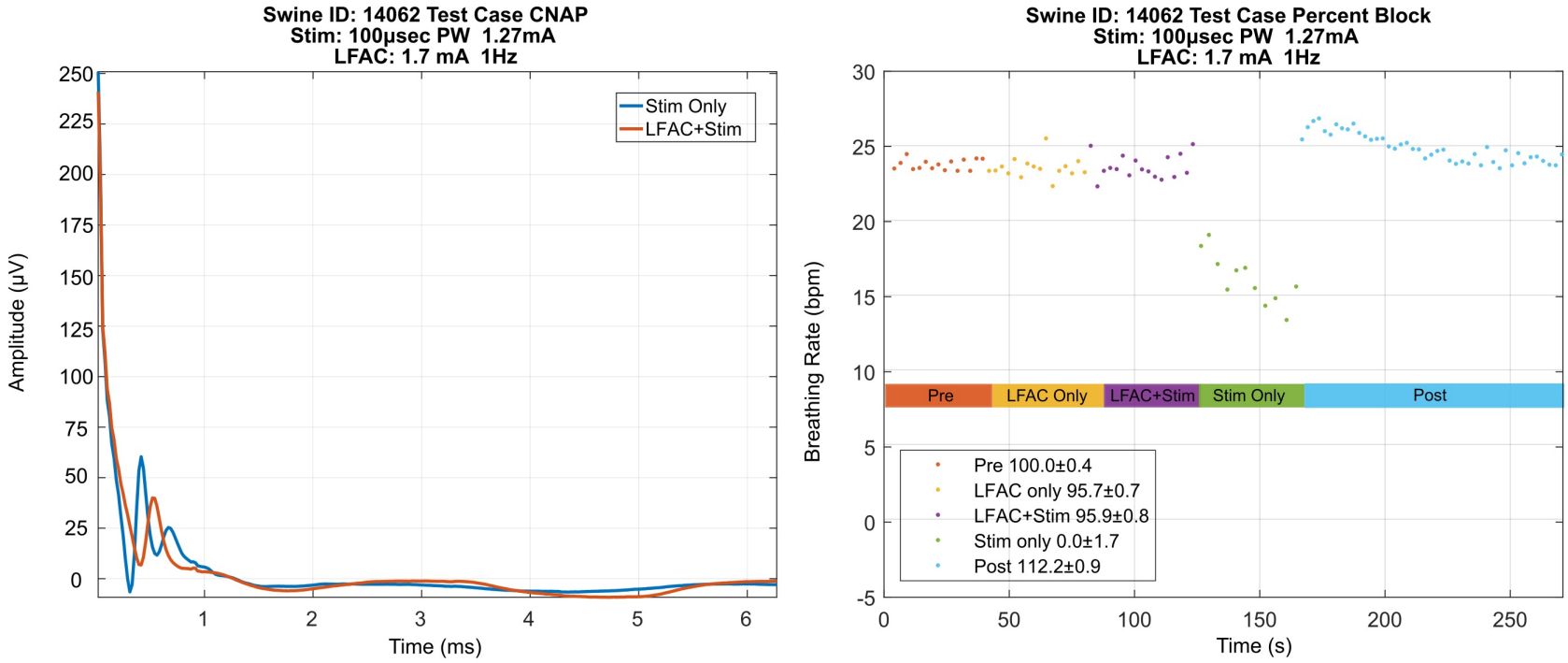

Figure 3.7. ENG recordings during an LFAC test case. In the 'Stim only' epoch (left panel) there are 2 clear CNAPs. The LFAC waveform during 'LFAC+Stim' slow these CNAPs down and cause a decrease in amplitude. The right panel shows the breathing rate and percent block during 'Stim only' and 'LFAC+Stim'

It is evident that there is a slowing effect and an amplitude reduction imparted by the LFAC waveform. The conduction velocities for the 1st peak and 2nd peak in the 'Stim Only' epoch are approximately 47 and 29 m/s, respectively. However, during 'LFAC+Stim' the conduction velocities decrease by approximately 10 m/s to 35.7 and 18.18 m/s, respectively.

The control case, *Figure 3.8*, shows the two CNAPs in the 'Stim Only' and 'LFAC+Stim' epochs superimposed on top of each other. Indicating that the fibers responsible for the Hering-Breuer reflex are likely fast A and B fibers, as has been shown in [92–94].

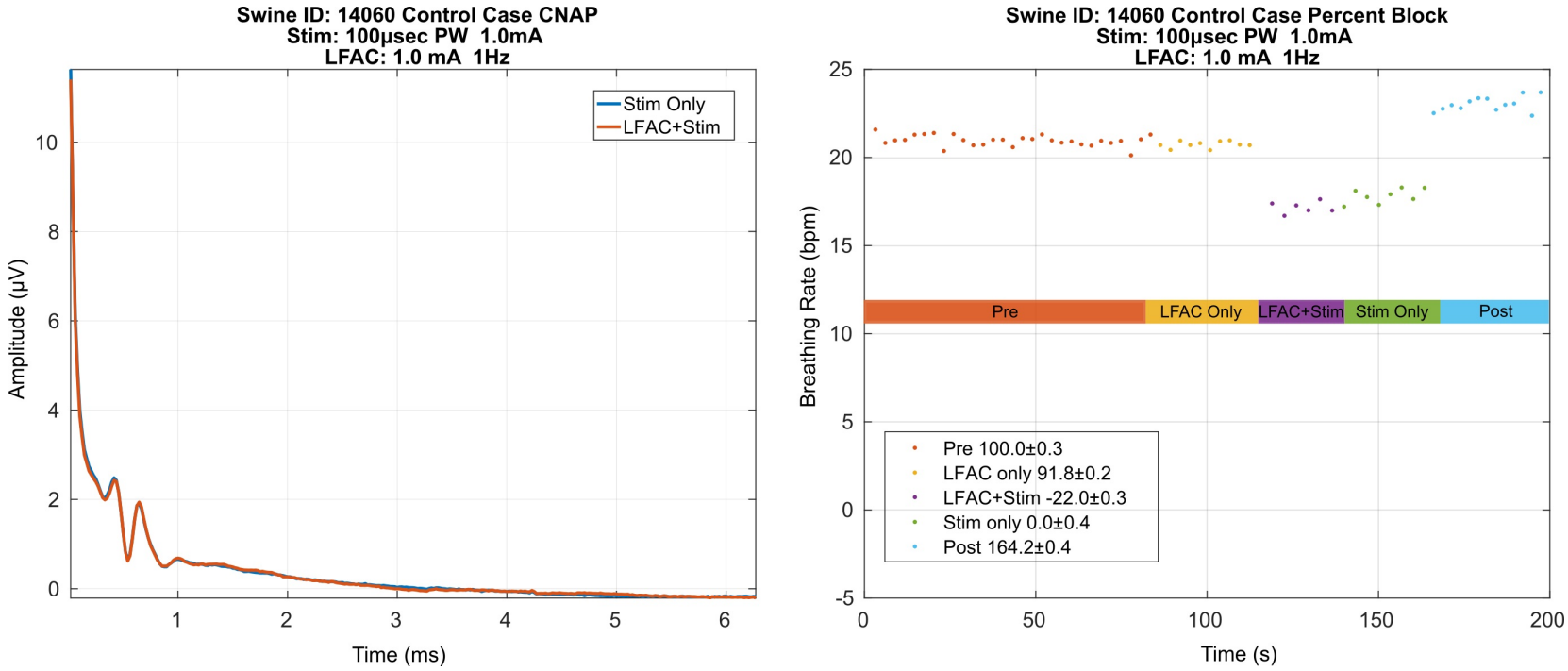

Figure 3.8. ENG recordings during an LFAC control experiment. During the 'Stim only' epoch (left panel) there are 2 clear CNAPs. Conversely to what occurs in the test case, the LFAC waveform in the 'LFAC+Stim' epoch does not affect the 2 CNAPs that are visible. The CNAPs visible in the 'LFAC+Stim' epoch are unaffected and superimposed on those seen during the 'Stim Only' epoch. This evidence further supports the hypothesis that LFAC block does not occur due to an electrode or waveform interaction. The right panel shows the breathing rate and percent block during 'Stim only' and 'LFAC+Stim' epochs in the control case

While CNAPs were observed on the oscilloscope during n = 5 of the experiments, neural recordings were only recovered in n = 2 due to a lack of gain in the remaining 3 experiments. However, the effects shown above were consistent and repeatable throughout all experiments. Additional examples of CNAPs in test and control cases are shown below (*Figure 3.9* and *Figure 3.10*, respectively).

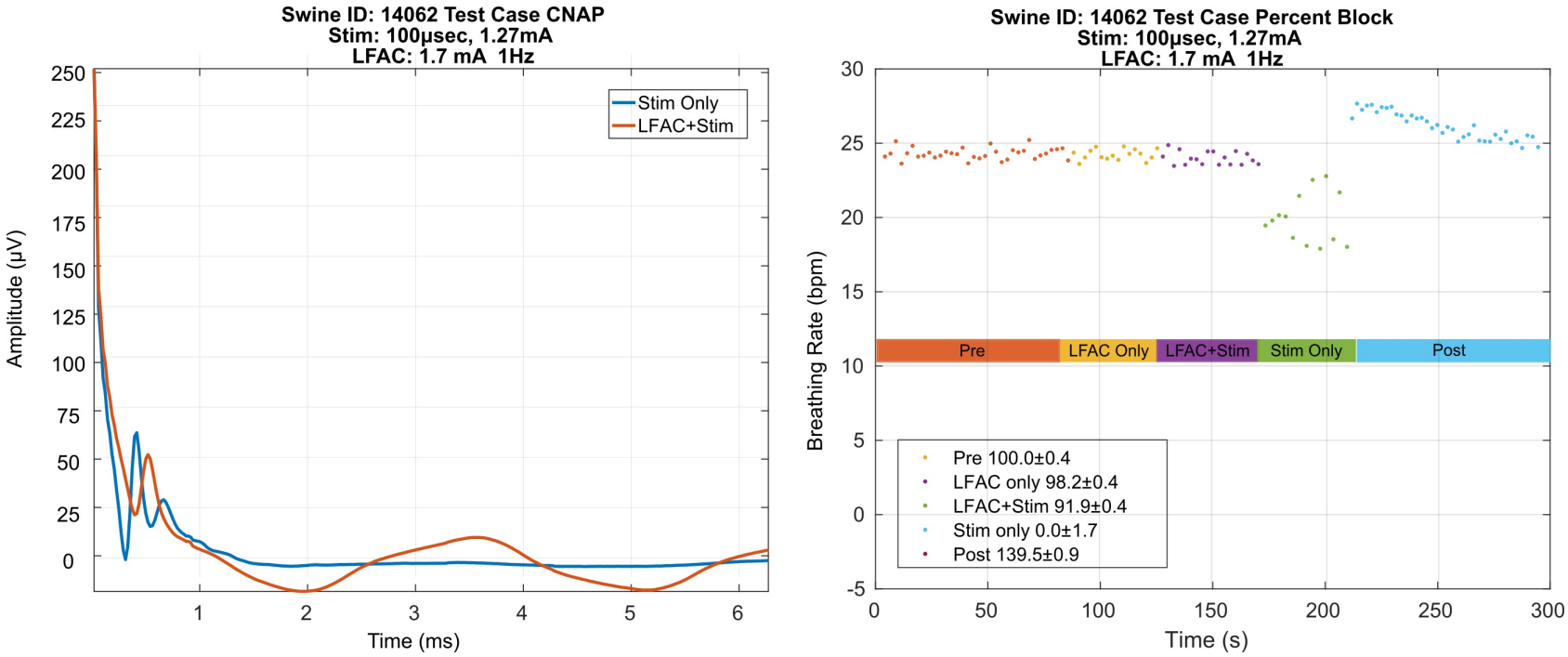

Figure 3.9. ENG recordings during an LFAC test experiment. This figure shows evidence of the change in neural activity in the 'LFAC+Stim' epoch due to the LFAC waveform. In the 'Stim only' epoch (left panel) there are 2 clear CNAPs. The LFAC waveform during 'LFAC+Stim' slow these CNAPs down and cause a decrease in amplitude. The right panel shows the respective breathing rate and percent block during 'Stim only' and 'LFAC+Stim'

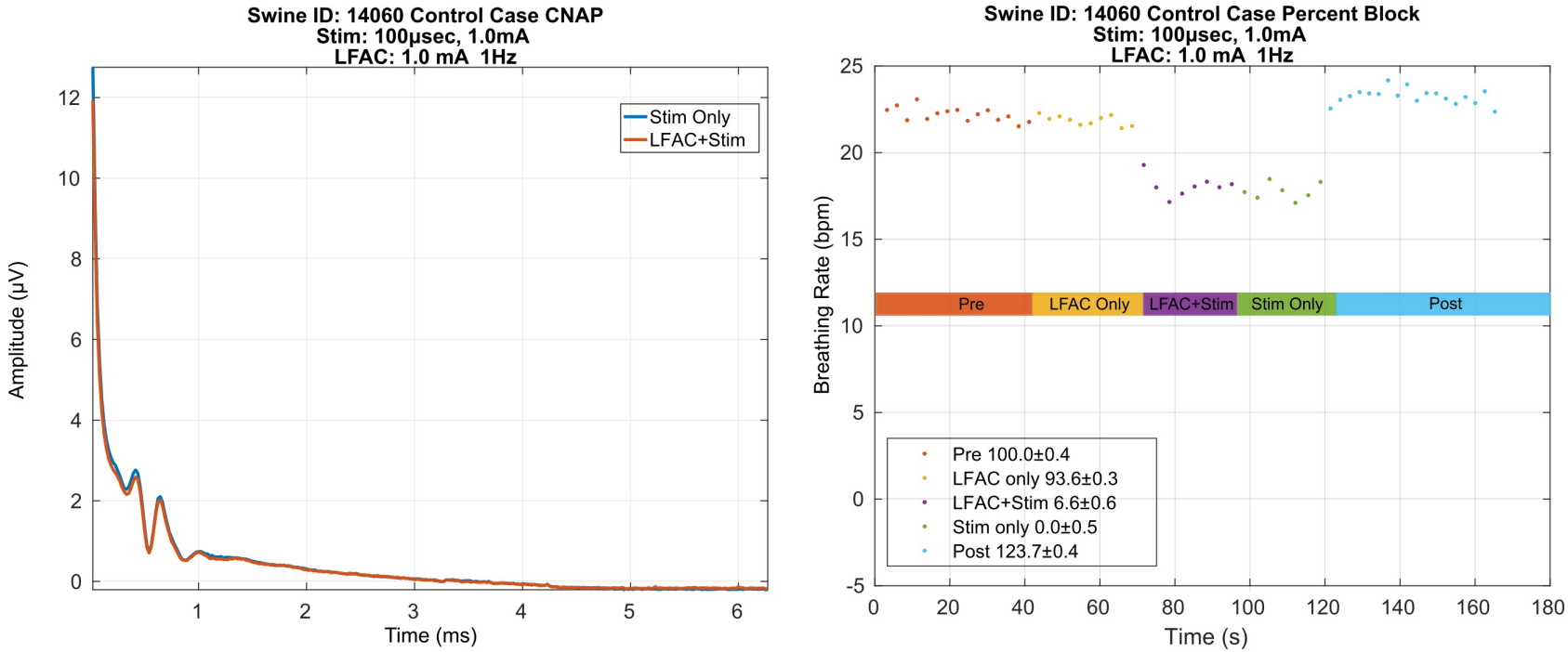

Figure 3.10. ENG recordings during an LFAC control experiment. During the 'Stim only' epoch (left panel) there are 2 clear CNAPs. Conversely to what occurs in the test case, the 'LFAC+Stim' epoch does not affect the 2 CNAPs that are visible. The CNAPs visible in the 'LFAC+Stim' epoch are unaffected and superimposed on those seen during the 'Stim Only' epoch. The right panel shows the respective breathing rate and percent block during 'Stim only' and 'LFAC+Stim' epochs in the control case

3.5 Discussion

With the use of the LFAC waveform at 1 Hz, $> 85\%$ block was achieved at average current levels of 1.1 mA_p. In comparison, kHFACb is generally achieved at currents between $1 - 10mA$ [59, 64, 69], higher than those required for LFAC. The LFAC conditioning waveform was well within the water window ($\sim$ 2.2 V_p) of the cuff electrode used. Additionally, the LFAC waveform, unlike DC block, allows for the reversal of the Faradaic reactions that occur at the tissue/electrode interface. These reactions can lead to nerve damage which is generally seen as a discoloration of the tissue. Removal of the nerve cuffs showed no observable damage or discoloration. However, damage can occur if the potential or current is not balanced due to an offset generating a direct current. This can lead to hydrolysis of water. Therefore, the potential was continually monitored throughout the experiment to ensure there was no offset. For clinical applications, continual monitoring and adjusting would not be feasible, thus a 'smart stimulator' may be needed to ensure and maintain balance as it is possible for the electrode potential to change and become polarized. Blocking effects were almost instantaneous without an onset response, which is a characteristic feature of kHFACb, and effects were immediately reversed when the LFAC waveform was discontinued, as seen in the 'Stim Only' epoch.

Neural activity was easily monitored throughout each experiment. This was made possible due to a characteristic feature of the LFAC waveform which is that the conditioning waveform is outside the bandwidth of the recording bandwidth of neural activity. There are two possible interpretations for the two CNAPs visible. The first interpretation is that in the 'LFAC+Stim' epoch, the first peak is the one attenuated and the peaks following were inverted. However, the more probable interpretation, consistent with *ex-vivo* and *in-silico* work [1], is that the LFAC waveform imposes a smearing or slowing effect on the CNAPs before block. The first peak shown is not only slowed down, but also attenuated. Meanwhile, the second peak is also slowed down and significantly attenuated to the point of almost complete annihilation. This indicates that LFAC blocks the slower, smaller nerve fibers first. This observation is also consistent with the *in-silico* and *ex-vivo* work [1].

The conduction velocities of 47 and 29 m/s point to A and B fibers as the potential mediators of the Hering-Breuer reflex which is line with the findings of Guz et al [92]. However, complete block of peak 2 resulted in the BRrate to assume at a rate comparable to that in the 'Pre' epoch. This evidence points to mainly B fibers as the mediators of the Hering-Breuer reflex.

In previous work, LFAC was applied to the vagus nerve of the rat to block a bradycardia induced state by vagal stimulation [85]. We had hypothesized that LFAC would not translate to large nerve bundles to achieve block of a biomarker. However, in the present work, we show that block was achieved in a larger nerve bundle and was successful in blocking a reflex mediated by the phrenic nerve. Furthermore, CNAP evidence showed a smearing effect prior to block and a preferential order of block. In the evidence presented here, the left vagus nerve was crushed to eliminate cardiac reflexes. In a previous study in the left vagus nerve of a rat, the nerve was crushed to eliminate cranial effects [85]. Crushing the nerve will not be an option in clinical applications, and standard nerve stimulation causes activation in both afferent and efferent fibers. Unidirectional activation can be achieved with the use of a second electrode for the delivery of LFAC to block unwanted activation. LFAC is an attractive alternative to other electrical blocking techniques in clinical applications due to the features such as no onset response, charge-balanced waveform, and low threshold characteristics.

CHAPTER 4. DISCUSSION

4.1 General Discussion

This thesis provides evidence of a novel blocking waveform *in-vivo*. The objective of this thesis was to parameterize the window of operation of the blocking low frequency alternating current (LFAC) waveform and to address the question of functionality. The voltage and current requirements will guide the development of *in-silico* models across different species. LFAC block fills the gap between direct current (DC) block at 0 Hz and kilohertz frequency alternating current block (kHFACb) greater than 1 kHz. Evidence of block has been shown *in-vivo* in rat and swine. The LFAC waveform blocked physiologically relevant biomarkers such as heart rate (HR) in rats and breathing rate (BR) in swine. In the rat study, vagal stimulation elicited an efferent volley of action potentials (AP) that resulted in a bradycardic state and if not discontinued or blocked, would result in death. In the swine study, vagal stimulation elicited an afferent volley of APs that resulted in the activation of the Hering-Breuer reflex. If vagal stimulation was not discontinued or blocked, it would result in the complete cessation of breathing which could result in death. The experimental paradigm was split into 5 epochs which consisted of recording the ECG or respiration during: Pre (baseline), LFAC only, LFAC + VStim, Vstim only, and Post (recovery). The 'LFAC only' epoch provided evidence that LFAC did not produce an onset response and at a fraction of the currents required for kHFACb. LFAC was able to produce functional changes in organ function by blocking the effect of vagal stimulation. Table below summarizes the drawbacks associated with the various electrical blocking techniques.

Table 4.1. Summary of electrical nerve conduction blocking techniques and their associated drawbacks

Electrical Blocking Technique		Onset Response/Activation	Hydrolysis	Reversibility	Current Thresholds
LFAC		No	No	Yes	~ 110μAp – 1.1mAp
Collision		Make or Break Activation	No	Yes	~ 0.5mA – 15mA
DC	Anodal	Break-Activation	Yes	Yes	~ 50μA – 7.0mAp
	Cathodal	Make-Activation	Yes	Yes	
kHFACb		Yes	No	Yes	~ 1mA – 10mA

4.2 Specific Discussion

4.2.1 Aim 1

Explore the effect of the LFAC waveform on a bradycardia induced state due to vagal stimulation.

The heart rate was normalized to the 'Pre' and 'Vstim only' epochs. The percent block during 'LFAC+VStim' when LFAC was delivered via a hook was calculated to be 86.6 $\pm$ 11% (n = 7) block at current levels 95 $\pm$ 38μA_p. When presented via a cuff electrode, 85.3 $\pm$ 4.60% block (n = 5) was achieved using current levels of 110 $\pm$ 65μA_p. The currents were well within the water window of the blocking electrode and less than half of the currents required for kHFACb block. This evidence suggest that LFAC can block the effect of a relevant biomarker imposed by vagal stimulation. The functional changes in the heart were not minor. Without block or if not discontinued, vagal stimulation alone would result in death of the animal.

These results suggest that LFAC can potentially modulate, or block, nerve activity to achieve a functional change in organ function, which was not predicted or able to be modeled *in-silico*. Preliminary electroneurogram (ENG) recordings during bradycardia point to the small A-delta and unmyelinated C-fibers as the nerve fibers mediating heart rate. This is consistent with the findings of McAllen et al [87]. With further investigations, LFAC could have the possibility of being applied clinically to alter a diseased state.

4.2.2 Aim 2

Compare the effect of electrode type on blocking a relevant biomarker.

The effect of electrode type on percent block during 'LFAC+VStim' was also investigated. One-way ANOVA for the electrodes were performed and showed that there was a statistical difference within the 5 epochs of the test sequence for the hook ($F(4,125) = 755.6$ and $Pr(>F) = 2e^{-}16$) and for the cuff ($F(4,70) = 2271$ and $Pr(>F) = 2e^{-}16$). Tukey post hoc results revealed that there was no significant difference between 'Pre' and 'LFAC only' in both the hook and the cuff ($p-adjusted = 0.99$ and $p-adjusted = 0.77$, respectively) indicating that the LFAC waveform does not cause an onset response.

Two-way ANOVA statistical analysis results supported the hypothesis that there was no significant difference between cuff and hook ($F(1,195) = 0.046$ and $Pr(> F) = 0.830$). Tukey post hoc results indicated that there was no statistical significant difference between 'Pre' and 'LFAC Only' ($p - adjusted = 0.98$). This further demonstrates that there is no onset response associated with LFAC. Significant differences were only due to treatment type, i.e., the 5 epochs of the waveform sequence. Two-way ANOVA statistical analysis results examining the effect of experimental case (test or control) and treatment (the 5 epochs of the experimental sequence) on normalized HR revealed a significant difference due to experimental case (F$(1,310) = 229.6$ and $Pr(> F) = 2e^{-}16$), a significant difference due to treatment ($F(4,310) = 1607.5$ and $Pr(> F) = 2e^{-}16$), and a significant difference between experimental case and treatment ($F(4,310) = 229.8$ and $Pr(> F) = 2e^{-}16$). Furthermore, Tukey post hoc results revealed that there were no significant differences in the 'Pre vs LFAC Only' epochs between and within the control and test cases. However, there was a significant difference in the 'LFAC+VStim' epoch between the control and test ($p - adjusted = 0$), as expected. It was hypothesized that the cuff electrodes would require less current due to less current leakage. LFAC delivered through the bipolar hook required currents of $95 \pm 38\mu A_p$. However, when presented via a bipolar cuff it required currents of $110 \pm 65\mu A_p$. The currents fall within similar ranges, however not enough replicates allowed for a statistical test. Furthermore, *Table 2.2* shows an increasing trend in currents. One possible explanation for this observation is a change in electrode impedance, indicating that the electrodes needed to be replatinized.

The statistical analysis results indicate that unlike kHFACb, LFAC does not cause an onset response when turned on whether LFAC is delivered via a hook or cuff. This makes LFAC a more attractive option as block also occurred at currents approximately less than half of those required for kHFACb. Furthermore, these results suggest that there was no significant functional difference between the cuff and hook. This evidence could drive the development for a non invasive clinical device.

4.2.3 Aim 3

Scalability of the LFAC waveform to different nerve diameters.

It was previously hypothesized that when LFAC was applied to larger nerve bundles, block would not be achieved due to lack of current penetration in a large nerve bundle. However, this hypothesis was rejected. When LFAC was applied to the cervical vagus nerve of swine (2.5*mm*), block of the Hering-Breuer reflex that is mediated by the phrenic nerve was achieved. LFAC achieved 87.2 $\pm$ 8.8 % (n = 5) block at current levels of 0.8 $\pm$ 0.3mA_p, which was well within the water window of the working electrode.

Block was achieved in the small nerve bundle of a rat with small contacts and in the human-sized vagus nerve in swine with larger contacts (*Table 4.2*). This evidence suggests that LFAC can be scaled to larger, human-sized autonomic nerve bundles. Furthermore, the electrode geometries that were used to achieve block will serve as a starting point for *in-silico* models to explore the 'best' or ideal electrode geometry and why they are deemed as such.

Table 4.2. Summary of cuff dimensions and parameters used for the rat and swine experiments

Cuff Dimensions		
Parameter	**Rat**	**Swine**
Cuff Length	5 mm	8 mm
Cuff Diameter	0.5 mm	2 mm
Contact Width	0.5 mm	1.5 mm
Edge to Edge Distance	1 mm	1.5 mm
Vagus Nerve Diameter	0.5 – 0.7 mm	2.0 – 2.5 mm

4.2.4 Aim 4

Explore the effect of LFAC on compound neural action potentials (CNAP).

An important feature of the LFAC waveform is that the frequency is outside the bandwidth of neural signals. ENG recordings during the swine experiments revealed that LFAC was able to block the B-fibers elicited during vagal stimulation which resulted in the activation of the Hering-Breuer reflex. Further examination of the CNAPs shows a preferential blocking order in which the slower fibers are blocked first, similar to DC block. Additionally, a smearing or slowing effect is evident. Both observations are consistent with the *in-silico* and *ex-vivo* work [1].

This evidence allows for the correlation of the observed and recorded functional changes in biomarkers with fiber type and conduction velocity. Furthermore, the observations presented, such as preferential order of block, converged and corroborated the *in-silico* models with *in-vivo* observations. This is a unique feature of the LFAC blocking technique in which small fibers are blocked first. An accurate *in-silico* model would allow for preliminary investigations prior to *in-vivo* experiments. The model could be used to predict electrode parameters required to achieve block.

4.3 Implications and Future Directions

The evidence presented here shows promise of a novel electrical blocking technique. There is potential for the LFAC waveform to be scaled to large caliber nerves. The realm of this study focused on autonomic nerves. Thus exploration of the effect of the LFACb waveform on somatic nerves to determine the capabilities of LFAC to block large fibers related to muscle twitching is needed.

Adequate levels of vagal stimulation were determined based on qualitative measures. The effects were titrated to cause an effect in heart rate and breathing. However, not enough of an effect that would cause the animal to crash and not recover upon the removal of vagal stimulation. Future studies could incorporate a quantitative measure to remove a possible variable that can result in variance from experiment to experiment.

Further investigations are needed to evaluate the frequency dependent window of block. *In-silico* work shows a frequency dependent window of block and activation. It also shows that lowering the frequency results in a higher current needed to achieve block. As frequency increases, the blocking threshold decreases. However, as the frequency continues to increase, LFAC causes activation and not block. Therefore, there is a specific window of operation for block before activation occurs. This window must be parameterized to evaluate what frequency results in the lowest current delivery while achieving block.

Additionally, in the work presented in this thesis, crushing the vagus nerve was crucial for isolating the biomarker and fibers of interest. However, this causes irreparable damage and is therefore, not an option in clinical settings. Standard electrical stimulation to the nerve causes activation of both efferent and afferent fibers. However, a second electrode can be used for the delivery of the LFAC waveform to block activation in the unwanted direction. Applications in which electrical stimulation is not necessary, such as spasticity, would only require a single electrode for LFAC.

Furthermore, nerve damage is still possible with the use of LFAC. This occurred in the early preliminary experiments when the potential or current wasn't balanced and was observed as discoloration of the tissue. Therefore, continuous monitoring of the DC offset was important. For clinical applications a 'smart stimulator' would be necessary not only to monitor and maintain balance but to also monitor and account for any potential change of the electrode that can occur due to polarization. Therefore, chronic studies are needed to further determine the long-term safety of LFAC.

Although LFAC was able to elicit a physiologically relevant change in a biomarker, whether HR or BR, complete block was not achieved. This is largely due to the duty cycle of the LFAC waveform. In these experiments, the duty cycle was approximately 25%. However, with the use of a second blocking electrode, the LFAC waveform can be delivered to each electrode. The waveforms can then be phased in such a way that the duty cycle reaches approximately 100%. This could potentially yield complete block. However, for certain applications of neural over activity, such as those that lead to spasticity, complete block may not be needed.

Further investigations are needed to evaluate the mechanism of LFAC or other blocking requirements that focus on electrode geometries. Furthermore, *in-silico* work, not presented in this thesis, suggests a closed state block of NAV1.7 [1]. Unlike DC block, LFAC blocks by inactivating the activation state variable m, and activating the inactivation state variable h. Whereas with DC block there is direct activation of h without activating m.

LFAC shows promise as a safe alternative to current blocking techniques. It has no associated onset response, as is associated with kHFACb block. In addition to that, it is a charge-balanced waveform which allows for the reversal of reactions occurring at the tissue/electrode interface, unlike DC block. The currents delivered were within the water window of the electrode, and there was no apparent injury to the nerve, which is generally observed as discoloration of the tissue or irreversible block. The evidence presented in this thesis focuses on autonomic nerves. However, work in the somatic system is needed to explore the capabilities of LFAC to block large fibers related to muscle twitching. While further investigations are needed, the evidence provided here indicates that LFAC has the potential to be a safe alternative to the other blocking techniques. It has the low threshold characteristics of cathodal block, a charge balanced waveform, and does not produce an onset response.

LIST OF REFERENCES

[1] M. Horn, C. Ahmed, and K. Yoshida, "Low Frequency Alternating Current Block - A New Method to Stop or Slow Conduction of Action Potentials," San Francisco, California.

[2] K. Yoshida and M. R. Horn, "Methods and systems for blocking nerve activity propagation in nerve fibers," U.S Patent US16/606,301, April, 2020.

[3] D. Purves, G. Augustine, D. Fitzpatrick, W. Hall, A.-S. LaMantia, R. Mooney, M. Platt, and L. White, *Neuroscience*, 6th ed. Oxford University Press, 2018.

[4] "Medical Physiology, 2e Updated Edition - 2nd Edition." [Online]. Available: https://www.elsevier.com/books/medical-physiology-2e-updated-edition/boron/978-1-4377-1753-2

[5] A. L. Hodgkin and A. F. Huxley, "Currents carried by sodium and potassium ions through the membrane of the giant axon of Loligo," *The Journal of Physiology*, vol. 116, no. 4, pp. 449–472, 1952, _eprint: https://physoc.onlinelibrary.wiley.com/doi/pdf/10.1113/jphysiol.1952.sp004717. [Online]. Available: https://physoc.onlinelibrary.wiley.com/doi/abs/10.1113/jphysiol.1952.sp004717

[6] H. S. Gasser and J. Erlanger, "THE RÔLE PLAYED BY THE SIZES OF THE CONSTITUENT FIBERS OF A NERVE TRUNK IN DETERMINING THE FORM OF ITS ACTION POTENTIAL WAVE," *American Journal of Physiology-Legacy Content*, vol. 80, no. 3, pp. 522–547, May 1927. [Online]. Available: https://www.physiology.org/doi/10.1152/ajplegacy.1927.80.3.522

[7] H. S. Gasser, "The Classification of Nerve Fibers," no. 3, p. 15.

[8] "The Nobel Prize in Physiology or Medicine 1944," library Catalog: www.nobelprize.org. [Online]. Available: https://www.nobelprize.org/prizes/medicine/1944/ceremony-speech/

[9] M. Piccolino, "Animal electricity and the birth of electrophysiology: the legacy of Luigi Galvani," *Brain Research Bulletin*, vol. 46, no. 5, pp. 381–407, Jul. 1998. [Online]. Available: http://www.sciencedirect.com/science/article/pii/S0361923098000264

[10] D. A. Groves and V. J. Brown, "Vagal nerve stimulation: a review of its applications and potential mechanisms that mediate its clinical effects," *Neuroscience & Biobehavioral Reviews*, vol. 29, no. 3, pp. 493–500, May 2005. [Online]. Available: http://www.sciencedirect.com/science/article/pii/S0149763405000199

[11] "The Vagus Nerve (CN X) - Course - Functions - TeachMeAnatomy," library Catalog: teachmeanatomy.info. [Online]. Available: https://teachmeanatomy.info/head/cranial-nerves/vagus-nerve-cn-x/

[12] R. H. Howland, "Vagus Nerve Stimulation," *Current Behavioral Neuroscience Reports*, vol. 1, no. 2, pp. 64–73, Jun. 2014. [Online]. Available: https://doi.org/10.1007/s40473-014-0010-5

[13] S. C. Schachter and C. B. Saper, "Vagus Nerve Stimulation," *Epilepsia*, vol. 39, no. 7, pp. 677–686, 1998, _eprint: https://onlinelibrary.wiley.com/doi/pdf/10.1111/j.1528-1157.1998.tb01151.x. [Online]. Available: https://onlinelibrary.wiley.com/doi/abs/10.1111/j.1528-1157.1998.tb01151.x

[14] G. M. De Ferrari and P. J. Schwartz, "Vagus nerve stimulation: from pre-clinical to clinical application: challenges and future directions," *Heart Failure Reviews*, vol. 16, no. 2, pp. 195–203, Mar. 2011. [Online]. Available: http://www.ulib.iupui.edu/cgi-bin/proxy.pl?url=https://search.ebscohost.com/login.aspx?direct=true&db=mnh&AN=21165697&site=eds-live

[15] H. Yuan and S. D. Silberstein, "Vagus Nerve and Vagus Nerve Stimulation, a Comprehensive Review: Part II," *Headache: The Journal of Head and Face Pain*, vol. 56, no. 2, pp. 259–266, 2016, _eprint: https://onlinelibrary.wiley.com/doi/pdf/10.1111/head.12650. [Online]. Available: http://headachejournal.onlinelibrary.wiley.com/doi/abs/10.1111/head.12650

[16] A. J. Rush, M. S. George, H. A. Sackeim, L. B. Marangell, M. M. Husain, C. Giller, Z. Nahas, S. Haines, R. K. Simpson, and R. Goodman, "Vagus Nerve Stimulation (VNS) for Treatment- Resistant Depressions: A Multicenter Study," *BIOL PSYCHIATRY*, p. 11.

[17] M. Roslin and M. Kurian, "The Use of Electrical Stimulation of the Vagus Nerve to Treat Morbid Obesity," *Epilepsy & Behavior*, vol. 2, no. 3, pp. S11–S16, Jun. 2001. [Online]. Available: https://linkinghub.elsevier.com/retrieve/pii/S1525505001902136

[18] P. Boon, I. Moors, V. De Herdt, and K. Vonck, "Vagus nerve stimulation and cognition," *Seizure*, vol. 15, no. 4, pp. 259–263, Jun. 2006. [Online]. Available: https://linkinghub.elsevier.com/retrieve/pii/S1059131106000409

[19] A. Mauskop, "Vagus nerve stimulation relieves chronic refractory migraine and cluster headaches," *Cephalalgia : an international journal of headache*, vol. 25, no. 2, pp. 82–86, Feb. 2005, place: England Publisher: Universitetsforlaget. [Online]. Available: https://www.ulib.iupui.edu/cgi-bin/proxy.pl?url=https://search.ebscohost.com/login.aspx?direct=true&db=mnh&AN=15658944&site=eds-live

[20] F. A. Koopman, S. S. Chavan, S. Miljko, S. Grazio, S. Sokolovic, P. R. Schuurman, A. D. Mehta, Y. A. Levine, M. Faltys, R. Zitnik, K. J. Tracey, and P. P. Tak, "Vagus nerve stimulation inhibits cytokine production and attenuates disease severity in rheumatoid arthritis," *Proceedings of the National Academy of Sciences*, vol. 113, no. 29, pp. 8284–8289, Jul. 2016. [Online]. Available: http://www.pnas.org/lookup/doi/10.1073/pnas.1605635113

[21] Li Shuyan, Scherlag Benjamin J., Yu Lilei, Sheng Xia, Zhang Ying, Ali Reza, Dong Yumei, Ghias Muhammad, and Po Sunny S., "Low-Level Vagosympathetic Stimulation," *Circulation: Arrhythmia and Electrophysiology*, vol. 2, no. 6, pp. 645–651, Dec. 2009, publisher: American Heart Association. [Online]. Available: https://www.ahajournals.org/doi/full/10.1161/circep.109.868331

[22] Vanoli E, De Ferrari G M, Stramba-Badiale M, Hull S S, Foreman R D, and Schwartz P J, "Vagal stimulation and prevention of sudden death in conscious dogs with a healed myocardial infarction." *Circulation Research*, vol. 68, no. 5, pp. 1471–1481, May 1991, publisher: American Heart Association. [Online]. Available: https://www.ahajournals.org/doi/10.1161/01.RES.68.5.1471

[23] M. Tosato, K. Yoshida, E. Toft, V. Nekrasas, and J. J. Struijk, "Closed-loop control of the heart rate by electrical stimulation of the vagus nerve," *Medical & Biological Engineering & Computing*, vol. 44, no. 3, pp. 161–169, Mar. 2006. [Online]. Available: https://www.ulib.iupui.edu/cgi-bin/proxy.pl?url=https://search.ebscohost.com/login.aspx?direct=true&db=aci&AN=21909084&site=eds-live

[24] P. J. Schwartz, G. M. D. Ferrari, A. Sanzo, M. Landolina, R. Rordorf, C. Raineri, C. Campana, M. Revera, N. Ajmone-Marsan, L. Tavazzi, and A. Odero, "Long term vagal stimulation in patients with advanced heart failure First experience in man," *European Journal of Heart Failure*, vol. 10, no. 9, pp. 884–891, 2008, _eprint: https://onlinelibrary.wiley.com/doi/pdf/10.1016/j.ejheart.2008.07.016. [Online]. Available: https://onlinelibrary.wiley.com/doi/abs/10.1016/j.ejheart.2008.07.016

[25] J.-M. Gracies, P. Nance, E. Elovic, J. McGuire, and D. M. Simpson, "Traditional pharmacological treatments for spasticity part II: General and regional treatments," *Muscle & Nerve*, vol. 20, no. S6, pp. 92–120, 1997. [Online]. Available: https://onlinelibrary.wiley.com/doi/abs/10.1002/\%28SICI\%291097-4598\%281997\%296\%20\%3C92\%3A\%3AAID-MUS7\%3E3.0.CO\%3B2-E

[26] J.-M. Gracies, E. Elovic, J. McGuire, and D. Simpson, "Traditional pharmacological treatments for spasticity part I: Local treatments," *Muscle & Nerve*, vol. 20, no. S6, pp. 61–91, 1997. [Online]. Available: https://onlinelibrary.wiley.com/doi/abs/10.1002/\%28SICI\%291097-4598\%281997\%296\%20\%3C61\%3A\%3AAID-MUS6\%3E3.0.CO\%3B2-H

[27] "Nerve block: How it works, types, and risks," library Catalog: www.medicalnewstoday.com. [Online]. Available: https://www.medicalnewstoday.com/articles/nerve-block

[28] A. H. Tilton, "Injectable Neuromuscular Blockade in the Treatment of Spasticity and Movement Disorders," *Journal of Child Neurology*, vol. 18, no. 1_suppl, pp. S50–S66, Jan. 2003. [Online]. Available: http://journals.sagepub.com/doi/10.1177/08830738030180010S0701

[29] S. Gündtiz, T. A. Kalyon, H. Dursun, H. Möhür, and F. Bilgiç, "Peripheral nerve block with phenol to treat spasticity in spinal cord injured patients," *Spinal Cord*, vol. 30, no. 11, pp. 808–811, Nov. 1992. [Online]. Available: http://www.nature.com/articles/sc1992156

[30] M. B. Lukban, R. L. Rosales, and D. Dressler, "Effectiveness of botulinum toxin A for upper and lower limb spasticity in children with cerebral palsy: a summary of evidence," *Journal of Neural Transmission*, vol. 116, no. 3, p. 319, Mar. 2009. [Online]. Available: https://www.ulib.iupui.edu/cgi-bin/proxy.pl?url=https://search.ebscohost.com/login.aspx?direct=true&db=edb&AN=36793488&site=eds-live

[31] A. L. Hodgkin and B. Katz, "The effect of temperature on the electrical activity of the giant axon of the squid," *The Journal of Physiology*, vol. 109, no. 1-2, pp. 240–249, Aug. 1949. [Online]. Available: https://www.ncbi.nlm.nih.gov/pmc/articles/PMC1392577/

[32] K. Y. H. Lagerspetz and A. Talo, "TEMPERATURE ACCLIMATION OF THE FUNCTIONAL PARAMETERS OF THE GIANT NERVE FIBRES IN LUMBRICUS TERRESTRIS L." p. 10.

[33] Callsen-Cencic and Mense, "Control of the unstable urinary bladder by graded thermoelectric cooling of the spinal cord: UNSTABLE URINARY BLADDER CONTROL," *BJU International*, vol. 84, no. 9, pp. 1084–1092, Dec. 2001. [Online]. Available: http://doi.wiley.com/10.1046/j.1464-410x.1999.00319.x

[34] P. Borgdorff and P. G. A. Versteeg, "An implantable nerve cooler for the exercising dog," *European Journal of Applied Physiology and Occupational Physiology*, vol. 53, no. 2, pp. 175–179, Oct. 1984. [Online]. Available: https://doi.org/10.1007/BF00422583

[35] A. R. Duke, M. W. Jenkins, H. Lu, J. M. McManus, H. J. Chiel, and E. D. Jansen, "Transient and selective suppression of neural activity with infrared light," *Scientific Reports*, vol. 3, Sep. 2013. [Online]. Available: https://www.ncbi.nlm.nih.gov/pmc/articles/PMC3764437/

[36] E. H. Lothet, K. L. Kilgore, N. Bhadra, N. Bhadra, T. Vrabec, Y. T. Wang, E. D. Jansen, M. W. Jenkins, and H. J. Chiel, "Alternating current and infrared produce an onset-free reversible nerve block," *Neurophotonics*, vol. 1, no. 1, p. 011010, Jul. 2014. [Online]. Available: http://neurophotonics.spiedigitallibrary.org/article.aspx?doi=10.1117/1.NPh.1.1.011010

[37] J. D. Sweeney, J. T. Mortimer, and D. R. Bodner, "Acute animal studies on electrically induced collision block of pudendal nerve motor activity," *Neurourology and Urodynamics*, vol. 8, no. 5, pp. 521–536, 1989, _eprint: https://onlinelibrary.wiley.com/doi/pdf/10.1002/nau.1930080516. [Online]. Available: https://onlinelibrary.wiley.com/doi/abs/10.1002/nau.1930080516

[38] J. Martau, J. Mortimer, D. Bodner, and G. Creasey, "Changes In Collision Block Threshold In Chronic Pudendal Nerve Implants," in *[1990] Proceedings of the Twelfth Annual International Conference of the IEEE Engineering in Medicine and Biology Society*, Nov. 1990, pp. 2244–2245.

[39] J. Mortimer, J. Sweeney, D. Bodner, and A. Ferguson, "An implantable cuff electrode for collision block of pudendal nerve motor activity," in *Proceedings of the Annual International Conference of the IEEE Engineering in Medicine and Biology Society*, Nov. 1988, pp. 1523–1524 vol.4.

[40] I. J. Ungar, J. T. Mortimer, and J. D. Sweeney, "Generation of unidirectionally propagating action potentials using a monopolar electrode cuff," *Annals of Biomedical Engineering*, vol. 14, no. 5, pp. 437–450, Sep. 1986. [Online]. Available: https://doi.org/10.1007/BF02367364

[41] C. Van Den Honert and J. T. Mortimer, "A Technique for Collision Block of Peripheral Nerve: Frequency Dependence," *IEEE Transactions on Biomedical Engineering*, vol. BME-28, no. 5, pp. 379–382, May 1981, conference Name: IEEE Transactions on Biomedical Engineering.

[42] J. D. Sweeney and J. T. Mortimer, "An Asymmetric Two Electrode Cuf for Generation of Unidirectionally Propagated Action Potentials," *IEEE Transactions on Biomedical Engineering*, vol. BME-33, no. 6, pp. 541–549, Jun. 1986, conference Name: IEEE Transactions on Biomedical Engineering.

[43] C. Van Den Honert and J. T. Mortimer, "A Technique for Collision Block of Peripheral Nerve: Single Stimulus Analysis," *IEEE Transactions on Biomedical Engineering*, vol. BME-28, no. 5, pp. 373–378, May 1981, conference Name: IEEE Transactions on Biomedical Engineering.

[44] J. D. Sweeney, J. T. Mortimer, and D. R. Bodner, "Animal study of pudendal nerve cuff electrode implants for collision block of motor activity," *Neurourology and Urodynamics*, vol. 9, no. 1, pp. 83–93, 1990, _eprint: https://onlinelibrary.wiley.com/doi/pdf/10.1002/nau.1930090109. [Online]. Available: https://onlinelibrary.wiley.com/doi/abs/10.1002/nau.1930090109

[45] J. Whitwam and C. Kidd, "THE USE OF DIRECT CURRENT TO CAUSE SELECTIVE BLOCK OF LARGE FIBRES IN PERIPHERAL NERVES," *British Journal of Anaesthesia*, vol. 47, no. 11, pp. 1123–1132, Nov. 1975. [Online]. Available: https://linkinghub.elsevier.com/retrieve/pii/S0007091217475374

[46] N. Bhadra and K. Kilgore, "Direct Current Electrical Conduction Block of Peripheral Nerve," *IEEE transactions on neural systems and rehabilitation engineering : a publication of the IEEE Engineering in Medicine and Biology Society*, vol. 12, pp. 313–24, Oct. 2004.

[47] N. Sperelakis and E. Kaneshiro, *Essentials of Membrane Physiology*, 2012. [Online]. Available: https://ebookcentral-proquest-com.proxy.ulib.uits.iu.edu/lib/iupui-ebooks/reader.action?docID=848958

[48] N. J. M. Rijkhoff and H. Wijkstra, "SELECTIVE DETRUSOR ACTIVATION BY ELECTRICAL SACRAL NERVE ROOT STIMULATION IN SPINAL CORD INJURY," p. 6.

[49] M. Sassen and M. Zimmermann, "Differential blocking of myelinated nerve fibres by transient depolarization," *Pflügers Archiv*, vol. 341, no. 3, pp. 179–195, Sep. 1973. [Online]. Available: https://doi.org/10.1007/BF00592788

[50] S. W. Kuffler and R. W. Gerard, "The small-nerve motor system to skeletal muscle," *Journal of Neurophysiology*, vol. 10, no. 6, pp. 383–394, Nov. 1947, publisher: American Physiological Society. [Online]. Available: http://journals.physiology.org/doi/abs/10.1152/jn.1947.10.6.383

[51] D. R. Merrill, M. Bikson, and J. G. R. Jefferys, "Electrical stimulation of excitable tissue: design of efficacious and safe protocols," *Journal of Neuroscience Methods*, vol. 141, no. 2, pp. 171–198, Feb. 2005. [Online]. Available: http://www.sciencedirect.com/science/article/pii/S0165027004003826

[52] D. M. Ackermann, N. Bhadra, E. L. Foldes, and K. L. Kilgore, "Separated Interface Nerve Electrode Prevents Direct Current Induced Nerve Damage," *Journal of neuroscience methods*, vol. 201, no. 1, pp. 173–176, Sep. 2011. [Online]. Available: https://www.ncbi.nlm.nih.gov/pmc/articles/PMC3099145/

[53] J. Miles, K. Kilgore, N. Bhadra, and E. Lahowetz, "Effects of ramped amplitude waveforms on the onset response of high-frequency mammalian nerve block," *Journal of neural engineering*, vol. 4, pp. 390–8, Jan. 2008.

[54] M. Tosato, K. Yoshida, E. Toft, and J. J. Struijk, "Quasi-trapezoidal pulses to selectively block the activation of intrinsic laryngeal muscles during vagal nerve stimulation," *Journal of Neural Engineering*, vol. 4, no. 3, pp. 205–212, Sep. 2007. [Online]. Available: http://stacks.iop.org/1741-2552/4/i=3/a=005?key=crossref.5a2fd61e15e4ea580f31a454ebb87f3b

[55] N. Accornero, G. Bini, G. L. Lenzi, and M. Manfredi, "Selective Activation of peripheral nerve fibre groups of different diameter by triangular shaped stimulus pulses." *The Journal of Physiology*, vol. 273, no. 3, pp. 539–560, 1977, _eprint: https://physoc.onlinelibrary.wiley.com/doi/pdf/10.1113/jphysiol.1977.sp012109. [Online]. Available: https://physoc.onlinelibrary.wiley.com/doi/abs/10.1113/jphysiol.1977.sp012109

[56] C. Tai, J. R. Roppolo, and W. C. de Groat, "Analysis of nerve conduction block induced by direct current," *Journal of Computational Neuroscience*, vol. 27, no. 2, pp. 201–210, Oct. 2009. [Online]. Available: http://link.springer.com/10.1007/s10827-009-0137-7

[57] N. Bhadra and K. L. Kilgore, "High-frequency electrical conduction block of mammalian peripheral motor nerve," *Muscle & Nerve*, vol. 32, no. 6, pp. 782–790, Dec. 2005. [Online]. Available: http://doi.wiley.com/10.1002/mus.20428

[58] "Direct current contamination of kilohertz frequency alternating current waveforms | Elsevier Enhanced Reader." [Online]. Available: https://reader.elsevier.com/reader/sd/pii/S0165027014001186language={en},urldate={2020-01-27},doi={10.1016/j.jneumeth.2014.04.002},

[59] K. L. Kilgore and N. Bhadra, "Reversible Nerve Conduction Block Using Kilohertz Frequency Alternating Current," *Neuromodulation: Technology at the Neural Interface*, vol. 17, no. 3, pp. 242–255, 2014. [Online]. Available: https://onlinelibrary.wiley.com/doi/abs/10.1111/ner.12100

[60] M. Gerges, E. L. Foldes, D. M. Ackermann, N. Bhadra, N. Bhadra, and K. L. Kilgore, "Frequency- and amplitude-transitioned waveforms mitigate the onset response in high-frequency nerve block," *Journal of Neural Engineering*, vol. 7, no. 6, p. 066003, Oct. 2010, publisher: IOP Publishing. [Online]. Available: https://doi.org/10.1088\%2F1741-2560\%2F7\%2F6\%2F066003

[61] T. L. Vrabec, T. E. Eggers, E. L. Foldes, D. M. Ackermann, K. L. Kilgore, and N. Bhadra, "Reduction of the onset response in kilohertz frequency alternating current nerve block with amplitude ramps from non-zero amplitudes," *Journal of NeuroEngineering and Rehabilitation*, vol. 16, no. 1, p. 80, Dec. 2019. [Online]. Available: https://jneuroengrehab.biomedcentral.com/articles/10.1186/s12984-019-0554-4

[62] D. M. Ackermann, E. L. Foldes, N. Bhadra, and K. L. Kilgore, "Effect of Bipolar Cuff Electrode Design on Block Thresholds in High-Frequency Electrical Neural Conduction Block," *IEEE Transactions on Neural Systems and Rehabilitation Engineering*, vol. 17, no. 5, pp. 469–477, Oct. 2009, conference Name: IEEE Transactions on Neural Systems and Rehabilitation Engineering.

[63] ——, "Electrode design for high frequency block: Effect of bipolar separation on block thresholds and the onset response," in *2009 Annual International Conference of the IEEE Engineering in Medicine and Biology Society*, Sep. 2009, pp. 654–657, iSSN: 1558-4615.

[64] M. Franke, T. Vrabec, J. Wainright, N. Bhadra, N. Bhadra, and K. Kilgore, "Combined KHFAC+DC nerve block without onset or reduced nerve conductivity after block," *Journal of neural engineering*, vol. 11, no. 5, p. 056012, Oct. 2014. [Online]. Available: https://www.ncbi.nlm.nih.gov/pmc/articles/PMC5705235/

[65] D. M. Ackermann, N. Bhadra, E. L. Foldes, and K. L. Kilgore, "Conduction block of whole nerve without onset firing using combined high frequency and direct current," *Medical & Biological Engineering & Computing*, vol. 49, no. 2, pp. 241–251, Feb. 2011. [Online]. Available: http://link.springer.com/10.1007/s11517-010-0679-x

[66] T. Vrabec, "DIRECT CURRENT BLOCK OF PERIPHERAL NERVE: ELECTRODE AND WAVEFORM DEVELOPMENT," p. 218.

[67] J. A. Tanner, "Reversible Blocking of Nerve Conduction by Alternating-Current Excitation," *Nature*, vol. 195, no. 4842, pp. 712–713, Aug. 1962, number: 4842 Publisher: Nature Publishing Group. [Online]. Available: http://www.nature.com/articles/195712b0

[68] B. R. Bowman and D. R. McNeal, "Response of Single Alpha Motoneurons to High-Frequency Pulse Trains," *Stereotactic and Functional Neurosurgery*, vol. 49, no. 3, pp. 121–138, 1986. [Online]. Available: https://www.karger.com/Article/FullText/100137

[69] K. L. Kilgore and N. Bhadra, "Nerve conduction block utilising high-frequency alternating current," *Medical & Biological Engineering & Computing*, vol. 42, no. 3, p. 394, May 2004. [Online]. Available: https://www.ulib.iupui.edu/cgi-bin/proxy.pl?url=https://search.ebscohost.com/login.aspx?direct=true&db=edb&AN=14048495&site=eds-live

[70] D. M. Ackermann, C. Ethier, E. L. Foldes, E. R. Oby, D. Tyler, M. Bauman, N. Bhadra, L. Miller, and K. L. Kilgore, "Electrical conduction block in large nerves: High-frequency current delivery in the nonhuman primate," *Muscle & Nerve*, vol. 43, no. 6, pp. 897–899, 2011, _eprint: https://onlinelibrary.wiley.com/doi/pdf/10.1002/mus.22037. [Online]. Available: https://onlinelibrary.wiley.com/doi/abs/10.1002/mus.22037

[71] K. L. Kilgore and N. Bhadra, "High Frequency Mammalian Nerve Conduction Block: Simulations and Experiments," in *2006 International Conference of the IEEE Engineering in Medicine and Biology Society*, Aug. 2006, pp. 4971–4974, iSSN: 1557-170X.

[72] L. Joseph and R. J. Butera, "Unmyelinated Aplysia Nerves Exhibit a Nonmonotonic Blocking Response to High-Frequency Stimulation," *IEEE Transactions on Neural Systems and Rehabilitation Engineering*, vol. 17, no. 6, pp. 537–544, Dec. 2009, conference Name: IEEE Transactions on Neural Systems and Rehabilitation Engineering.

[73] R. Williamson and B. Andrews, "Localized electrical nerve blocking," *IEEE Transactions on Biomedical Engineering*, vol. 52, no. 3, pp. 362–370, Mar. 2005, conference Name: IEEE Transactions on Biomedical Engineering.

[74] L. Joseph and R. J. Butera, "High-Frequency Stimulation Selectively Blocks Different Types of Fibers in Frog Sciatic Nerve," *IEEE Transactions on Neural Systems and Rehabilitation Engineering*, vol. 19, no. 5, pp. 550–557, Oct. 2011, conference Name: IEEE Transactions on Neural Systems and Rehabilitation Engineering.

[75] N. Bhadra, N. Bhadra, K. Kilgore, and K. J. Gustafson, "High frequency electrical conduction block of the pudendal nerve," *Journal of Neural Engineering*, vol. 3, no. 2, pp. 180–187, Jun. 2006. [Online]. Available: https://www.ncbi.nlm.nih.gov/pmc/articles/PMC3375816/

[76] M. Camilleri, J. Toouli, M. Herrera, B. Kulseng, L. Kow, J. Pantoja, R. Marvik, G. Johnsen, C. Billington, F. Moody, M. Knudson, K. Tweden, M. Vollmer, R. Wilson, and M. Anvari, "Intra-abdominal vagal blocking (VBLOC therapy): Clinical results with a new implantable medical device," *Surgery*, vol. 143, no. 6, pp. 723–731, Jun. 2008. [Online]. Available: https://linkinghub.elsevier.com/retrieve/pii/S0039606008001827

[77] J. M. Cuellar, K. Alataris, A. Walker, D. C. Yeomans, and J. F. Antognini, "Effect of High-Frequency Alternating Current on Spinal Afferent Nociceptive Transmission: High-Frequency Alternating Current Inhibits Spinal DHN," *Neuromodulation: Technology at the Neural Interface*, vol. 16, no. 4, pp. 318–327, Jul. 2013. [Online]. Available: http://doi.wiley.com/10.1111/ner.12015

[78] D. M. Ackermann, N. Bhadra, M. Gerges, and P. J. Thomas, "Dynamics and sensitivity analysis of high-frequency conduction block," *Journal of Neural Engineering*, vol. 8, no. 6, p. 065007, Oct. 2011. [Online]. Available: https://iopscience.iop.org/article/10.1088/1741-2560/8/6/065007

[79] B. Bromm, "Spike frequency of the nodal membrane generated by high-frequency alternating current," *Pflügers Archiv*, vol. 353, no. 1, pp. 1–19, Mar. 1975. [Online]. Available: https://doi.org/10.1007/BF00584507

[80] D. Trenchard and J. G. Widdicombe, "ASSESSMENT OF DIFFERENTIAL BLOCK OF CONDUCTION BY DIRECT CURRENT APPLIED TO THE CERVICAL VAGUSNERVE," p. 8.

[81] N. Bhadra, T. L. Vrabec, N. Bhadra, and K. L. Kilgore, "Reversible conduction block in peripheral nerve using electrical waveforms," *Bioelectronics in Medicine*, vol. 1, no. 1, pp. 39–54, Jan. 2018. [Online]. Available: https://www.futuremedicine.com/doi/10.2217/bem-2017-0004

[82] Y. A. Patel and R. J. Butera, "Differential fiber-specific block of nerve conduction in mammalian peripheral nerves using kilohertz electrical stimulation," *Journal of Neurophysiology*, vol. 113, no. 10, pp. 3923–3929, Jun. 2015. [Online]. Available: https://www.physiology.org/doi/10.1152/jn.00529.2014

[83] N. Rijkhoff, E. Koldewijn, P. van Kerrebroeck, F. Debruyne, and H. Wijkstra, "Acute animal studies on the use of an anodal block to reduce urethral resistance in sacral root stimulation," *IEEE Transactions on Rehabilitation Engineering*, vol. 2, no. 2, pp. 92–99, Jun. 1994.

[84] P. Thoren, J. T. Shepherd, and D. E. Donald, "Anodal block of medullated cardiopulmonary vagal afferents in cats," *Journal of Applied Physiology*, vol. 42, no. 3, pp. 461–465, Mar. 1977. [Online]. Available: https://www.physiology.org/doi/10.1152/jappl.1977.42.3.461

[85] L. M. Mintch, I. Muzquiz, M. R. Horn, M. Carr, and K. Yoshida, "Reversible Conduction Block in Peripheral Mammalian Nerve Using Low Frequency Altenating Current," San Francisco, California.

[86] G. C. Santa Cruz Chavez, B.-Y. Li, P. A. Glazebrook, D. L. Kunze, and J. H. Schild, "An afferent explanation for sexual dimorphism in the aortic baroreflex of rat," *American Journal of Physiology - Heart and Circulatory Physiology*, vol. 307, no. 6, pp. H910–H921, Sep. 2014. [Online]. Available: https://www.ncbi.nlm.nih.gov/pmc/articles/PMC4166749/

[87] R. M. McAllen and K. M. Spyer, "The location of cardiac vagal preganglionic motoneurones in the medulla of the cat." *The Journal of Physiology*, vol. 258, no. 1, pp. 187–204, Jun. 1976. [Online]. Available: http://doi.wiley.com/10.1113/jphysiol.1976.sp011414

[88] W. A. Huang, N. G. Boyle, and M. Vaseghi, "Cardiac Innervation and the Autonomic Nervous System in Sudden Cardiac Death," *Cardiac Electrophysiology Clinics*, vol. 9, no. 4, pp. 665–679, Dec. 2017, publisher: Elsevier. [Online]. Available: https://www.cardiacep.theclinics.com/article/S1877-9182(17)30102-8/abstract

[89] H. Johannessen, D. Revesz, Y. Kodama, N. Cassie, K. P. Skibicka, P. Barrett, S. Dickson, J. Holst, J. Rehfeld, G. van der Plasse, R. Adan, B. Kulseng, E. Ben-Menachem, C.-M. Zhao, and D. Chen, "Vagal Blocking for Obesity Control: a Possible Mechanism-Of-Action," *Obesity Surgery*, vol. 27, no. 1, pp. 177–185, Jan. 2017. [Online]. Available: https://doi.org/10.1007/s11695-016-2278-x

[90] E. L. Foldes, D. M. Ackermann, N. Bhadra, and K. L. Kilgore, "Counted cycles method to quantify the onset response in high-frequency peripheral nerve block," in *2009 Annual International Conference of the IEEE Engineering in Medicine and Biology Society*, Sep. 2009, pp. 614–617, iSSN: 1558-4615.

[91] L. Richardson, C. Ahmed, C. Smolik, and K. Yoshida, "3D printed hinged multi-contact cuff electrodes for rapid prototypeing and testing," Nottwil, Switzerland, Aug. 2018.

[92] A. Guz and D. W. Trenchard, "Pulmonary stretch receptor activity in man: a comparison with dog and cat," *The Journal of Physiology*, vol. 213, no. 2, pp. 329–343, Mar. 1971. [Online]. Available: http://doi.wiley.com/10.1113/jphysiol.1971.sp009385

[93] R. M. McAllen, A. D. Shafton, B. O. Bratton, D. Trevaks, and J. B. Furness, "Calibration of thresholds for functional engagement of vagal A, B and C fiber groups in vivo," *Bioelectronics in Medicine*, vol. 1, no. 1, pp. 21–27, Nov. 2017, publisher: Future Medicine. [Online]. Available: https://www.futuremedicine.com/doi/10.2217/bem-2017-0001

[94] R. Chang, D. Strochlic, E. Williams, B. Umans, and S. Liberles, "Vagal Sensory Neuron Subtypes that Differentially Control Breathing," *Cell*, vol. 161, no. 3, pp. 622–633, Apr. 2015. [Online]. Available: http://www.sciencedirect.com/science/article/pii/S0092867415003098

APPENDIX A. INSTRUMENTATION SETUP

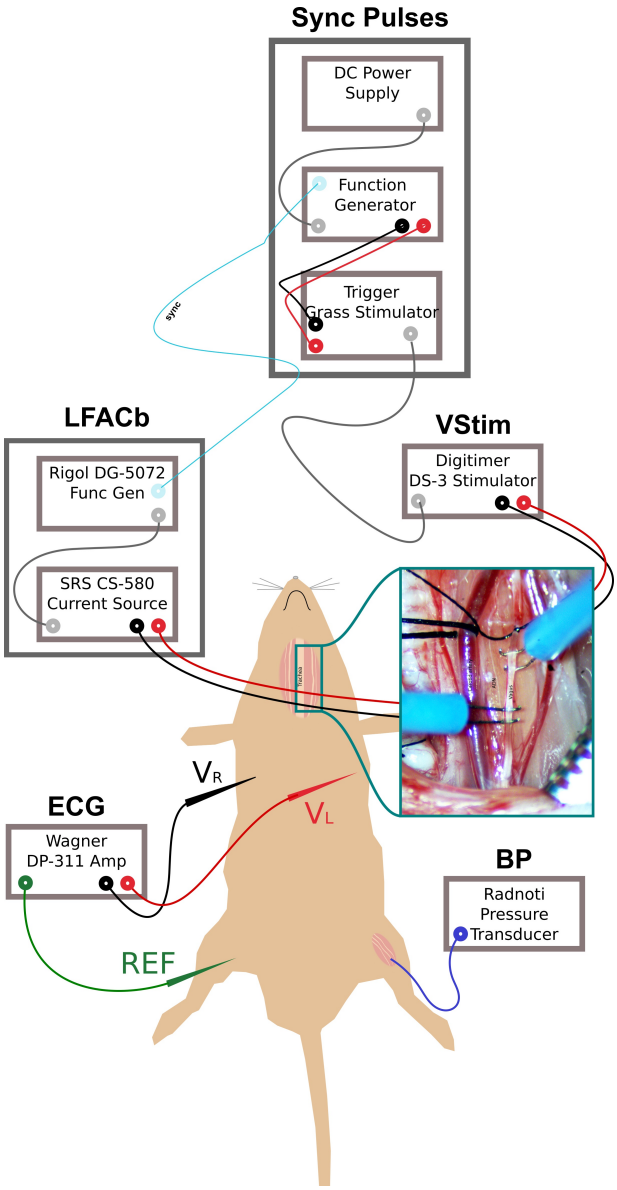

Figure A.1. General instrumentation set up for the rat

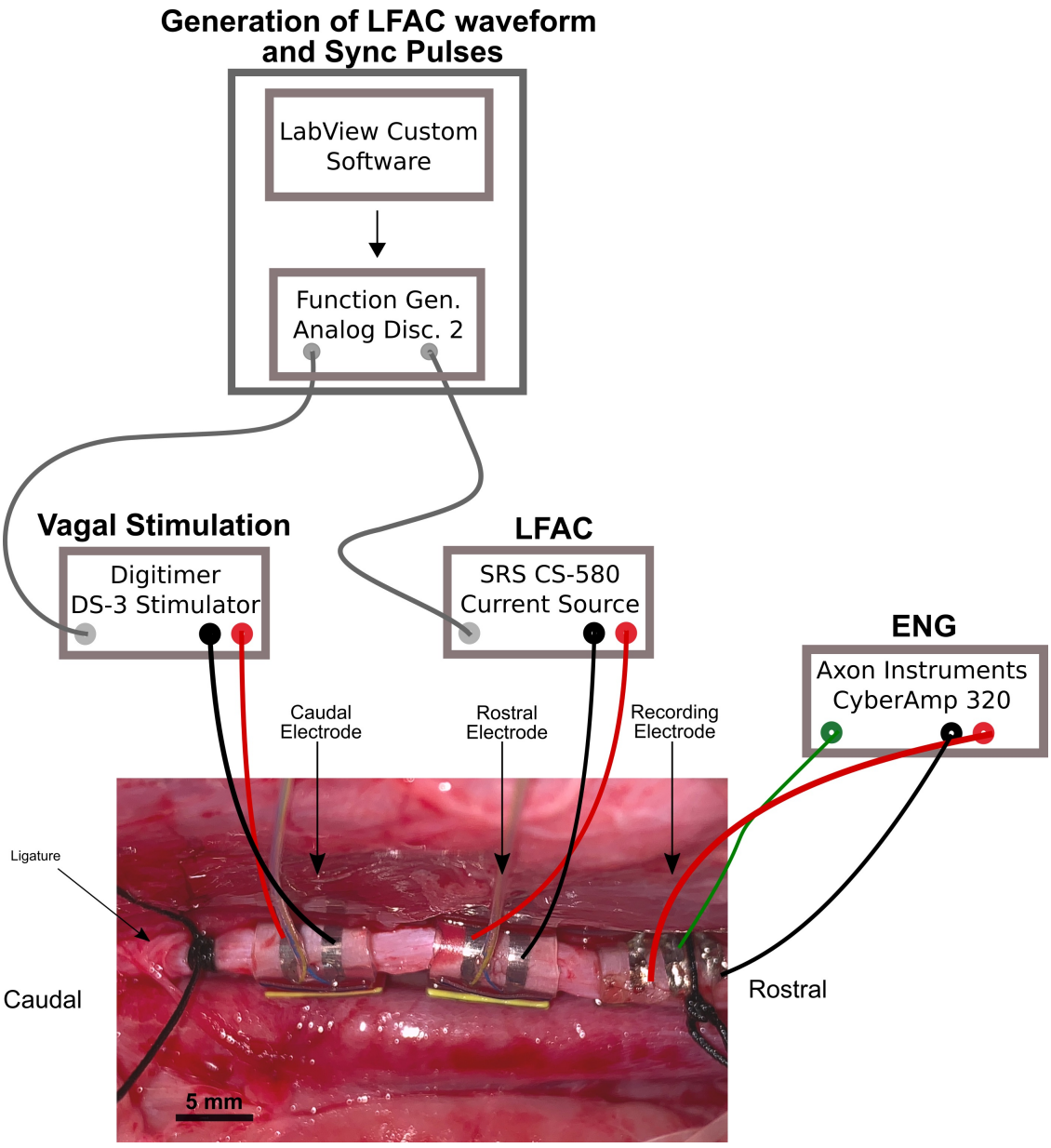

Figure A.2. General instrumentation set up for the swine